



University of Kentucky  
UKnowledge

---

University of Kentucky Doctoral Dissertations

Graduate School

---

2003

## A SPATIAL MODEL FOR EVALUATING VARIABLE-RATE FERTILIZER APPLICATION ACCURACY

JOHN PATRICK FULTON

*University of Kentucky*, [jfulton@bae.uky.edu](mailto:jfulton@bae.uky.edu)

[Right click to open a feedback form in a new tab to let us know how this document benefits you.](#)

---

### Recommended Citation

FULTON, JOHN PATRICK, "A SPATIAL MODEL FOR EVALUATING VARIABLE-RATE FERTILIZER APPLICATION ACCURACY" (2003). *University of Kentucky Doctoral Dissertations*. 248.  
[https://uknowledge.uky.edu/gradschool\\_diss/248](https://uknowledge.uky.edu/gradschool_diss/248)

This Dissertation is brought to you for free and open access by the Graduate School at UKnowledge. It has been accepted for inclusion in University of Kentucky Doctoral Dissertations by an authorized administrator of UKnowledge. For more information, please contact [UKnowledge@lsv.uky.edu](mailto:UKnowledge@lsv.uky.edu).

ABSTRACT OF DISSERTATION

JOHN PATRICK FULTON

THE GRADUATE SCHOOL  
UNIVERSITY OF KENTUCKY  
2003

A SPATIAL MODEL FOR EVALUATING VARIABLE-RATE FERTILIZER  
APPLICATION ACCURACY

---

ABSTRACT OF DISSERTATION

---

A dissertation submitted in partial fulfillment  
of the requirements for the degree of  
Doctor of Philosophy in Biosystems and Agricultural Engineering  
in the College of Engineering  
at the University of Kentucky

By  
John Patrick Fulton  
Lexington, KY

Director: Dr. Scott A. Shearer, Professor of Biosystems and Agricultural Engineering  
Lexington, KY

2003

Copyright © John Patrick Fulton 2003

## ABSTRACT OF DISSERTATION

### A SPATIAL MODEL FOR EVALUATING VARIABLE-RATE FERTILIZER APPLICATION ACCURACY

The popularity of variable-rate technology (VRT) has grown. However, the limitations and errors of this technology are generally unknown. Therefore, a spatial data model was developed to generate “as-applied” surfaces to advance precision agricultural (PA) practices. A test methodology based on ASAE Standard S341.2 was developed to perform uniform-rate (UR) and variable-rate (VR) tests to characterize distribution patterns testing four VRT granular applicators (two spinner spreaders and two pneumatic applicators). Single-pass UR patterns exhibited consistent shapes for three of the applicators with patterns shifts observed for the fourth applicator. Simulated overlap analysis showed that three of the applicators performed satisfactorily with most CVs less than 20% while one applicator performed poorly (CVs > 25%). The spinner spreaders over-applied at the margins but the pneumatic applicators under-applied suggesting a required adjustment to the effective swath spacing. Therefore, it is recommended that CVs accompany overlap pattern plots to ensure proper calibration of VRT application.

Quantification of the rate response characteristics for the various applicators illustrated varying delay and transition times. Only one applicator demonstrated consistent delay and transition times. A sigmoidal function was used to model the rate response for applicators. One applicator exhibited a linear response during a decreasing rate change. Rate changes were quicker for the two newer VR control systems signifying advancement in hydraulic control valve technology. This research illustrates the need for standard testing protocols for VRT systems to help guide VRT software developers, equipment manufacturers, and users.

The spatial data model uses GIS functionality to merge applicator descriptive patterns with a spatial field application file (FAF) to generate an ‘as-applied’ surface representing the actual distribution of granular fertilizer. Field data was collected and used to validate the “as-applied” spatial model. Comparisons between the actual and predicted application rates for several fields were made demonstrating good correlations for one applicator (several  $R^2 > 0.70$ ), moderate success for another applicator ( $0.60 < R^2 < 0.66$ ), and poor relationships for the third applicator ( $R^2 < 0.49$ ). A comparison of the actual application rates to the prescription maps generated  $R^2$  values between 0.16 and 0.81

demonstrating inconsistent VRT applicator performance. Thus, “as-applied” surfaces provide a means to properly evaluate VRT while enhancing researchers’ ability to compare VR management approaches.

KEYWORDS: As-applied surfaces and maps, Distribution patterns, Pneumatic and spinner disc applicators, Precision agriculture, Variable-rate technology

Multimedia Element Used: jpfult03.pdf

John Patrick Fulton

December 19, 2003

A SPATIAL MODEL FOR EVALUATING VARIABLE-RATE FERTILIZER  
APPLICATION ACCURACY

By  
John Patrick Fulton

Dr. Scott A. Shearer  
*Director of Dissertation*

Dr. Dwayne R. Edwards  
*Director of Graduate Studies*

December 19, 2003

## RULES FOR THE USE OF DISSERTATIONS

Unpublished dissertations submitted for the Doctor's degree and deposited in the University of Kentucky Library are as a rule open for inspection, but are to be used only with due regard to the rights of the authors. Bibliographical references may be noted, but quotations or summaries of parts may be published only with the permission of the author, and with the usual scholarly acknowledgments.

Extensive copying or publication of the dissertation in whole or in part also requires the consent of the Dean of the Graduate School of the University of Kentucky.

DISSERTATION

JOHN PATRICK FULTON

THE GRADUATE SCHOOL  
UNIVERSITY OF KENTUCKY  
2003



A SPATIAL MODEL FOR EVALUATING VARIABLE-RATE FERTILIZER  
APPLICATION ACCURACY

---

DISSERTATION

---

A dissertation submitted in partial fulfillment  
of the requirements for the degree of  
Doctor of Philosophy in Biosystems and Agricultural Engineering  
in the College of Engineering  
at the University of Kentucky

By  
John Patrick Fulton

Lexington, KY

Director: Dr. Scott A. Shearer, Professor of Biosystems and Agricultural Engineering

Lexington, KY

2003

Copyright © John Patrick Fulton 2003

Dedicated to my parents, Thomas and Barbara Fulton, and to the Agricultural community, in an effort to positively influence and enhance the future of farming.

## ACKNOWLEDGEMENTS

This dissertation represents the end of my formal education as a student. There exist many people who have provided inspiration up to this point in my life: GOD, family, friends, teachers, coaches, strangers, and many others. The list is long but everyone is to thank for their positive influence on my life. However, while I cannot mention everyone, I follow with personal thanks to several individuals who have made the completion of this dissertation possible.

First and foremost, I thank God for his never ending love and support. Through all the highs and lows, He has always been present, providing strength and inspiration.

I want to thank Dr. Scott Shearer, first for his friendship and then for all his guidance and mentoring. He is a family friend and has provided me with great opportunities during my time at the University of Kentucky. Scott has influenced my life and career path while supplying countless hours of advice. Thanks for everything Scott.

I am grateful for everything that Drs. Wells and Stombaugh have provided. They have both been good role models and educated me on many of the teaching and research facets that I will implement in my future academia career. Their friendship, with them and their families, has provided many memorable experiences during my stay in Lexington.

Thanks is also extended to Dr. Carl Dillon. I really appreciate him serving on my committee and the countless hours of discussion on precision agriculture and related topics. He taught me the importance of having cooperative research outside of the engineering profession and no matter how good of a system one designs, it must be economical. I also thank Dr. Murdock for being on my committee, his friendship, and bringing to light the importance of agronomics to my research.

I want to extend a sincere thanks to Tim Smith. Tim has had a tremendous impact on my life as both a mentor and friend. He has constantly provided direction on many of my research projects and taught me so much about engineering. Tim is a super person and I appreciate all that he has done for me.

I appreciate everything that Steve Higgins and Dennis Hancock have done. Steve has been a long time friend and we have had many memorable working experiences. He was a large asset for all the field work and it could not have been completed without him. Dennis has been a positive influence on me during the short period that we have known each other. He provided me with a wealth of knowledge in the agronomy field plus taking time for all the discussions revolving around precision agriculture and the future of farming.

I want to give the utmost appreciation to the shop guys (Carl King, Lee “Dave” Rehtin, Ed Roberts, and Ed Hutchins) for all their assistance during this research. However, I want to thank them most for

their friendship and sharing of life experiences. I believe the phrase “field talk” was developed during this research and provided the fondest memories.

More personally, I would like to thank Ed Hutchins. Ed was an integral part to the completion of this research by providing countless hours to my research. There are only a handful of people in my life that have had a large influence on me, and Ed is one. He has been a real life educator and a good person. Thanks Ed!

Lastly, I want to thank my family: grandparents, uncles, aunts, and cousins. They have all been an inspiration during my life, supplying an endless amount of support. Thanks to my sister, Catherine, and her husband, Brian, for all their love and encouragement, along with my nephew, Adam, who brought smiles during the late nights. I also thank the special person in my life, Kate; for all of her love, support, and help. She made many sacrifices during the completion of my dissertation and I could have not done it without her. The last two people I want to thank are my parents. Your love, continual support, encouragement, and guidance in all that I do in life are unparalleled. I love both you and thank you, who you are and what you provide in my life. You are the BEST.

# TABLE OF CONTENTS

<b>ACKNOWLEDGEMENTS .....</b>	<b>iii</b>
<b>TABLE OF CONTENTS .....</b>	<b>v</b>
<b>LIST OF TABLES.....</b>	<b>vii</b>
<b>LIST OF FIGURES.....</b>	<b>ix</b>
<b>LIST OF FILES.....</b>	<b>xiii</b>
<b>CHAPTER ONE INTRODUCTION.....</b>	<b>1</b>
PREFACE.....	1
JUSTIFICATION.....	2
OBJECTIVES.....	4
ORGANIZATION OF DISSERTATION.....	4
<b>CHAPTER TWO REVIEW OF LITERATURE.....</b>	<b>5</b>
<b>CHAPTER THREE PERFORMANCE ASSESSMENT AND MODEL DEVELOPMENT OF A VARIABLE-RATE, SPINNER-DISC FERTILIZER APPLICATOR.....</b>	<b>11</b>
INTRODUCTION.....	11
SUB-OBJECTIVES.....	12
OVERVIEW OF APPLICATOR.....	12
METHODOLOGY.....	12
RESULTS AND DISCUSSION.....	15
SUMMARY.....	25
<b>CHAPTER FOUR SIMULATION OF UNIFORM- AND VARIABLE-RATE APPLICATION OF GRANULAR MATERIALS.....</b>	<b>27</b>
INTRODUCTION.....	27
SUB-OBJECTIVES.....	28
METHODOLOGY.....	28
RESULTS AND DISCUSSION.....	36
SUMMARY.....	42
<b>CHAPTER FIVE COMPARISON OF VARIABLE-RATE GRANULAR APPLICATION EQUIPMENT...44</b>	
INTRODUCTION.....	44
SUB-OBJECTIVES.....	44
OVERVIEW OF APPLICATORS.....	45
METHODOLOGY.....	48
RESULTS AND DISCUSSION.....	54
SUMMARY.....	77
<b>CHAPTER SIX AS-APPLIED SPATIAL DATA MODEL FOR EVALUATION OF VARIABLE-RATE FERTILIZER APPLICATION ACCURACY.....</b>	<b>80</b>
INTRODUCTION.....	80
SUB-OBJECTIVES.....	81
METHODOLOGY.....	81
RESULTS AND DISCUSSION.....	89
SUMMARY.....	103

<b>CHAPTER SEVEN CONCLUSION .....</b>	<b>106</b>
CONCLUSIONS .....	106
SUGGESTIONS FOR FUTURE WORK .....	107
<b>APPENDIX A APPLICATOR DESCRIPTION FILES (ADF'S) .....</b>	<b>109</b>
<b>APPENDIX B SPATIAL MODEL AVENUE SCRIPT .....</b>	<b>111</b>
<b>REFERENCES .....</b>	<b>137</b>
<b>VITA .....</b>	<b>141</b>

## LIST OF TABLES

Table 3.1. Average transverse distribution pattern statistical results for single-pass tests. ....	18
Table 3.2. Desired uniform application rate along with statistical information for actual applied rate for multiple-pass tests.....	20
Table 3.3. Input parameters for each sigmoidal line fit according to distance from center transverse position. ....	22
Table 3.4. Slope and y-intercept for linear line fit for high to low rate change according to distance from center transverse position. ....	23
Table 3.5. Correlation coefficient comparing the actual potash application to the predicted application. .	24
Table 4.1. Prescription map summary information.....	30
Table 4.2. Standardized distribution pattern data.....	31
Table 4.3. Summary for the various layers of fields B and C.....	35
Table 4.4. Summary information for the "as-applied" surface for field A.....	36
Table 4.5. Rate difference categorization between the "as-applied" surface and prescription map for field A. ....	38
Table 4.6. Comparison of various layers. ....	41
Table 5.1. Applicator characteristics.....	45
Table 5.2. Single-pass UR summary statistics for the New Leader applicator.....	55
Table 5.3. Single-pass UR summary statistics for the Gandy applicator.....	55
Table 5.4. Single-pass UR summary statistics for the AgChem applicator. ....	56
Table 5.5. Simulated multiple pass summary statistics (progressive method).....	65
Table 5.6. ANOVA results for the various applicators.....	68
Table 5.7. Sigmoidal regression results for New Leader rate transitions. ....	72
Table 5.8. Sigmoidal regression results for Gandy rate transitions. ....	73
Table 5.9. Sigmoidal regression results for the AgChem rate transitions.....	73
Table 5.10. Regression results for the Newton Crouch rate transitions.....	75
Table 5.11. Rate transition characteristics. ....	75
Table 6.1. Application ranges. ....	82
Table 6.2. Applicator characteristics.....	83
Table 6.3. Example ADF for the New Leader: NL.dbf (only left half of file shown). ....	83
Table 6.5. Summary data for validation comparisons.....	90
Table 6.6. Validation results for various offsets and patterns.....	91
Table 6.7. Statistics for the “as-applied” surfaces and difference maps. ....	101
Table 6.8. Rate difference categorization between the “as-applied” surface and prescription map. ....	101

Table 6.9. Comparison of the actual applications versus the prescription map. .... 102



# LIST OF FIGURES

Figure 1.1. U.S. farms, land in farms, and average acres per farm from 1850 to 1997 (source: compiled by ERS from Census of Agriculture data and reported by USDA) .....	1
Figure 2.1. Example cumulative distribution pattern from adjacent overlap passes.....	6
Figure 3.1. Collection pan matrix for the single-pass tests.....	14
Figure 3.2. Collection pan matrix for the multiple-pass tests.....	14
Figure 3.3. Theoretical Gaussian distribution pattern.....	15
Figure 3.4. Actual uniform 56.0 kg/ha application surface.....	16
Figure 3.5. Actual uniform 168.1 kg/ha application surface.....	16
Figure 3.6. Mean distribution pattern for uniform 56.0 kg/ha application rate.....	16
Figure 3.7. Mean distribution pattern for uniform 168.1 kg/ha application rate.....	17
Figure 3.8. Modeled 56.0 kg/ha application surface.....	18
Figure 3.9. Modeled 168.1 kg/ha application surface.....	19
Figure 3.10. Actual UR application surface for the 56.0 kg/ha multiple-pass test.....	19
Figure 3.11. Actual UR application surface for the 168.1 kg/ha multiple-pass test.....	19
Figure 3.12. Rate change application surface for the VRT spinner spreader truck (change from 56.0 to 168.1 kg/ha).....	20
Figure 3.13. Rate change application surface for the VRT spinner spreader truck (change from 168.1 to 56.0 kg/ha).....	20
Figure 3.14. Example application rate change dynamics for 56.0 to 168.1 kg/ha (longitudinal application rates averaged for transverse distance 2.67 and -2.67 m).....	22
Figure 3.15. Example application rate change dynamics for 168.1 to 56.0 kg/ha (longitudinal application rates averaged for transverse distance 2.67 and -2.67 m).....	23
Figure 3.16. Modeled rate change application surface (56.0 to 168.1 kg/ha).....	24
Figure 3.17. Modeled rate change application surface (168.1 to 56.0 kg/ha).....	24
Figure 3.18. Predicted vs. observed collection pan contents for 56.0 to 168.1 kg/ha application rate change.....	25
Figure 3.19. Predicted vs. observed collection pan contents for 168.1 to 56.0 kg/ha application rate change.....	25
Figure 4.1. Application prescription map and field application file for field A.....	28
Figure 4.2. Application prescription map, field application file, and validation points for field B.....	29
Figure 4.3. Application prescription map, field application file, and validation points for field C.....	29
Figure 4.4. Low, medium, and high distribution patterns.....	31
Figure 4.5. Polygon assignment to point B showing: (a) length and heading determination for proper orientation, and (b) division into 13 sub-polygons for distribution pattern allocation.....	32

Figure 4.6. Grid generation (only left half shown) for specification of the "as-applied" surface for field A. ....	33
Figure 4.7. Generated "as-applied" surface for field A.....	33
Figure 4.8. "As-applied" surface superimposed on the prescription map for field A. ....	33
Figure 4.9. "As-applied" surface superimposed on the prescription map for field B. ....	34
Figure 4.10. "As-applied" surface superimposed on the prescription map for field C. ....	35
Figure 4.11. Prescribed versus the "as-applied" (predicted) application rates.....	37
Figure 4.12. Difference between the "as-applied" surface and prescription map for field A. ....	38
Figure 4.13. Plot of the correlation coefficient versus offset distance for field B. ....	40
Figure 4.14. Plot of the correlation coefficient versus offset distance for field C. ....	40
Figure 4.15. Plot of predicted versus actual application rates for field B. ....	40
Figure 4.16. Plot of predicted versus actual application rates for field C. ....	41
Figure 5.1. Newton Crouch spinner disc applicator; a) isometric view of applicator b) rear view showing spinner discs, and c) hydraulic drive motor and source fluid power control valve for apron chain. ...	46
Figure 5.2. New Leader L3020G spinner disc applicator a) side view of applicator b) rear view showing spinner discs, and c) hydraulic drive motor and control valve for apron belt.....	46
Figure 5.3. Gandy Orbit-Air pneumatic applicator; a) isometric view of applicator b) fluted metering rollers, c) centrifugal blower and Rawson hydraulic control system, and d) deflector plates. ....	47
Figure 5.4. AgChem AirMax 2000 pneumatic applicator; a) isometric view of applicator b)deflector plates, c) centrifugal blower, and d) hydraulic drive for apron chains. ....	47
Figure 5.5. AgChem prescription map generated by SGIS for the 336.2 to 112.1 kg/ha rate transition. ...	48
Figure 5.6. Material collection and test site layout. ....	49
Figure 5.7. New Leader UR collection pan matrix. ....	50
Figure 5.8. Gandy UR collection pan matrix. ....	51
Figure 5.9. AgChem collection pan matrix for single-pass UR and VR tests along with the desired rate transition line fed into SGIS. ....	51
Figure 5.10. New Leader collection pan matrix for single-pass, rate transition tests. ....	52
Figure 5.11. Gandy collection pan matrix for single-pass, rate transition tests. ....	53
Figure 5.12. Characterized distribution patterns for the New Leader. ....	58
Figure 5.13. Characterized distribution patterns for the Gandy.....	58
Figure 5.14. Characterized distribution patterns for the AgChem. ....	58
Figure 5.15. Uniform application surfaces for the New Leader - a) 56.0 kg/ha, b) 112.1 kg/ha, c) 224.2 kg/ha, and d) 336.2 kg/ha. ....	59
Figure 5.16. Uniform application surfaces for the Gandy - a) 56.0 kg/ha, b) 112.1 kg/ha, c) 224.2 kg/ha, and d) 336.2 kg/ha. ....	60
Figure 5.17. Uniform application surfaces for the AgChem – a) 112.1 kg/ha, b) 224.2 kg/ha, c) 336.2 kg/ha, and d) 448.3 kg/ha. ....	60

Figure 5.18. Simulated overlap distribution pattern for Newton Crouch.....	61
Figure 5.19. Simulated overlap distribution pattern for New Leader. ....	62
Figure 5.20. Simulated overlap distribution pattern for the Gandy. ....	62
Figure 5.21. Simulated overlap distribution pattern for the AgChem.....	63
Figure 5.22. The effect of swath spacing on the CV for the Newton Crouch applicator. ....	64
Figure 5.23. Standardized distribution patterns for the Newton Crouch. ....	66
Figure 5.24. Standardized distribution patterns for the New Leader. ....	67
Figure 5.25. Standardized distribution patterns for the Gandy. ....	67
Figure 5.26. Standardized distribution patterns for the AgChem. ....	67
Figure 5.27. Rate transition surfaces for the New Leader; a) 112 to 336 kg/ha and b) 336 to 112 kg/ha. .	70
Figure 5.28. Rate transition surface for the Gandy; 112 to 336 kg/ha and b) 336 to 112 kg/ha. ....	70
Figure 5.29. Rate transition surfaces for the AgChem; a) 112 to 336 kg/ha and b) 336 to 112 kg/ha.....	71
Figure 5.30. Example illustration for characterizing rate change dynamics (New Leader 0.0 m transverse position). ....	74
Figure 6.1. Application of offset and definition of transects. ....	84
Figure 6.2. Transect designation and delineation into equal length sections (New Leader example with 19 sub-polygons). ....	84
Figure 6.3. Resulting pattern polygon layer and grid overlay for specification of the “as-applied” surface. ....	85
Figure 6.4. The application prescription map, FAF, and validation points for field 11 (Applied using New Leader). ....	86
Figure 6.5. The application prescription map, FAF, and validation points for field 230 (Applied using New Leader). ....	87
Figure 6.6. The application prescription map, FAF, and validation points for field 12 (Applied using Gandy). ....	87
Figure 6.7. Rawson controller output versus the prescribed application rate. ....	89
Figure 6.8. Plot of predicted versus actual application rate: a) field 11 and b) field 8 (New Leader). ....	94
Figure 6.9. Plot of predicted versus actual application rate: a) field 10 and b) field 12 (Gandy). ....	94
Figure 6.10. “As-applied surface superimposed on the prescription map for field 10 (Gandy). ....	96
Figure 6.11. “As-applied surface superimposed on the prescription map for field 8: a) “as-applied” surface and prescription map only, and b) FAF included (New Leader). ....	97
Figure 6.12. “As-applied surface superimposed on the prescription map for field 11: a) “as-applied” surface and prescription map only, and b) FAF included (New Leader). ....	98
Figure 6.13. Difference between the “as-applied” surface and prescription map for field 10. ....	99
Figure 6.14. Difference between the “as-applied” surface and prescription map for field 8. ....	100
Figure 6.15. Difference between the “as-applied” surface and prescription map for field 11. ....	100
Figure 6.16. Plot of desired versus actual application rates for field 10. ....	102

Figure 6.17. Plot of desired versus actual application rates: a) field 11 and b) field 8 (New Leader)..... 103

## LIST OF FILES

jpgfult03.pdf.....4.7 MB

# CHAPTER ONE

## INTRODUCTION

### PREFACE

Farming remains one of the major businesses within the United States and even the World. As with any business, profitability drives decision making and competitiveness in a tight profit margin industry. The number of farms within the U.S. peaked in 1935 at nearly 7 million, but a dramatic decline occurred during the 1940's, 50's, and 60's, and has continued through the next millennium at a slower pace (USDA, 2003; fig. 1.1). As of 1997, approximately 1.9 million farms remain; however, the total farm acreage within the U.S. has not decreased at the same pace (USDA, 2003). These statistics indicate the remaining farmers are managing more acres. With this trend comes the fact that farmers or farm managers are now relying on hired help to perform much of the field work. Farm managers spend less time in the field than they once might have.

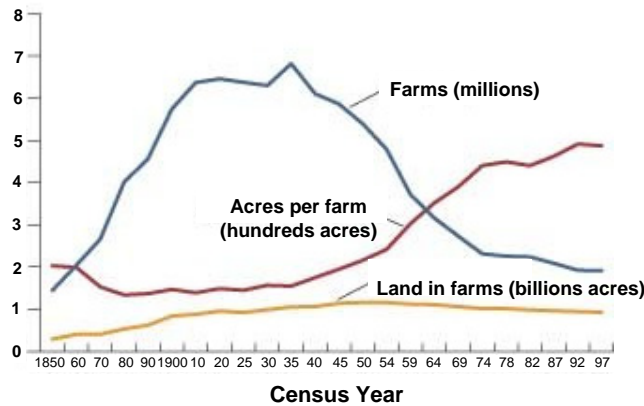


**Figure 1.1. U.S. farms, land in farms, and average acres per farm from 1850 to 1997 (source: compiled by ERS from Census of Agriculture data and reported by USDA)**

The population of the United States and World continues to increase rapidly. In 2000, the U.S. population was estimated at just over 251 million, but it is projected that the U.S. population will exceed 403 million by 2050 (U.S. Census Bureau, 2002), a 43% increase in just 50 years. With the U.S. population increasing, feeding the population and securing our future food resources will be at the hands of the American farmer. Can the American farmer become more efficient and possibly increase production to meet future food demands? The answer could rest on whether farmers can be provided with tools to make informed management decisions. Precision agriculture (PA) is a set of new tools that farmers adopted in mid 1990's to improve the profitability of crop production. Now, crop, fertility, and

soil spatial variability can be managed. More specifically, farmers can make site-specific management decisions and implement these decisions based on spatial variability and productivity potential.

The development of the Global Positioning System (GPS) by the Department of Defense (DoD) has facilitated the implementation of PA. GPS provides timely position fixes on the earth. Coupling GPS with sensors and other instruments permits spatial attributes to be collected by farmers. Yield monitors provide crop performance data via a grain mass-flow sensor mounted downstream of the cleaning shoe on agricultural combines. These data are tagged with GPS information for map generation. Sometimes yield variability can be explained while other times the exact cause is unknown. Additional spatial information such as grid soil sampling, digital soil maps, and soil electrical conductivity may provide clues to the potential cause of this variability.

Grid soil sampling provides a method to characterize fertility levels and pH within a field. Many farmers attempt to manage this variability using variable-rate technology (VRT). With VRT, inputs (fertilizers and lime) are applied in accordance with local soil fertility levels. VRT offers the potential for more effective utilization of inputs that would reduce costs and increase profits.

In theory, VRT provides benefits based on the assumption that when VRT is put into practice, it performs as expected. The performance of VRT equipment has not been well documented and most accept it as an accurate method for applying inputs. However, until the performance of VRT is known, it is difficult to draw conclusions about the economics and agronomics associated with VRT. Therefore, this dissertation presents a methodology to generate “as-applied” maps for assessing the accuracy of VRT application and to answer many of the questions surrounding the performance of VRT equipment.

## **JUSTIFICATION**

Site-specific management (SSM) and site-specific farming (SSF) are common terms used to describe PA. The concept of PA has been traced back to as early as 1929 when Linsley and Bauer (1929) built a framework to manage soil pH variability. Today, with computer technology, agriculture has moved into the information age, providing farmers with better information to manage operations. SSM adds the spatial dimension to crop diagnostics and input application recommendations, plus the automation of data collection expands the quantity of available spatial information while reducing the cost of it (Lowenberg-DeBoer and Swinton, 1997). Profitability will be a major outcome of PA (Lowenberg-DeBoer and Swinton, 1997) but profitability assessment behind SSM suggested by current literature only offers broad principles (Fairchild and Duffy, 1993) while not incorporating all economic factors. Further, it has been acknowledged that many economic studies on VRT of fertilizers, most showing VRT as non profitable, are inconclusive as a result of improper data collection along with procedural problems (Lowenberg-DeBoer and Swinton, 1997). The adoption of PA hinges on several key factors for farmers. These factors

include access to information about the technology, confidence in this information, and favorable outcomes resulting from this information (Lowenberg-DeBoer and Swinton, 1997). In part, a missing piece of information necessary to assess the economic value of SSM is the actual representation of inputs. The recognized spatial application rate must be reported back to the management system to analyze site-specific crop response and adjust future applications (van Bergeijk et al., 2001). The quantification of VRT application errors is not well developed for proper assessment of this technology.

Yule et al. (1996) reported that SSF allows for the application of economic optimum dressing in each part of the field. Allocation of inputs to fields is based on site-specific information. However, the assumption is that SSF can be correctly executed with existing technology and the resulting spatial data authenticates crop and field conditions. To capture some of the unexpected profits from PA technology and improve its performance, the operation of equipment must be precise (Mowitz, 2003). This requires that VRT equipment is in proper working order, be calibrated correctly, and perform as advertised. Questions regarding the accuracy of VRT continue to arise, but most have put VRT into practice expecting the advertised performance. The key to VR liming is accurate development of lime application maps, accurate application control, and sufficient crop response (Pierce and Warncke, 2000) to offset the additional costs of VRT. For fertilizer application, improvements to the basic spreader are the first priority for full utilization of modern technology on these machines (Möller and Svensson, 1991). Currently, standard methodologies do not exist for assessing VRT application accuracy. Therefore, a standard approach is needed to evaluate VRT performance.

The collection of accurate spatial data such as yield, fertility, and “as-applied” maps leads to forming customized crop input application recommendations. A disconnection currently exists between regional-scale recommendations and the spatial data being collected using modern technologies (Lowenberg-DeBoer and Swinton, 1997). The development of site-specific crop response relationships can lead to site-specific recommendations to optimize input use efficiency thereby boosting the farmer’s bottom line. The potential profitability of variable-rate (VR) fertilization has not been realized (Lowenberg-DeBoer and Swinton, 1997). Spatially tailored input applications add value to site-specific information (Bullock et al., 2002). A major piece of missing information from today’s PA spatial data sets is the actual distribution of material during field application. As with any scientific study, unless it is known what actually happens or how it happens, the activity of interest cannot be evaluated. Thus, to formulate site-specific crop response relationships, actual portrayal of field application of inputs is required.



## **OBJECTIVES**

The overall goal of this research was to develop and validate a methodology to post-process field application files (FAF) to create “as-applied” maps for assessing VR application. The specific research objectives are:

- To characterize the distribution patterns of uniform- and variable-rate granular application equipment,
- To develop a spatial model for generating “as-applied” surfaces using logged field data and the distribution characterization patterns, and
- To validate the “as-applied” model through the collection and analysis of field data.

## **ORGANIZATION OF DISSERTATION**

The presentation of this research is in manuscript format, indicating particular chapters represent separate manuscripts, each covering a distinct aspect of this research. The research and results (contained in Chapters Three through Six) cover the development of methodologies to characterize distribution patterns from granular VRT applicators and then using this information along with FAFs to generate “as-applied” surfaces. A method for characterizing and modeling distribution patterns and rate changes from a VR spinner spreader is provided in Chapter Three. Chapter Four describes the development and initial validation of the spatial data model to create “as-applied” surfaces. Chapter Five compares four different VR granular applicators to identify potential errors associated with VRT granular applicators while characterizing the distribution patterns from these applicators for use in the “as-applied” spatial model. Modifications and validation of the “as-applied” spatial data model are presented in Chapter Six.

Chapter One and Seven include introductory and concluding remarks to the research, respectively. Chapter One provides an introduction to this research followed by the motivation behind it and overall objectives. Chapter Seven provides the conclusions and suggestions for future work. To reduce redundancy within the dissertation, a single, comprehensive literature review is presented in Chapter Two to overview previous work and relevant background information. A single reference section and Appendices are placed at the end of the dissertation.

## CHAPTER TWO

### REVIEW OF LITERATURE

Precision agriculture (PA) allows farmers to manage fields on a much finer resolution when compared with the traditional "whole field" basis. Many believe that the use of PA practices allows for better nutrient management by applying only what is required for crop growth thereby providing agronomic, economic and environmental advantages over the traditional approach: blanket application. Implementation of PA usually consists of breaking a field into smaller units called management zones. Doerge (1999) defined a management zone as a sub-region of a field expressing homogeneous combination of yield limiting factors for which a single rate of a specific crop input is suitable. While VRT has become an accepted method in the agricultural community for spatially varying inputs, elimination of application errors through proper calibration and operation is critical to ensure accurate VRT performance. With VRT equipment, more complexity is introduced with rate changes during application requiring a new level of knowledge and skill to utilize this technology. Those implementing PA technologies have had trouble with the lack of available technical information and training programs to assemble and utilize PA systems (Leer, 2003).

ASAE standard S341.2, Procedure for Measuring Distribution Uniformity and Calibrating Granular Broadcast Spreaders (ASAE Standards, 2000), provides a uniform procedure for testing, assessing the performance, and reporting the test results of broadcast spreaders. The standard outlines a methodology by which to assess the distribution pattern of a broadcast spreader using a 1-D row of pans. Specifications for test setup, collection devices, test procedures, effective swath width, and specification of testing application rate, and other protocol are clearly defined in this standard. While the standard addresses uniform-rate (UR) application, it does not include considerations for testing VRT equipment. To date, no standard or defined test protocol has been published to evaluate VRT. One concern is actually what should be tested to quantify application accuracy of VRT; individual components making up a VR system or a VR system as a whole unit. More importantly, very few VRT equipment manufacturers provide sufficient control of the application rate for VR fertilization (Cointault et al., 2003) and future research is required to understand the effects of various sources of VRT errors (Schueller and Wang, 1994). Thus, standard test and reporting procedures are needed to assess VRT equipment.

Chaplin et al. (1995) investigated the distribution of granular material application in the field. They described a methodology based on ASAE standard S341.2 (ASAE Standards, 1997) and performed tests for a single-disk mounted fertilizer spreader. Fulton et al. (2001) modified ASAE S341.2 to include a 2-D

array of collection pans to assess VR application of granular products to assist in testing VRT granular applicators. The 2-D matrix of pans permitted the characterization of distribution patterns along with the ability to capture distribution patterns during rate changes. Capturing rate changes within the test matrix also allowed for quantification of system latency for VRT equipment. Molin et al. (2002) derived a method using pans to determine the time for rate changes of a VR fertilizer spreader to occur. Pans were placed on either side of the spreader's centerline path at 25% of the effective swath width. These two longitudinal rows of pans were used to collect material during prescribed rate changes.

The coefficient of variation (CV) provides a means to quantify application variability and accuracy. ASAE S341.2 requires CVs to be reported when testing applicators while manufacturers and custom applicators have adopted CV calculations as an acceptable approach to quantifying application accuracy. Lower CVs indicate uniform distribution patterns. Spinner spreaders tend to exhibit CVs varying from 5% to 10%; however, terrain irregularities can greatly increase CVs to the upper 20's or lower 30's (Parish, 1991). Sogaard and Kierkegaard (1994) reported that CVs in the range of 15% to 20% are typical of field tests for spinner spreaders.

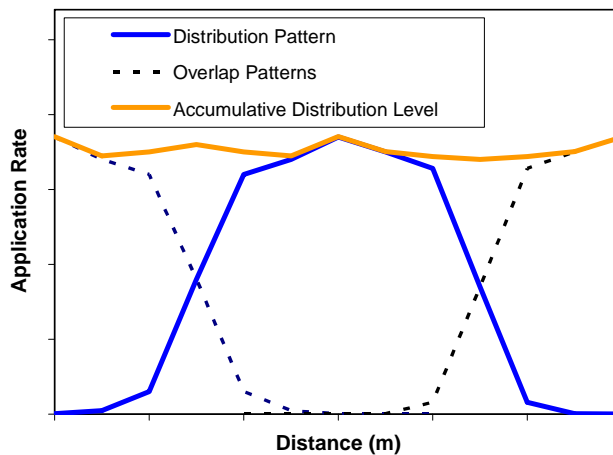


**Figure 2.1. Example cumulative distribution pattern from adjacent overlap passes.**

Spinner disc spreaders rely on distribution pattern overlap to achieve application requiring a wider testing width than the effective spread width (fig. 2.1). Over- and under-lap on parallel passes creates application errors. Marchenko and Chernikov (1977) determined varying swath width for spreaders under normal operation, which creates potential application errors by not maintaining the correct pass-to-pass distance. Dorr and Pannel (1992) reported that 10% of a field had either over- or under-lapping patterns. Thus, consistency at the proper pass-to-pass distance is important. Similarly, vehicle speed (Parish and Chaney, 1986; Parish, 1987) and rough terrain (Parish, 1991) affect the performance of a spinner spreader. Parish (1991) showed that the CV increased from 10% to 30% when moving from operating on

a smooth to a rough surface. Pettersen et al. (1991) investigated how the distribution pattern of a twin-disc spreader was influenced by fertilizer particle size. Their results showed that different particle sizes produce varying spatial distributions. They provided a detailed test method for collecting fertilizer samples and used interpolation techniques to generate continuous distribution patterns. Thus, several factors influence application quality of spinner spreaders under traditional UR application but provide no indication about how VRT might introduce additional errors for granular applicators.

Variable-rate technology adds another dimension to granular fertilizer application. Instead of the applicator rate remaining at a fixed value during field operation, a dynamic response of the system is required to achieve VR application. Applicator dynamics have an important effect on VRT applicator performance (Schueller and Wang, 1994). A complement of components, such as a GPS receiver, computer, VR software, and VR controller are integrated to make VRT work. Each component produces some level of error which is then translated into an overall VRT system error. The overall error can be a summation of individual component errors understanding that interaction effects can exist. The addition of VRT components may require unique calibration procedures and operation of equipment to minimize application errors when contrasted with traditional practices. Most work on VRT has been directed towards hardware and software development, and the implementation of these VR systems. Research has lagged behind assessing the application accuracy of these systems and identifying potential sources of errors. Concerns have been articulated about accuracy with VR application of pesticides and fertilizers when using application maps (Goense, 1997).

Research suggests that dynamic weighing of the fertilizer spreader to automatically calibrate the flow control device during fertilizer application (van Bergeijk et al., 2001) is needed to maintain proper deposition of granular material from a VRT system. However, accurate metering is independent of accurate distribution of material from an applicator. The resulting mass flow must be correctly distributed for site-specific application of fertilizers (van Bergeijk et al., 2001). An optical sensor (Grift and Hofstee, 2002) or imaging system (Cointault et al., 2003) could be used to predict where fertilizer particles land and provide continuous assessment of material distribution during field application. Asymmetrical irregularities in distribution patterns can occur (Roth et al., 1985). Thus, real-time distribution pattern assessment and material deposition would provide feedback tools for maintaining uniform application of VRT granular applicators. Cointault et al. (2003) cited that accurate spatial fertilizer application requires control of the instantaneous fertilizer flow and distribution. Currently, no commercially available spreaders possess both of these features.

Quantifying the VRT system latency or delay time allows the “look-ahead” feature provided in most software packages to be properly set assuming similar system response for increasing and decreasing rate changes. Schueller (1989) described liquid fertilizer mixing and flow control to minimize material

transport lag times. He concluded that rate and mixture variations are improved by: (1) controlling flow to each system component, (2) decreasing the response times of the pumps and valves involved, (3) minimizing the volume of connecting hoses, (4) adequate mixing, and (5) mixing as close as possible to the nozzles. It was also found that varying the pump speed or re-circulation flows were viable options for flow control. The key feature noted is the existence of lag or delay time of the whole system. For liquid application, transport lag of a VRT injector ranged from 15 to 55 seconds indicating that the lag time varies across the boom for each nozzle (Anglund and Ayers, 2003). These delay times produce application errors by having the rate transition occur after or before the desired time. Considerable improvement in VRT performance can be made with command feed forward control (Schueller and Wang, 1994). Errors are also introduced in distribution patterns with the existence of substantial lag times at different nozzles or application points across the spread width.

Molin et al. (2002) reported the response time of a VR fertilizer spinner spreader was 3.1 seconds for an increasing step rate change and 5.6 seconds for the decreasing step change. The VR spreader also applied less than the desired rate during these tests up to -27% in one case. A detailed description of calibration was not provided. These results indicate that different “look-ahead” times are required to properly adjust rate changes to the desired location in time. Currently available software designed for VR control only permits one “look-ahead” time to be set. Another concern was the under-application of material during the VR tests which could indicate that different calibration procedures are needed for VRT applicators to maintain the desired spread quantity.

Reichenberger and Russnogle (1989) described a system that simplifies precision fertilizer application. The system utilized a laptop computer and a fifth wheel to determine location. An application rate map was stored in the computer's memory, and machine application rates were controlled with feedback from the fifth wheel. The unit was reported to be ready for modifications that would allow application of liquid fertilizer, chemical injection, planting, and the development of yield maps. While the fifth wheel provided feedback for position information, feedback about the actual application rate was needed to ensure this system applies the prescribed amount.

Olieslagers et al. (1996) described the fertilizer distribution of a spinning disc spreader. Many parameters, including orifice position and angular speed of the discs, affect the distribution pattern of disc spreaders. VRT application, accomplished by changing the mass deposition rate on spinner discs, leads to a fluctuating spreader pattern, which results in large deviations from intended application rates. Olieslagers et al. (1997) suggested that continuous change in various spreader adjustments might be needed to maintain a uniform distribution pattern when changing rates on the go. They also stated that future work should be concentrated on the particle dynamics of granular materials and resulting distribution pattern when varying material deposition rates on the go.

Research has suggested that adjusting ground speed (not the mass flow) is desirable to regulate the required rate while the rotational speed of the disc remains constant with its velocity independent of driving speed (Hofstee, 1995). Most, if not all, VRT systems adjust the mass flow of material rather than the operator continuously vary the ground speed. Varying mass flow is preferred since speed adjustments is controlled solely by the operator while generating a tedious task for a driver and accelerating driver fatigue. However, automated guidance provides a solution for controlling ground speed in order to reduce application errors that exist when varying mass flow. Future research could help address whether it would be desirable to control ground speed, mass flow, or both simultaneously to minimize VRT application errors. This research might suggest that prescribed ground speeds be generated along with the application rates for VRT application.

Fulton et al. (2001) demonstrated distribution variability at different rates from a spinner spreader by performing fixed and VR application of murate of potash. They cited that distribution variability could compound application errors when moving to VR application with spinner spreaders. Additionally, pattern shifts during rate changes (Fulton et al., 2001; Olieslagers et al., 1997) plus the existence of system latency (Fulton et al., 2001) causing delayed rate changes creates other sources of application errors for VRT equipment. The problem with pattern shifts is not as easily rectified but needs to be addressed to maintain distribution uniformity at various application rates. Potential solutions involve modification of the spreader hardware (i.e. adjustment of divider position simultaneously with apron chain speed adjustments), or other technology such as continuously adjustable spinner fins to maintain the desired distribution pattern.

Research on VRT has shown mixed results about yield and economic advantages. Variable-rate nitrogen (N), phosphorous (P), and potassium (K) have increased crop yield and/or decreased fertilizer quantities for potatoes (*Solanum tuberosum* L.) (Cambouris et al., 1999) and irrigated sorghum (*Sorghum bicolor* L. Moench) (Yang et al., 1999). Varying the rates of N, P, and K demonstrated no substantial yield increase (Carr et al., 1991) or economic gain (Wibawa et al., 1993) over UR application. In areas of low soil-test P, VR at times reduced the overall amount of P applied but seldom increased corn (*Zea mays* L.) or soybean (*Glycine Max* L. Merr.) yields (Mallarino, 1999). Net returns were not consistently increased in wheat, corn, and soybeans even though P and K were redistributed within fields using VRT (Lowenberg-Deboer and Aghib, 1999). Modeling of VR lime determined potential for economic gains in corn and soybeans (Bongiovanni and Lowenberg-Deboer, 2000). However, no increase in crop yield was observed with VR lime and P (Weisz et al., 2003). Swinton and Lowenberg-Deboer (1998) reported VR was profitable in high value crops such as sugar beets, sometimes profitable in corn, but never profitable for low value crops such as wheat with the cost of grid soil sampling being the main profit limitation of VR.

One of the driving forces behind PA is the potential positive environmental impact it could provide. VRT has the ability to minimize over-application of inputs thereby reducing runoff of chemicals and fertilizer into water sources. Lowenberg-DeBoer and Swinton (1997) stated that the three forces bringing PA to North America are technology, competition, and environmental concerns and public policies. These researchers stated that incorporation of environmental impacts into SSM management algorithms is needed. However, the profitability of SSM technology is site-specific and therefore will be determined on a farm-by-farm or field-by-field basis. The economic value of PA based on environmental impact is difficult to assess. Some studies have found VR nitrogen application to be better than UR application for both water quality and profitability (English et al., 1999; Thrikawala et al., 1999; Babcock and Pautsch, 1998; Schnitkey et al., 1996). On the other hand, some research has demonstrated little or no benefits of VR application in water quality or profitability (Watkins et al., 1998; Qui and Prato, 1999). And in some cases, VRT might improve water quality without generating higher profits when compared with UR application (Wang et al., 2003).

The purest form of PA will be attained when site-specific yield response and production functions are defined. These will provide true spatial management of inputs and provide direction for making informed decisions. A field has potentially spatially dependent production functions (Yule et al., 1996) which is indicative of the complexity of yield limiting factors. However, spatial quantification of the actual distribution of inputs will be required to close the loop for the development of site-specific response relationships. Yield maps quantify spatial crop performance while spatial fertility maps provide the nutrient levels within the soil. Errors in the representation of spatial data exist for yield monitoring (Arslan and Clovin, 1998; Bashford et al., 1995; Jasa et al., 2000; Kettle and Peterson, 1998; Strubbe et al., 1996) and fertility maps (Mueller et al., 2001). However, with future technological advances, yield and fertility map accuracy should improve. Generation of accurate “as-applied” maps remain an impediment to defining spatial response relationships. The actual distribution of material is a pre-requisite to site-specific crop response analyses and for making future application adjustments (J. van Bergeijk et al., 2001). Several years of yield, fertility, and application data will be required to draw meaningful inferences relative to customized production functions. PA is providing the tools to facilitate on-farm investigators develop such production functions.

## **CHAPTER THREE**

# **PERFORMANCE ASSESSMENT AND MODEL DEVELOPMENT OF A VARIABLE-RATE, SPINNER-DISC FERTILIZER APPLICATOR**

### **INTRODUCTION**

Current commodity prices and pressure from environmental regulations are causing the production agricultural sector to seek more competitive methods of producing food and fiber products. With the development of the global positioning system (GPS) and variable-rate technology (VRT), precision agriculture (PA) is now becoming a common practice on many U.S. farms. GPS and VRT have the potential to improve productivity and profitability while conserving and protecting our natural resource base.

Traditional methods of fertilizer and chemical application tend to treat all areas of a field the same, regardless of variability in soil and landscape features. With the traditional approach, soil cores are pulled at random throughout a field and mixed into a single composite sample. These samples are then analyzed to compute fertility recommendations for nutrient application levels. Depending on the soil tests, nutrients (phosphorus, potash, and nitrogen) or agricultural lime are then applied in broadcast or banded fashion to the entire field. Prior to PA, the variability within many fields was accepted as a factor that producers could do little to correct. In fact, this variability was quantified and used as justification for modifying recommended fertilizer applications rates to insure crop yields are not limited.

Searcy (1995) defined Site-Specific Crop Management as "the use of local soil and crop parameters to make precise application of production inputs to small areas with similar characteristics." Spatial variability occurs with respect to many parameters (soil type, fertility, topsoil depth, and slope) that affect crop production. Therefore, the potential exists to vary production inputs (fertilizer, seed, and chemicals) as a function of field location.

Linsley and Bauer (1929) outlined a practice to intensively sample and map soil pH variation for determining areas for lime application at various levels. This demonstration predates today's efforts, in which technology makes site-specific management (SSM) a reality. Concerns still exist with regard to whether SSM is profitable when compared with traditional field-average application practices. Application uniformity and accuracy are important elements of this assessment. Therefore, tests were conducted to assess and characterize distribution pattern variability of a spinner disc spreader, and then mathematically model uniform-rate (UR) and variable-rate (VR) application of granular materials. Such a



model can then be used to predict overall application efficiency and estimate the deviation from the desired distribution patterns. This approach can also be used to investigate and specify appropriate management grid resolution for PA practices based on equipment limitations.

## **SUB-OBJECTIVES**

The purpose of this investigation was to characterize and model the distribution of granular material from a VRT applicator. Specific objectives were:

- To conduct UR and VR distribution tests to characterize the discharge pattern of a spinner-disc VR fertilizer applicator, and
- To model VR application of murate of potash (KCl) fertilizer.

## **OVERVIEW OF APPLICATOR**

The Biosystems and Agricultural Engineering Department at the University of Kentucky maintains a custom-built VR fertilizer applicator, modeled after a Newton Crouch (Model 54) spreader that uses two spinner discs to apply granular products. Granular material was supplied to the twin spinners using a traditional apron chain. A Gerotor motor (Model DT9906223DZ1) was used to power the apron chain drive. Flow to this motor was controlled using a Source Fluid Power motorized control valve along with additional pressure-compensated valves (Model MFC16-20-12V-7) to control the fluid bypassed for speed control. The truck was equipped with a Midwest Technologies, Inc., TASC 6200 controller to vary the speed of the apron chain, thereby controlling the rate of material deposition on the spinners.

The TASC 6200 was interfaced to a laptop computer through an RS-232 serial data link. The apron chain drive motor was equipped with a magnetic speed sensor as part of the feedback control for the system. An Omnistar 7000 1-Hz receiver with C-band differential correction was mounted on top of the truck and linked to the laptop via a second RS-232 serial port. Agris's FieldLink, software version 2.15, was used to acquire GPS positioning information and communicate the requisite application rate to the TASC 6200 controller. FieldLink was used to record the test site boundary and establish a rate change line or two polygons for testing rate changes from low to high or high to low.

## **METHODOLOGY**

Field tests were conducted at the Animal Research Center located in Woodford County, Kentucky to evaluate the VR spinner disc spreader while applying granular murate of potash (KCl) fertilizer. Application rate, distribution, and the effect of rate changes via DGPS were evaluated by modifying ASAE standard S341.2 to include a two-dimensional array of collection pans. Test cases investigated

included: (1) UR application at a low rate, (2) UR application at a high rate, (3) VR application from a low to high rate, and (4) VR application from a high to low rate. Single-pass tests were performed for each of these cases to assess application accuracy and characterize rate changes. Additionally, the effect of overlap on spread uniformity was evaluated by performing multiple parallel passes for only the high and low fixed fertilizer applications rates. Therefore, a total of six tests were performed.

Tests were conducted *in situ* at UR and VR to assess the application accuracy. All field tests were conducted on days when sustained wind speeds were less than 8.0 km/hr at a height of 1.5 m above the ground, and the slope of the test site was less than 2% (*ASAE Standards*, 1997). All tests were run with the hopper filled to approximately 40% to 50% capacity, as defined by ASAE standard S341.2.

ASAE standard S341.2 was followed to fabricate aluminum collection pans for testing the spreader. The pans measured 40.6 cm wide, 50.8 cm long, and 10.2 cm in height. An aluminum divider with a 10.2 cm × 10.2 cm grid and 5.1 cm height was also fabricated to place inside each tray to minimize material movement out of the tray. Pans were placed uniformly in a two-dimensional array for collection of discharged granular materials for both single and multiple passes. The size of the array normal to the direction of travel included 13 collection pans, spaced evenly across the anticipated distribution width. Parallel to the axis of travel, there were 13 evenly spaced rows of collection trays. Figures 3.1 and 3.2 show the two different pan arrays used for testing the applicator. Spacing in the direction of travel was determined as a function of controller response and applicator ground speed to ensure that complete rate change patterns were captured. The narrow array spacing of the multiple-pass tests required the omission of two longitudinal rows of trays to allow room for the wheels of the spinner spreader truck within the collection matrix (fig. 3.2).

Many factors directly affect fertilizer distribution and application accuracy, such as systematic errors associated with machine calibration and metering efficiency. To minimize the combined effect of these factors and achieve accurate fertilizer distribution, the spreader truck was calibrated prior to performing the tests. The best distribution was achieved by adjusting the position of the rear divider until a uniform Gaussian transverse distribution was achieved for an average application rate of potash (fig. 3.3). A one-dimensional array of 13 pans was used during this process. Spinner speeds were set at 550 rpm, with the gate opening positioned at 4.4 cm above the floor of the bed. The truck was operated in second gear and at 1800 rpm, which resulted in a ground speed of 20.4 km/hr for all tests.

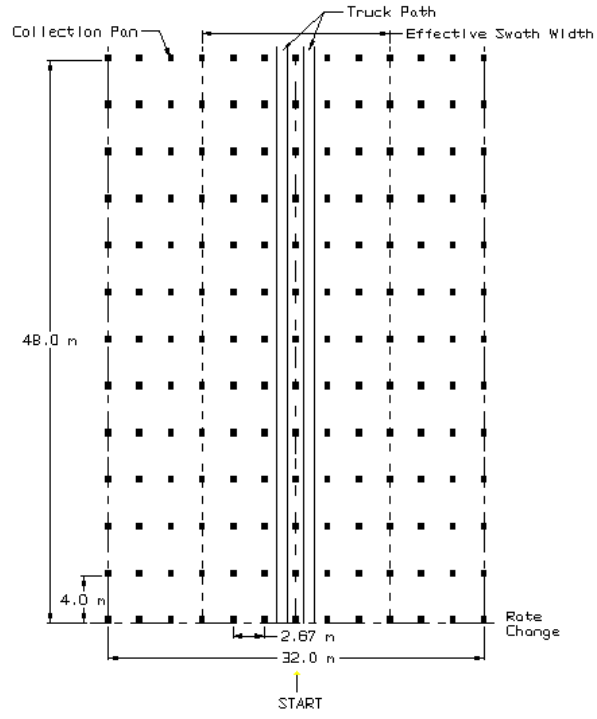


**Figure 3.1. Collection pan matrix for the single-pass tests.**

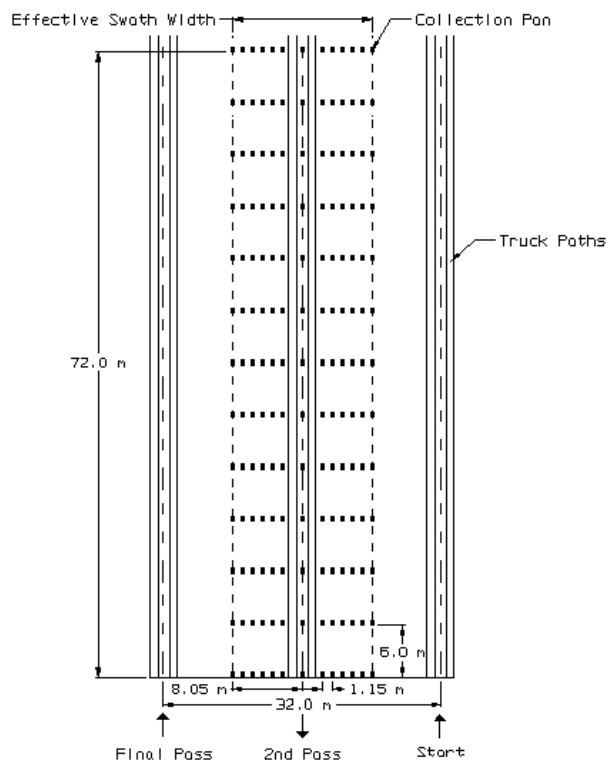


**Figure 3.2. Collection pan matrix for the multiple-pass tests.**

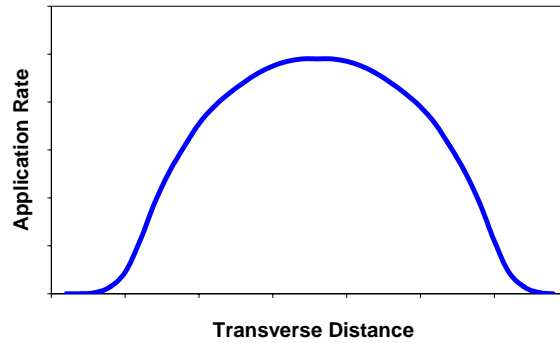


**Figure 3.3. Theoretical Gaussian distribution pattern.**

Test application rates were made at 25% and 75% (*ASAE Standards*, 1997) of the maximum application rate, as recommended by the University of Kentucky's Lime and Fertilizer Recommendations for murate of potash (AGR-1, 1998). AGR-1 recommends a maximum application of 134 kg/ha of potash ( $K_2O$ ) for corn production. Murate of potash ( $KCl$ ) is 60%  $K_2O$  (0-0-60), and therefore an application rate of 56.0 kg/ha was selected for the low rate and 168.1 kg/ha was selected for the high rate. For these particular tests, the potash used had a density of  $1041 \text{ kg/m}^3$  and moisture content less than 1% (wet basis).

The center of each swath was flagged so that the driver had a visual guide when traversing the test site. Potash was collected within the swath width of the spreader using the collection trays. Collection pan contents were collected, bagged, and labeled for each of the field tests. All samples were then weighed and recorded to the nearest hundredth of a gram. Surface plots were generated in Surfer Version 6.04 (Surfer, 1996) for a visual verification of data collection.

## **RESULTS AND DISCUSSION**

Figures 3.4 and 3.5 present the UR single application surfaces for the 56.0 and 168.1 kg/ha application rates. The 56.0 kg/ha application surface appears somewhat uniform with minimal irregularities. Distribution irregularities can be attributed to particle dynamics and shearing of the material mass at the apron chain-spinner interface. Figures 3.4 and 3.5 illustrate evidence of application irregularities when looking at longitudinal cross-sections. The surface plot in figure 3.4 hints that an M-shaped pattern (less material than desired at the center of the pattern) is occurring. In fact, the plot of the mean transverse application rate for the uniform 56.0 kg/ha, presented in figure 3.6, shows a slight decrease in material at the center of the pattern. For the most part, the spreader does an acceptable application job at the low rate.

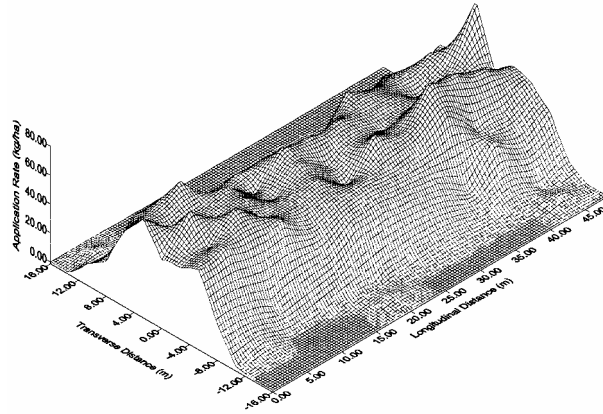


Figure 3.4. Actual uniform 56.0 kg/ha application surface.

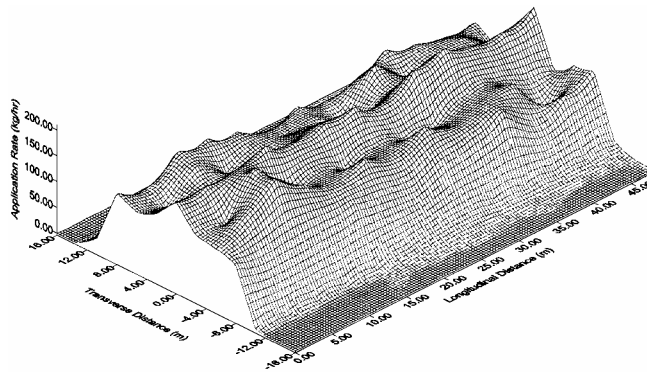


Figure 3.5. Actual uniform 168.1 kg/ha application surface.

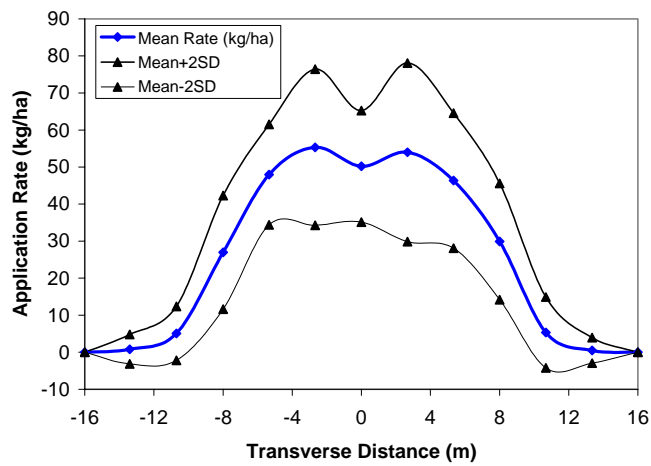
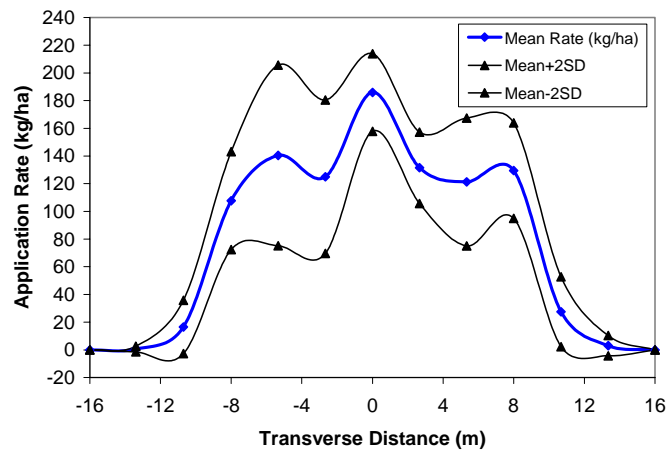


Figure 3.6. Mean distribution pattern for uniform 56.0 kg/ha application rate.

Figure 3.5 shows similar irregularities as figure 3.4 and the resulting pattern shift from the desired Gaussian pattern. The W-shaped pattern results when more material is applied at the pattern's center than on either side of the center. Figure 3.7 is a plot of the mean transverse application pattern and

demonstrates this W-shaped pattern. Both the high and low rate tests were performed with identical truck settings. The shift in pattern is consistent with the conclusions of Olieslagers et al. (1997) that concurrent changes in the spreader settings (divider position, spinner speed, adjustable fins, etc.) are needed to maintain a Gaussian distribution. One note, figures 3.6 and 3.7 present negative application rates when plotting the two, standard deviations which is not possible but illustrated to depict the variability in the mean application pattern.



**Figure 3.7. Mean distribution pattern for uniform 168.1 kg/ha application rate.**

The mean transverse distribution application patterns for the 56.0 and 168.1 kg/ha uniform single passes are presented in table 3.1 along with standard deviations and coefficients of variation (CV). The CV is low at the center of the pattern and increases towards the edges. This increase can be attributed to the small amount of material collected in the outside pans. Typically, these pans accumulate few particles, so an additional particle or two results in higher CVs. This explains the high CV in the low-rate tests in comparison to the high-rate tests. Looking at only the center seven pans (representing the effective swath width), the CVs appears acceptable, with the majority of the CVs for each test around 20%. The test area was a hay field with some topographic relief. Sogaard and Kierkegaard (1994) stated that the CV would definitely increase under actual field tests from the desired 5-10% to 15-20%.

The mean transverse application rates for the UR low and high tests were used to model the application of both and are presented in figures 3.8 and 3.9. The strength of the relationship for uniform rates will be discussed later.

The uniform application test plots for multiple passes are presented in figures 3.10 and 3.11. These surfaces show a wide variation in application distribution, with the center and outer pans receiving more material than the others. Table 3.2 summarizes the target application rate along with the statistical parameters for each test. The actual application rate is slightly larger than the desired rate. Both tests show a range in application rates with a coefficient of variation of 21% for the 56.0 kg/ha rate test and

20% for the 168.1 kg/ha rate test. While the spreader is applying at or near the target rate, the quality of distribution is less than desirable but typical for spinner spreaders.

**Table 3.1. Average transverse distribution pattern statistical results for single-pass tests.**

Test	Transverse position (m)	Mean application rate (kg/ha)	Standard deviation (kg/ha)	CV (%)
56.0 kg/ha	16	0	0	0
	13.35	0.5	1.7	360.6
	10.68	5.4	4.8	89.4
	8	29.9	7.8	26.2
	5.34	46.3	9.1	19.7
	2.67	54.0	12.0	22.3
	0	50.2	7.5	15.0
	-2.67	55.3	10.5	19.0
	-5.34	48.0	6.8	14.1
	-8	27.0	7.7	28.4
	-10.68	5.1	3.7	71.9
	-13.35	0.8	2.0	245.3
	-16	0	0	0
168.1 kg/ha	16	0	0	0
	13.35	3.1	3.7	119.9
	10.68	27.5	12.6	45.9
	8	129.4	17.2	13.3
	5.34	121.3	23.1	19.0
	2.67	131.5	12.9	9.8
	0	185.9	14.0	7.5
	-2.67	125.0	27.7	22.1
	-5.34	140.4	32.6	23.2
	-8	107.7	17.7	16.4
	-10.68	16.5	9.6	58.3
	-13.35	0.6	1.0	160.4
	-16	0	0	0

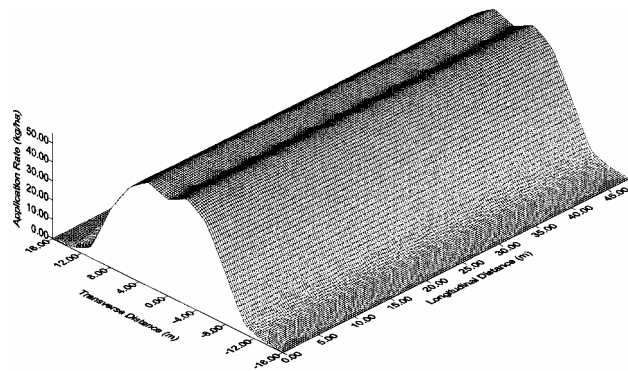


**Figure 3.8. Modeled 56.0 kg/ha application surface.**

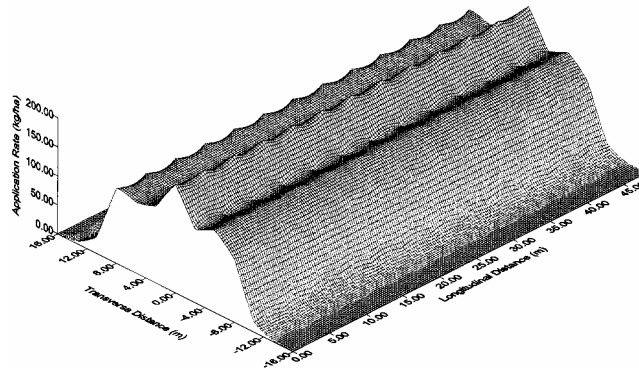


**Figure 3.9. Modeled 168.1 kg/ha application surface.**

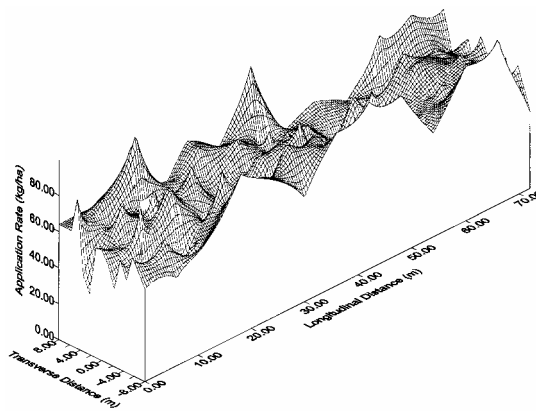


**Figure 3.10. Actual UR application surface for the 56.0 kg/ha multiple-pass test.**

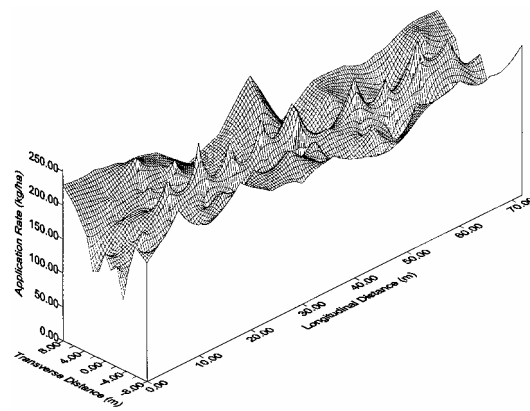


**Figure 3.11. Actual UR application surface for the 168.1 kg/ha multiple-pass test.**



**Table 3.2. Desired uniform application rate along with statistical information for actual applied rate for multiple-pass tests.**

Desired rate (kg/ha)	% Difference	Actual applied rate				
		Mean (kg/ha)	Min. (kg/ha)	Max. (kg/ha)	Std dev. (kg/ha)	CV (%)
56.0	10.9	62.1	30.5	99.7	13.2	21.3
168.1	2.7	172.7	86.2	253.7	34.6	20.0

Figures 3.12 and 3.13 present the application surfaces for rate changes from 56.0 kg/ha to 168.1 kg/ha and from 168.1 to 56.0 kg/ha, respectively. The zero longitudinal distance denotes the desired transition in the rate change. For these particular tests, the look-ahead time in the FieldLink control software was set at zero so that the system latency could be characterized using the test-pan data.

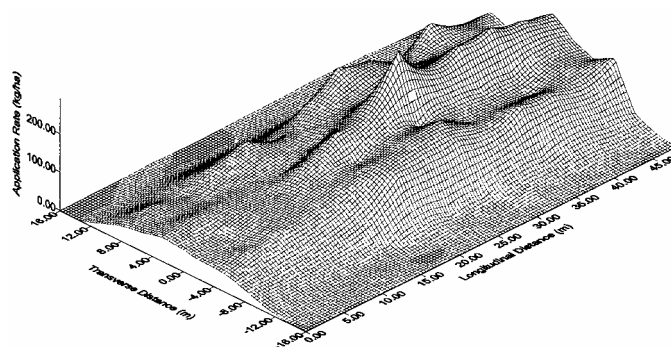


**Figure 3.12. Rate change application surface for the VRT spinner spreader truck (change from 56.0 to 168.1 kg/ha).**

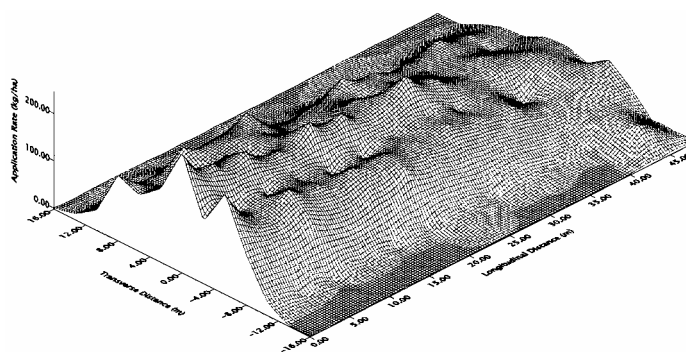


**Figure 3.13. Rate change application surface for the VRT spinner spreader truck (change from 168.1 to 56.0 kg/ha).**

The rate change surface for an application rate-change from 56.0 to 168.1 kg/ha (fig. 3.12) demonstrates what was seen in the uniform tests. The spreader does a good job of distributing potash at 56.0 kg/ha, but as the rate change occurs, the pattern shifts from Gaussian to W-shaped. The same type of

pattern shift occurred when adjusting the rate from 168.1 to 56.0 kg/ha but in reverse (fig. 3.13). The results portrayed in both of these figures provide insight into problems, such as the time required to make rate changes and the presence pattern shifts, of VR application with disc spinner spreader. Additionally, the rate change characteristics were different in each of these tests. The difference in the rate change from high to low and low to high was probably due to the characteristics of the controller.

The next step was to model the VR application process shown in figures 3.12 and 3.13. Symmetry with respect to the center of the pattern was assumed for transverse distribution. Correspondingly, equidistant longitudinal rows from the center pans were averaged to create seven longitudinal data sets to represent the rate change dynamics. The center row was used as is and not averaged with any of the other rows. Pans in the last longitudinal row collected little or no material and were set to zero application rate for both tests. Only nine of the 52 outside collection pans in both of the rate change tests contained any material. An important facet for modeling the application rate change was to utilize the same regression function on each particular test to simplify the process.

Sigma Plot 4.0 (Sigma Plot, 1997) was used to fit a sigmoidal curve to each of the data sets for the rate change from 56.0 to 168.1 kg/ha. The basic function used was:

$$\hat{y} = y_o + \frac{a}{1 + e^{\left(\frac{x_o - x}{b}\right)}} \quad (1)$$

where

- $\hat{y}$  = predicted application rate
- $y_o$  = minimum predicted application rate
- $a$  = range of the predicted application rate
- $x$  = longitudinal position
- $x_o$  and  $b$  = constants calibrated based on the  $x$  values.

Figure 3.14 shows the results of fitting the rate change dynamics to the average of the  $\pm 2.67$  m data points along with the 95% regression confidence interval for the initial sigmoidal function using the original parameters in table 3.3. The curve has an  $R^2$  of 0.98, suggesting a good model fit. Table 3.3 presents the results for all six data sets along with the equation coefficients and  $R^2$  values. Zero application rate values in the average data, representing the transverse pan position  $\pm 13.35$ , were set equal to 0.01 so that Sigma Plot could perform the analysis. The  $\pm 13.35$  transverse position data resulted in a less than desirable fit ( $R^2$  of 0.64). Similar to the outside pans, these pans collected very few particles and an addition of one or two potash granules produced more variation from pan to pan, unlike those pans located nearer the center of distribution which receive more potash.

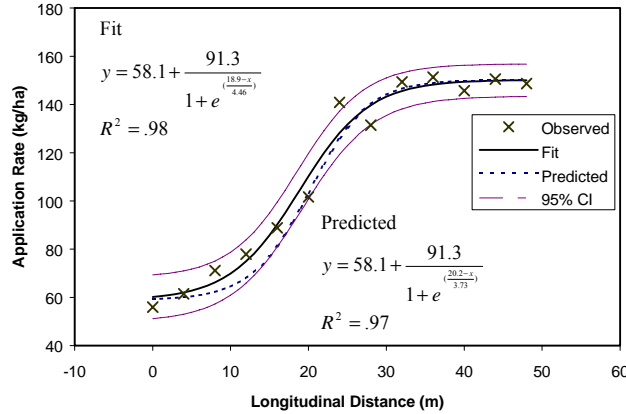


**Figure 3.14. Example application rate change dynamics for 56.0 to 168.1 kg/ha (longitudinal application rates averaged for transverse distance 2.67 and -2.67 m).**

**Table 3.3. Input parameters for each sigmoidal line fit according to distance from center transverse position.**

Parameter	Transverse pan position (m)							Constants
	0	2.67	5.34	8.0	10.68	13.35	16.0	
<i>a</i>	167.54	91.31	78.85	102.94	41.55	5.44	-	
<i>b</i>	2.95	4.46	3.09	3.81	8.0	0.06	-	3.73
<i>x<sub>o</sub></i>	18.15	18.89	14.76	16.86	30.81	21.73	-	20.2
<i>y<sub>o</sub></i>	58.06	58.90	52.90	34.67	15.19	1.37	-	
<i>R<sup>2</sup></i>	0.88	0.98	0.89	0.94	0.92	0.64	-	

Constants were calculated for parameters *b* and *x<sub>o</sub>* by averaging these parameters, since these values were fairly consistent, thereby simplifying the family of equations. Figure 3.14 presents the new simplified function and is labeled "predicted." The new function differs slightly but is contained within the 95% regression confidence interval and has an *R<sup>2</sup>* value of 0.97. The simplified equations for each of the data sets do a good job of predicting the "actual" application rate. Each equation was then applied to the six longitudinal rows to calculate a predicted application rate for each pan.

The same procedure was employed to model the rate change from 168.1 to 56.0 kg/ha. However, a simple linear model was used to describe the rate change as opposed to the sigmoidal function. Figure 3.15 presents the rate change dynamics for the average longitudinal applications rate for the ±2.67 m pan position along with the 95% regression confidence interval for the linear fit. The results for each linear fit are summarized in table 3.4. Although a linear prediction equation did a better job than the sigmoidal, the overall fit was not as good as the results for the rate change from 56.0 to 168.1 kg/ha, as shown by the lower *R<sup>2</sup>* values. This could be seen with more distribution irregularities, as shown in figure 3.13 and figure 3.12. Similar to the low to high rate change results, the fit of the ±13.35 data was questionable at

best ( $R^2 = 0.29$ ). Two outlier data points were deleted for this analysis. Each occurred at 44 meters for the 10.68 and 13.35 transverse position. These points were extremely high, skewing the fit of the linear regression model ( $R^2 = 0.23$  for the  $\pm 10.68$  data, and  $R^2 = 0.01$  for the  $\pm 13.35$  data) for these two data sets. Several elements could have contributed to the high values at this location, such as larger, denser fertilizer particles, which traveled farther.

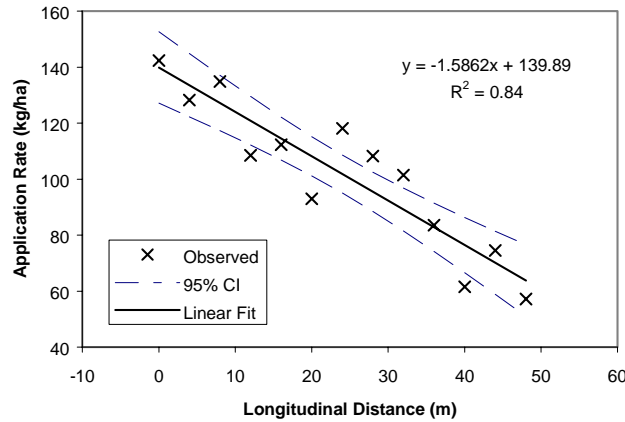


**Figure 3.15. Example application rate change dynamics for 168.1 to 56.0 kg/ha (longitudinal application rates averaged for transverse distance 2.67 and -2.67 m).**

**Table 3.4. Slope and y-intercept for linear line fit for high to low rate change according to distance from center transverse position.**

Parameter	Transverse pan position (m)						
	0	2.67	5.34	8.0	10.68	13.35	16.0
<i>m</i>	-3.19	-1.5862	-1.8509	-1.5662	-0.4311	-0.1161	-
<i>b</i>	223.62	139.89	144.61	121.48	30.81	5.7802	-
$R^2$	0.86	0.84	0.87	0.87	0.58	0.29	-

The predicted values were then used to create surface plots, which model the rate changes. Figures 3.16 and 3.17 contain the modeled surfaces for the rate change from 56.0 to 168.1 kg/ha and from 168.1 to 56.0 kg/ha, respectively. At first glance, figures 3.12 and 3.16 are very similar, except that many of the irregularities seen in figure 3.12 are smoothed out in figure 3.16. The same results can be seen when comparing figures 3.13 and 3.17. Using the coefficient of correlation to compare the actual data used to generate the models to the predicted data shows a good fit for both models. Table 3.5 contains the coefficient of correlation for each of the rate changes, as well as the data for each of the single-pass uniform application tests. The high correlation coefficients are expected since the original collected data used to develop the models were used for the comparison. The high correlation coefficient for the 168.1

to 56.0 kg/ha rate change (0.96) may not have been anticipated due to the low  $R^2$  values seen in table 3.4, but it can be explained because a majority of the product was distributed within 8.0 m of the center pans.

**Table 3.5. Correlation coefficient comparing the actual potash application to the predicted application.**

Test	SSE	Correlation coefficient
56.0 kg/ha	7265.8	0.96
168.1 kg/ha	43184.2	0.97
56.0 to 168.1 kg/ha	45592.4	0.97
168.1 to 56.0 kg/ha	39689.5	0.96

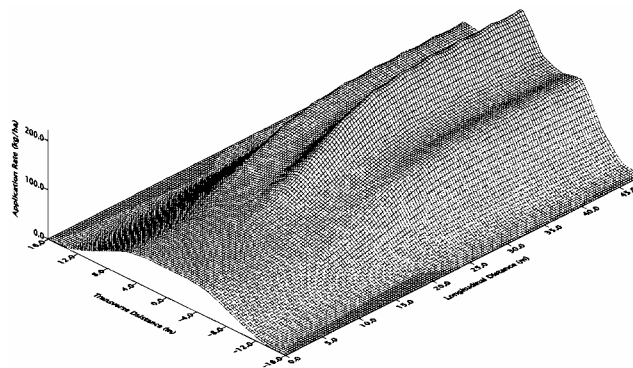


**Figure 3.16. Modeled rate change application surface (56.0 to 168.1 kg/ha).**

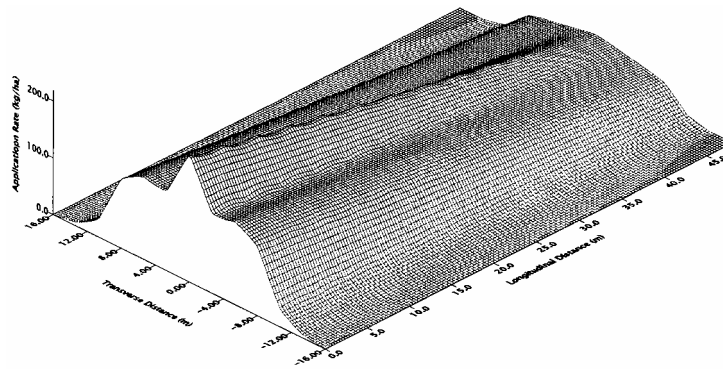


**Figure 3.17. Modeled rate change application surface (168.1 to 56.0 kg/ha).**

Figures 3.18 and 3.19 contain plots of the predicted versus observed data points for all of the 169 pans in each test. In both cases, a high percentage of the data points are along the one-to-one line. From these results, it appears that a model can be developed that does a good job of approximating the actual VR and uniform distribution for this spreader truck.

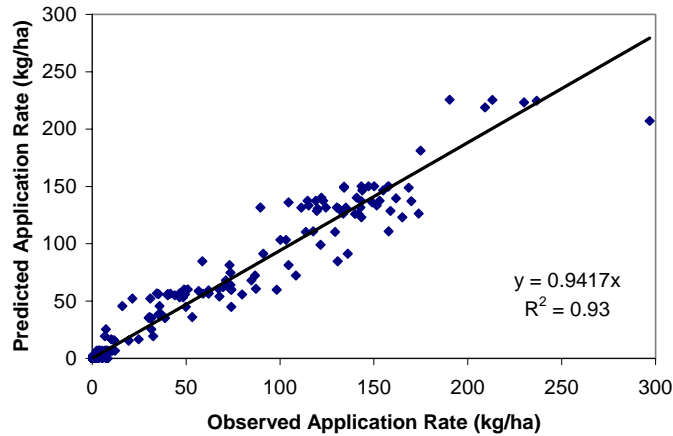


**Figure 3.18. Predicted vs. observed collection pan contents for 56.0 to 168.1 kg/ha application rate change.**

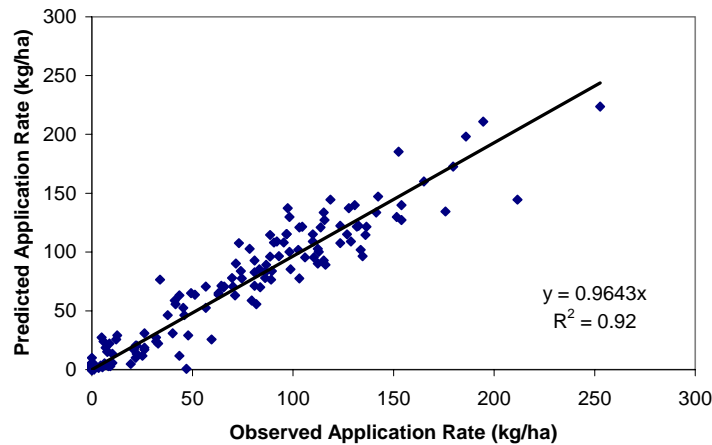


**Figure 3.19. Predicted vs. observed collection pan contents for 168.1 to 56.0 kg/ha application rate change.**

## SUMMARY

This investigation was conducted to assess the accuracy of a VR fertilizer applicator and to determine whether uniform- and variable-rate application of potash could be modeled. Uniform and VR tests were performed using a  $13 \times 13$  matrix of collection pans to gather material spread by a spinner spreader truck. The results of these tests showed the distribution variability existing with spinner spreaders. Coefficient of variations above 20% were calculated for the average transverse distribution patterns for both the 56.0 and 168.1 kg/ha uniform tests.

Uniform and VR applications were mathematically modeled from the collected data. A sigmoidal function was used to describe rate change from 56.0 to 168.1 kg/ha, while a linear function described the rate change from 168.1 to 56.0 kg/ha. The average transverse distribution pattern was used to model

uniform application at 56.0 and 168.1 kg/ha. Comparing the modeled application surface to the actual collected material for each test showed that the modeled application at uniform rates of 56.0 and 168.1 kg/ha, the modeled rate change from 56.0 to 168.1 kg/ha, and the modeled rate change from 168.1 to 56.0 kg/ha did a good job of projecting the actual distribution. Further, the comparison between 56.0 and 168.1 kg/ha distribution patterns showed that there existed a need to change the spreader adjustments to maintain a uniform pattern. The spinner spreader did a good job of applying material at 56.0 kg/ha (with only a slight M-shaped pattern), but at the higher rate of 168.1 kg/ha, the distribution pattern shifted from the desirable Gaussian shape to the less desirable W-shaped pattern. The shift to a W-shaped pattern at the 168.1 kg/ha application rate was also observed in the rate change tests. Therefore, adjustable fins on the spinners or concurrent movement of the rear divider during rate changes might improve pattern shifts at different rates, and thereby improve application accuracies.

Further field-testing will enable the development of a simulation model for predicting application accuracy using a field application file (FAF) containing the applicator DGPS application traverse and information about the applied amount at each DGPS point. In return, the field investigation will allow for characterization and modeling of VR application of granular materials with the ability to assess deviation from the desired application. This will help determine and refine the acceptable management grid resolution based on the spreader truck's limitations for PA. These results also lend information to corrective equipment management procedures to help in reducing application errors. Determining the distribution pattern variability of VRT equipment may illustrate limitations, thereby allowing producers to select the optimal economic sampling and management grid resolution.

The actual distribution model and the calculated application error can also be used to assess operator and equipment performance. Overlap and under-lap can be determined to see if driver error seriously affects application accuracy. Alternately, users may choose to look at the sensitivity of spinner spreaders to perform adjustments.

## **CHAPTER FOUR**

# **SIMULATION OF UNIFORM- AND VARIABLE-RATE APPLICATION OF GRANULAR MATERIALS**

### **INTRODUCTION**

Variable-rate technology (VRT) used in conjunction with the global positioning system (GPS) has become a common practice implemented by precision agriculture (PA) practitioners. VRT appears to provide a method for improving input use efficiency by applying near-optimum rates based on local soil conditions and crop requirements. This reduction of over- and under-application of inputs enhances productivity and profitability while reducing environmental impacts. These positive outcomes are predicated on the accuracy of VRT equipment. However, many studies have shown that errors exist in VRT systems. GPS receivers exhibit position and latency errors. VRT controllers have limited response time and steady-state rate error. Consequently, the use of prescription maps for economic and agronomic analysis can generate misleading results. However, some errors can be minimized through software corrections and hardware calibration.

Of more critical importance to application accuracy is the deposition or application consistency of product across the application width of the machine. Manufacturers and producers have acknowledged the existence of deposition variability. However, producers continue to use the equipment despite these errors.

Today, many software and hardware manufacturers offer two-way communications between VRT software and VR controllers. The software packages not only send the desired application rate to the VR controller, but they also record the actual application data returned by the VR controller. This application data represents a spatial application quantity point file describing the location and amount of product that passes through the metering device. The main limitations of these data sets are that they do not represent actual product distribution after it leaves the metering devices. In particular, they do not account for possible distribution pattern inaccuracies at various application rates, over- and under-lap on parallel passes, the offset distance between the GPS antenna and the point of application, and system latency. These application errors are evident on spinner spreaders applying granular material. Consequently, even the use of the logged field application data for economic and agronomic analysis can generate misleading results. Therefore, a better quantification of spatial material deposition in the field is necessary for accurate economic and agronomic analyses.



## SUB-OBJECTIVES

While VRT equipment offers a method to better match nutrient application rates to localized soil conditions, limitations of the distribution equipment often result in application errors. The goal of this project was to develop a method to post-process field application files (FAF) to create accurate "as-applied" surfaces. The specific objectives were:

- To generate an "as-applied" surface for granular fertilizer and agricultural lime using the distribution patterns determined by Fulton et al. (2001) and the FAF logged during field application with a VR spinner disc spreader,
- To validate the "as-applied" surface generating spatial data model,
- To compare the "as-applied" surface to the desired prescription surface, and
- To assess the effect of GPS receiver offset distances and receiver latency on the accuracy of the spatial data model.

## METHODOLOGY

Three fields located in Shelby County, Kentucky, were used to collect experimental data during application of murate of potash (KCl) applied using the same spinner spreader used by Fulton et al. (2001). Field A (9.6 ha) was used for developing the "as-applied" spatial data model and illustrating its assessment capabilities. Fields B (9.2 ha) and C (34.2 ha) served for validating the "as-applied" spatial data model. The fields were subdivided into 0.4 ha square management zones. Fields A, B, and C contained 31, 25, and 89 management zones, respectively. Some individual management zones were larger or smaller than 0.4 ha due to irregular field shapes. The SSToolbox (SST, 1999) software package was used to generate the application prescription maps (figs. 4.1, 4.2, and 4.3). Prescription maps were based on the University of Kentucky's Lime and Fertilizer recommendations for murate of potash (AGR-1, 1998). Table 4.1 provides summary information for all three fields and application prescription maps.

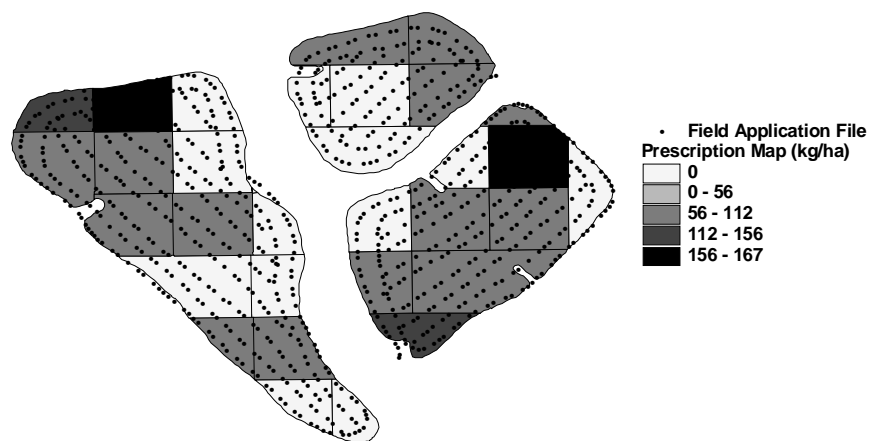


**Figure 4.1. Application prescription map and field application file for field A.**

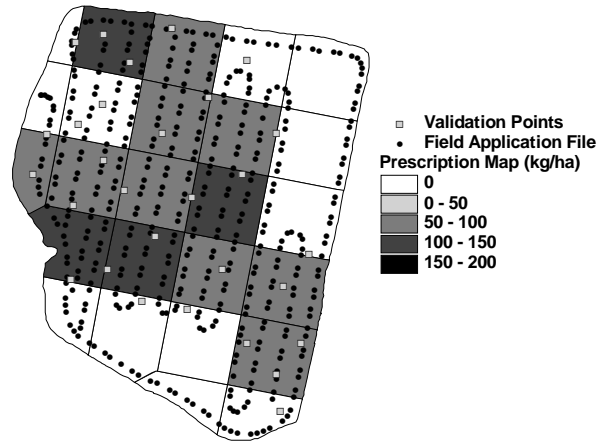


**Figure 4.2. Application prescription map, field application file, and validation points for field B.**

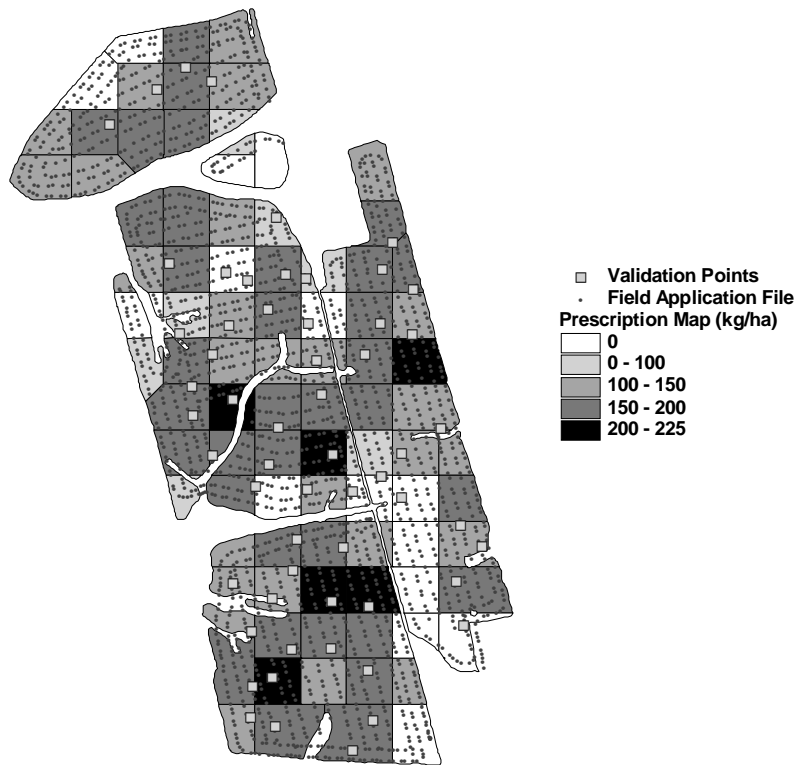


**Figure 4.3. Application prescription map, field application file, and validation points for field C.**

AgView software by GIS Solutions (GIS, 1999) was used to execute the VR control and generate the FAF. Based on the spinner spreader's location during application, AgView used the prescription map to pass the desired application rates to a MidTech TASC 6200 controller. In turn, the MidTech controller regulated the amount of murate of potash being applied and simultaneously echoed the accumulated applied volume back to AgView. AgView recorded the position and volume of applied fertilizer at each

location and saved this information as a spatial data layer in ESRI's "shape file" format (figs. 4.1, 4.2, and 4.3).

**Table 4.1. Prescription map summary information.**

<b>Prescription Map</b>	<b>Field A</b>	<b>Field B</b>	<b>Field C</b>
Field area (ha)	9.6	9.2	34.3
Number of zones	31	25	89
Application rate (kg/ha)			
Minimum	0.0	0.0	0.0
Maximum	166.2	145.3	211.0
<b>Range (kg/ha)</b>	<b>Percent of Area (%)</b>		
0.0	37.6	44.9	15.9
0.1 - 100.0	42.0	38.2	5.9
100.1 - 125.0	10.5	8.1	10.8
125.1 - 150.0	2.4	8.8	17.7
150.1 - 175.0	7.5	0.0	27.2
175.1 - 212.0	0.0	0.0	22.5

The first step in the analysis process was to re-project the FAFs from geographic coordinates (WGS 84) into the State Plane, Kentucky North coordinate system using ArcView's projection utility (ESRI, 1999). Either State Plane or Universal Transverse Mercator (UTM) coordinates are required to create polygons with area properties for representing the distribution of murate of potash. Projecting data from WGS 84 (decimal degrees) into a Euclidean coordinate system simplifies dimensional analysis, such as measuring distances and generating defined shapes, within software code.

Previous work using the same VR spinner spreader truck for modeling of VR application of murate of potash permits the selection of transverse distribution patterns to describe VR application (Fulton et al., 2001). For simplicity and initial program development, three distribution patterns were chosen to represent high, medium, and low application rates (fig. 4.4). The modeled uniform 168.1 and 56.0 kg/ha distribution patterns determined by Fulton et al. (2001) were used to represent the high and low rates, respectively. The medium rate was selected as 112.1 kg/ha, and the associated distribution pattern was extracted from the appropriate location of the rate change (56.0 to 168.1 kg/ha) application surface created by Fulton et al. (2001). Each distribution pattern was scaled using its summed deposition for that pattern. The application rate ranges for these three categories and the standardized distribution patterns are presented in table 4.2.

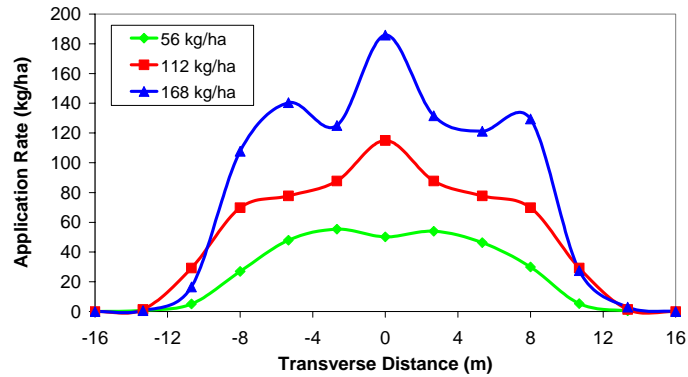


Figure 4.4. Low, medium, and high distribution patterns.

Table 4.2. Standardized distribution pattern data.

Range (kg/ha)	Pattern Location (m)												
	-16.00	-13.35	-10.68	-8.00	-5.34	-2.67	0.00	2.67	5.34	8.00	10.68	13.35	16.00
0 – 84.0	0.00	0.00	0.02	0.09	0.14	0.17	0.16	0.17	0.15	0.08	0.02	0.00	0.00
84.1 – 140.0	0.00	0.00	0.05	0.11	0.12	0.14	0.18	0.14	0.12	0.11	0.05	0.00	0.00
140.1 - 250.0	0.00	0.00	0.03	0.13	0.12	0.13	0.19	0.13	0.14	0.11	0.02	0.00	0.00

Next, the FAFs were used in combination with the appropriate distribution patterns to create an "as-applied" surface for this field. To merge this data and create the "as-applied" surface, an Avenue script was developed for ArcView® 3.2 (ESRI, 1999). A single script was written to read the re-projected shape file, determine the applied volume, and then assign application polygons at each point representing the appropriate distribution pattern.

The first function performed by the script was to compute the amount of murate of potash applied per point by taking the difference in the total amount between consecutive points. A new column was generated within the database file to represent the quantity of material applied per point. The next step was to create polygons at each of the logged GPS fixes. This rectangular polygon was further subdivided into 13 equal-width rectangular sub-polygons, which were each assigned an application rate based upon the amount of material applied at the corresponding point.

An offset distance that helped improve the positioning of the application polygons was included to account for separation distance between the GPS antenna and actual point of application on the spreader. The GPS antenna on most spreaders is mounted on the cab or near the front of the spreader, while the spinners or application point is at the rear. In most cases, the applied material lands behind the dispersion point of the spinner discs. The Avenue script performs this spatial shift by moving all the points in the re-projected FAF back in time based on each point's current position and heading.

Spread width was set at 34.7 m based on the single-pass test data collected by Fulton et al. (2001). The length of the polygon was calculated from the distance between the midpoint of the GPS fix of interest and the GPS fixes on either side (fig. 4.5a). Based on these dimensions, a rectangular polygon was generated and assigned to each GPS fix. To orient the polygon, the heading of the spreader truck was determined by calculating the azimuth between the point of interest and the next point in time (fig. 4.5a). The polygon was then rotated perpendicular to the heading, as shown in figure 4.5.

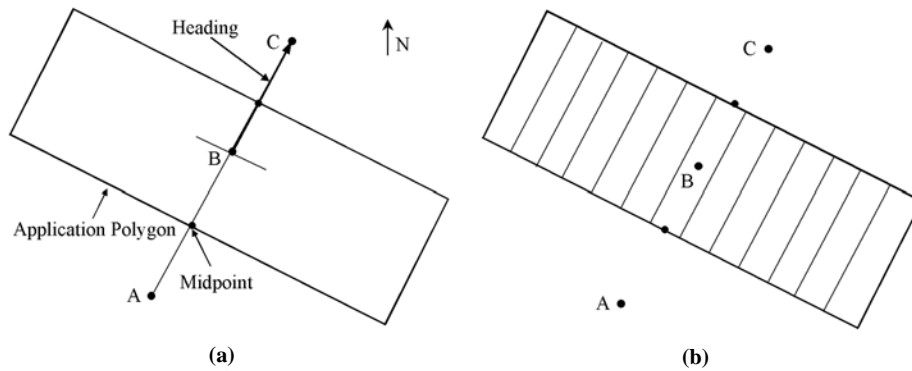


**Figure 4.5. Polygon assignment to point B showing: (a) length and heading determination for proper orientation, and (b) division into 13 sub-polygons for distribution pattern allocation.**

Once oriented, the polygon was sub-divided (normal to the direction of travel) into 13 equal sub-polygons to facilitate the assignment of the distribution pattern (fig. 4.5b). The resulting distribution pattern polygon layer can be seen in figure 4.6. The start and end of pass points required a slightly altered method for applying a polygon since three consecutive points (one on either side of the point of interest) did not exist for determining a midpoint and heading. To resolve this situation, a ghost point was placed at a distance from the point of interest equal in magnitude to the distance between the point of interest and the adjacent point in the opposite direction. This provided a means to calculate a heading and assign a polygon for these unique cases.

The next step performed within the Avenue script was assigning the amount of applied material to each polygon. The normalized distribution patterns in table 4.2 were used to specify the distribution of material applied at each sub-polygon. The amount of murate of potash applied at the point of interest was multiplied by the scaled level of deposition for each sub-polygon. The applied quantity of material in each polygon was converted to an application rate by dividing this quantity by the polygon area.

A matrix of points was generated (fig. 4.6) for specification of the "as-applied" surface. Only half of the matrix is shown to better display the polygon layer. The user was prompted for the grid spacing. A 3.05 m spacing was chosen for field A. At each point, the application rates were summed for all intersecting polygons to estimate the total application rate, thus creating the "as-applied" surface (fig. 4.7).

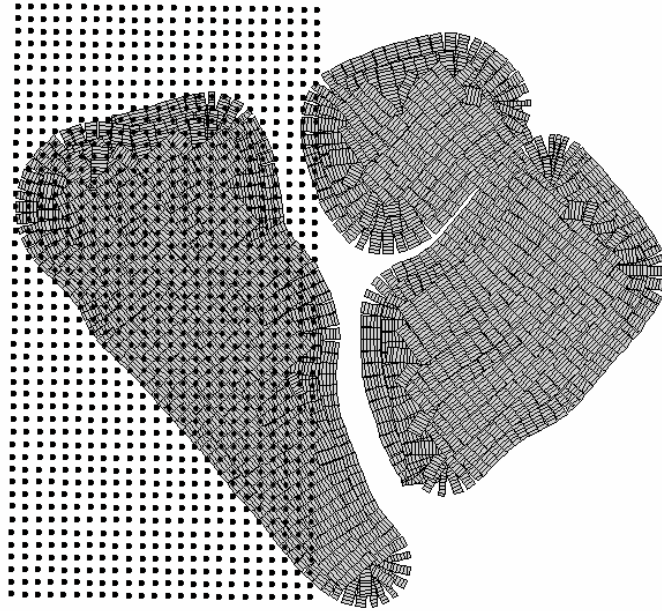


Figure 4.6. Grid generation (only left half shown) for specification of the "as-applied" surface for field A.

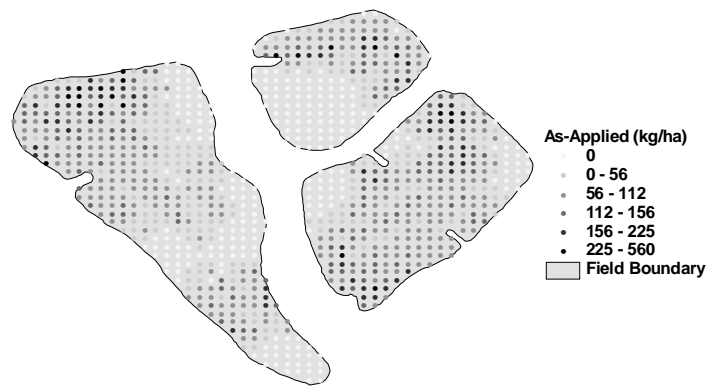


Figure 4.7. Generated "as-applied" surface for field A.

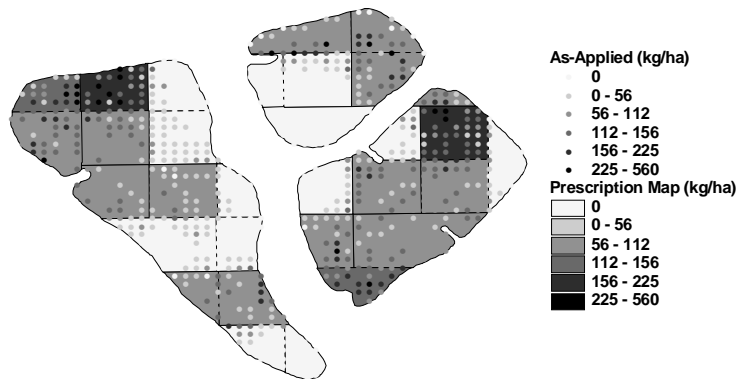
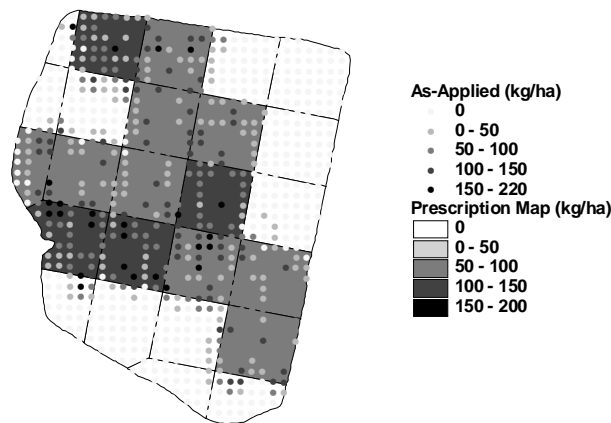


Figure 4.8. "As-applied" surface superimposed on the prescription map for field A.

The last step was to compare the "as-applied" surface to the prescription map to assess application accuracy for field A. Figure 4.8 shows the "as-applied" surface superimposed over the prescription map for field A with corresponding legends used for each map to provide a visual portrayal of application errors. Thus, visible points indicate deviations from the prescription map.

Validation of the "as-applied" spatial data model consisted of randomly placing collection pans within fields B and C. A total of 29 and 58 pans were placed in fields B and C, respectively, to collect applied murate of potash. Fulton et al. (2001) described collection pan size, which was in accordance with ASAE Standard S341.2 (ASAE Standards, 1997). The prescription maps were uploaded into the control system of the VRT applicator. An experienced driver was instructed to apply as normal, ignoring the collection pans during application. Figures 4.2 and 4.3 illustrate the application traverse for each field representing the FAF created by AgView. A foam marker was used for guidance. For these fields, the operator did not drive over some management zones that required zero application in order to save time. Subsequent to application, test pan locations were recorded using a DGPS receiver (figs. 4.2 and 4.3). The murate of potash collected in each pan was bagged, identified, and weighed. The ratio of sample mass to pan collection area provided the actual application rate.

Each field's validation points were imported into ArcView<sup>®</sup> 3.2 along with the "as-applied" files. The "as-applied" procedure was implemented as described above by re-projecting all shape files into Kentucky State Plane North and then executing the Avenue script. For fields B and C, the Avenue script was executed twice. The first run used the validation shape files in place of the matrix layer to predict the application rates for each validation point. These predicted results were then compared to the actual application rates to assess the "as-applied" spatial data model accuracy. The second run was used to generate an "as-applied" surface for each field (figs. 4.9 and 4.10). The generated "as-applied" surfaces are a 10 × 10 m grid of points. Table 4.3 contains summary statistics for the validation points (actual and predicted) and "as-applied" surfaces for these two fields.



**Figure 4.9. "As-applied" surface superimposed on the prescription map for field B.**

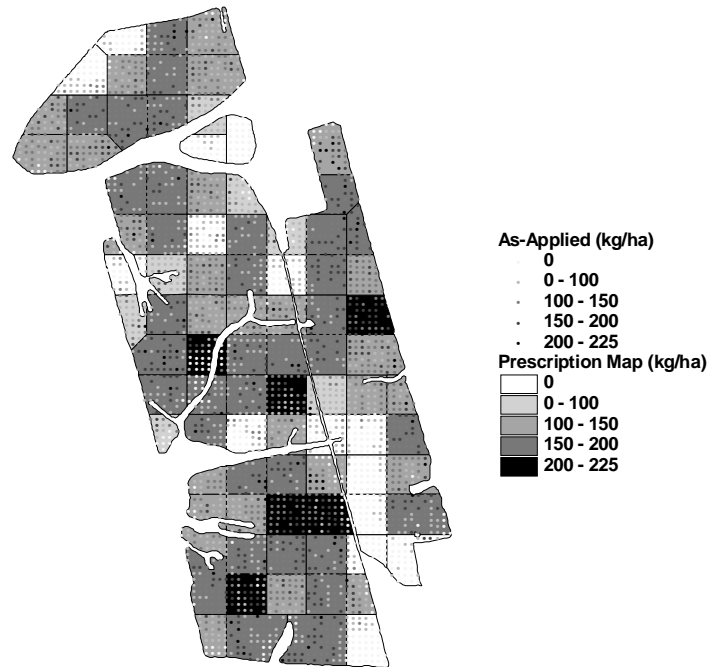


Figure 4.10. "As-applied" surface superimposed on the prescription map for field C.

Table 4.3. Summary for the various layers of fields B and C.

Validation Points	Field B	Field C
Number of points	29	58
<b>Predicted application rate (kg/ha)</b>		
Minimum	0.0	0.0
Maximum	141.1	233.4
<b>Actual application rate (kg/ha)</b>		
Minimum	0.0	0.0
Maximum	133.3	292.4
<b>As-Applied Surface</b>		
Number of points	909	3420
Application rate (kg/ha)		
Minimum	0.0	0.0
Maximum	218.7	803.5

Finally, the effect of different offsets on the validity of the spatial data model was investigated. The Avenue script was executed repeatedly using different offsets for each field. The actual and predicted data for each offset was compared to determine the best offset for each field.



## RESULTS AND DISCUSSION

The prescribed application rates for field A ranged from 0.0 to 166.2 kg/ha for the various management zones (table 4.1). Zones requiring no murate of potash made up 37.6% of the field area, which is depicted in figure 4.1. A total of 16 zones, or 62.4% of the field area, required some application of murate of potash.

The "as-applied" surface (fig. 4.7) shows a large range in the predicted application rates for field A. A total of 952 points represented the "as-applied" surface with rates ranging from 0 to 557 kg/ha (table 4.4). Figure 4.8 presents an overlay of the "as-applied" surface and prescription map for field A. The legends for these layers are equivalent; therefore, visible points correspond to deviations from the desired application rates. Variability existed within all the management zones; those zones requiring the highest application rates had the most variability. Zones requiring no application typically exhibited less variability, which would be expected since no material was applied.

**Table 4.4. Summary information for the "as-applied" surface for field A.**

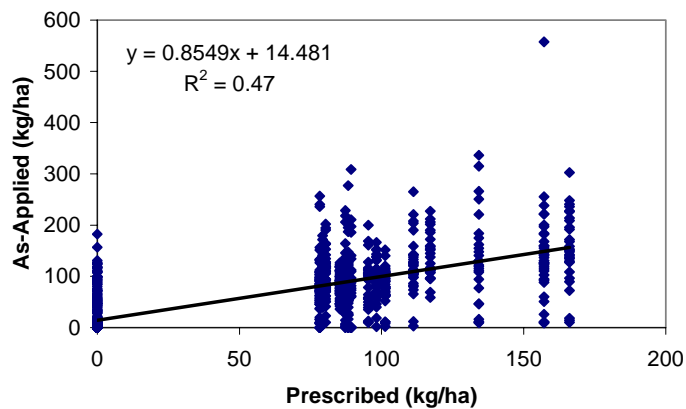
<b>Total number of points</b>		952	
<b>Application rate (kg/ha)</b>			
<b>Minimum</b>		0.0	
<b>Maximum</b>		557.3	
		<b>Percent Correct (%)</b>	
<b>Range (kg/ha)</b>	<b>Percent of Points</b>	<b>Within 5 kg/ha</b>	<b>Within 10 kg/ha</b>
0.0	40.0	72.0	80.0
78.3 - 80.0	11.8	8.0	18.8
80.1 - 90.0	21.6	16.5	27.7
90.1 - 100.0	7.1	13.2	23.5
100.1 - 110.0	3.9	10.8	27.0
110.1 - 120.0	6.4	14.8	29.5
120.1 - 166.2	9.6	6.6	12.1

Table 4.4 provides a statistical breakdown of the distribution of application rates for the "as-applied" surface. As expected, the best results were in zones requiring zero application. Forty percent of the points received 0.0 kg/ha, with 80% of those points within 10 kg/ha of the desired 0.0 kg/ha application rate. The results do not indicate that application errors were rate sensitive for the spreader. None of the rate categories appear to generate larger errors than others. However, the percent correct numbers seem to show that the spreader performed slightly better in the range from 80 to 120 kg/ha. The two outermost ranges, disregarding the 0 kg/ha category, showed the greatest errors for both the within 5 kg/ha and within 10 kg/ha columns.

Few points from the "as-applied" surface were close to the desired application rates of the prescription map. The number of correct points for the within 10 kg/ha column was between 12% and 29% for most application ranges. These small percentages represent deviations from the prescription map that is indicative of poor application by the VRT spinner spreader.

Seven percent of the points were greater than the maximum application rate (166.2 kg/ha) called for by the prescription map. These high values could be attributed to errors ranging from control issues, such as hydraulic flow variations during rate changes, to multiple overlaps at headlands. It appears that many of the high rates occurred near the headlands.

The prescribed applications rates were compared to the "as-applied" (predicted) rates using linear regression (fig. 4.11). The relatively low  $R^2$  value of 0.47 indicated a weak relationship between the predicted and prescribed application rates. An  $R^2$  of 0.70 or higher would seem to specify a more acceptable application job. It must also be recognized that shortcomings of the model may contribute to the low application accuracy.



**Figure 4.11. Prescribed versus the "as-applied" (predicted) application rates.**

A difference map was created to compare the "as-applied" surface to the prescription map (fig. 4.12) to show the areas receiving over- and under-application of murate of potash. The legend was selected so that larger symbols indicate larger deviations. The plus signs indicate over-application, while the minus signs represent under-application. Circles represent only slight variation from the desired prescription applications. As discussed above, the most accurate applications occurred in the zones requiring no application, with 95% of the circles falling within the 13 zero application zones. A few larger symbols can be seen, but most of the difference appears to fall between -50 and 50 kg/ha. Table 4.5 presents a breakdown for rate difference ranges found in the legend of figure 4.12. Nearly 79% of the points occurred between -50 and 50 kg/ha. Very few points (1.4%) were in the ranges of -150 to -400 kg/ha and 150 to 400 kg/ha. The summary statistics indicate more over-application than under-application, which

could be indicative of the operator not maintaining a large enough pass-to-pass spacing. The benefit of a difference surface is that it provides a quick visual assessment of application errors.

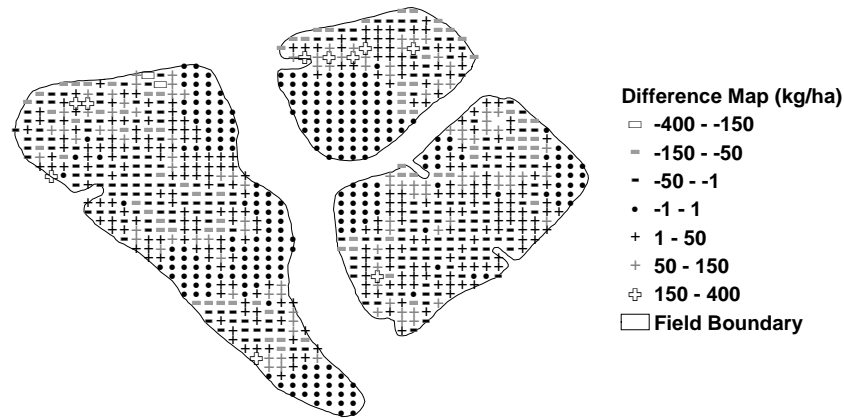


**Figure 4.12. Difference between the "as-applied" surface and prescription map for field A.**

**Table 4.5. Rate difference categorization between the "as-applied" surface and prescription map for field A.**

Rate Difference Range (kg/ha)	Percent
-150 to -400	0.2
-50 to -150	8.6
-1 to -50	22.1
-1 to 1	28.0
1 to 50	28.6
50 to 150	11.3
150 to 400	1.2

Deviations from the desired application rate may be attributed to many factors. The control system was incapable of performing instantaneous rate changes at zone boundaries, thereby creating a situation in which the desired rate at zone boundaries was rarely achieved. This was most prevalent along zone boundaries that specify no application (fig. 4.8). Additionally, the AgView software used in this study incorporated a "look-ahead" feature that initiates rate changes early to compensate for actuator lag. A three second "look-ahead" time was used for this spreader system based on the results of Fulton et al. (2001). Similarly, the "as-applied" points around the field boundary seemed to receive reduced rates. This is apparent in management zones at the top of figure 4.8. These under-applied areas could result from the proximity to the periphery of the field, where parallel overlapping passes by the spreader were not performed.

The path chosen by the operator influenced material application accuracy for fields A and C. Many times, the operator was unable to navigate parallel to management zone boundaries (figs. 4.1 and 4.3). For

these fields, the operator drove diagonally to the management zones since that provided the longest, straightest parallel passes for covering these irregular shaped fields. The application pattern in field B was parallel to the zones (fig. 4.2). There were noticeably more errors in fields A and C, especially in the zone corners where the spreader was in a particular zone for only a brief period of time. These data suggest orienting management zones parallel to the field traverse thereby improving application accuracy. Misalignment of zones to traffic patterns is typical with irregular-shaped fields. Regardless of the chosen traffic pattern, the "as-applied" spatial data model should properly predict the application of granular materials.

Another factor affecting application accuracy was pass-to-pass spacing. The effective spread width of this applicator was 16.0 m. However, parallel passes and spacing varied in all three fields, as can be observed in figures 4.1, 4.2, and 4.3.

The validation of the "as-applied" spatial data model focused on its predictability and not on comparing the "as-applied" surfaces to the application prescriptions. Figures 4.9 and 4.10 demonstrate that significant differences exist between the prescription maps and "as-applied" surfaces for fields B and C. The legends for each layer are the same; therefore, the appearance of a point illustrates deviation from the desired application. Both "as-applied" surfaces show noticeable deviation from the prescription maps for VR application of murate of potash.

Various offset distances were used in the model to determine the effect on the "as-applied" surfaces. The user-selected offset distance serves to compensate for GPS latency and antenna position in relation to the application point. The predicted application rates for each offset were then compared to the actual application data. An offset of 5.5 m produced the highest correlation ( $R = 0.67$ ) for field B, with 5.8 m and 6.1 m offsets resulting in correlations of 0.66 (fig. 4.13). The highest correlation (0.76) for field C was found at an offset of 4.9 m (fig. 4.14). A polynomial regression line was fit to the offset data. The polynomial fit for field B (fig. 4.13) indicates that the appropriate offset is somewhere around 5.5 m. However, a poor polynomial fit was found for field C (fig. 4.14). From this fit, an offset of 3.5 m provided the best results. Therefore, offsets of 5.5 m for field B and 4.9 m for field C were selected for analyzing the validity of the model. These were the highest correlation coefficients computed for each field. Thus, these offsets were entered into the model for predicting the application rate at each validation point.

The reason for the different offsets for each field is unknown. It would be expected that the same offset distance would generate the highest correlation coefficient for predicting the application rates on each field. However, only a 0.6 m variation existed, which is relatively small compared to the size of the machine. The same spreader setup was used on each field, but the difference could be that application occurred on different days at varying ground speeds, field terrain differences, and air speed and direction.

Variations in murate of potash sources (particle density and origin) may have contributed to the differences.

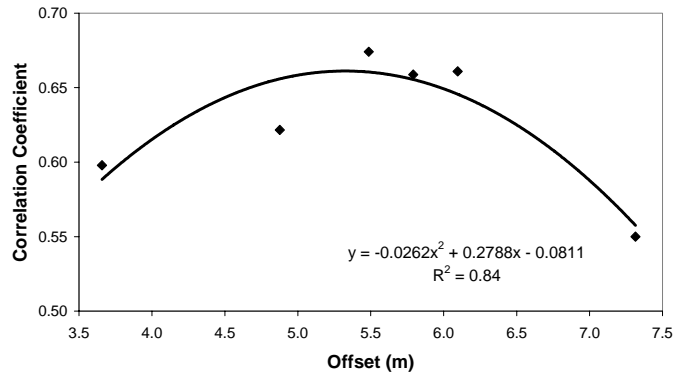


Figure 4.13. Plot of the correlation coefficient versus offset distance for field B.

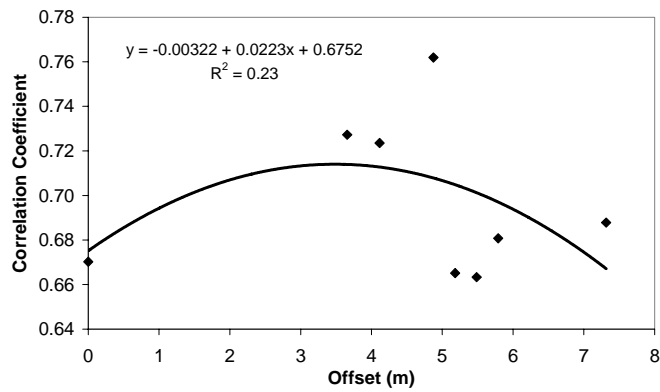


Figure 4.14. Plot of the correlation coefficient versus offset distance for field C.

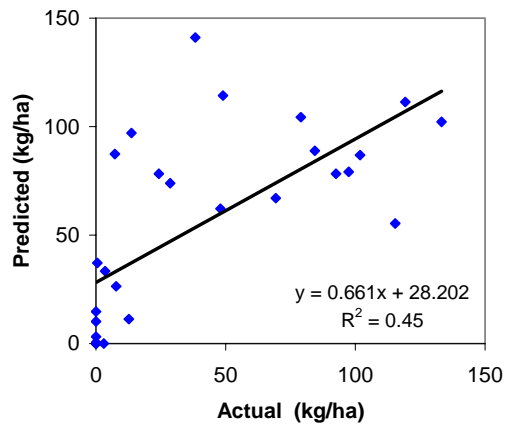
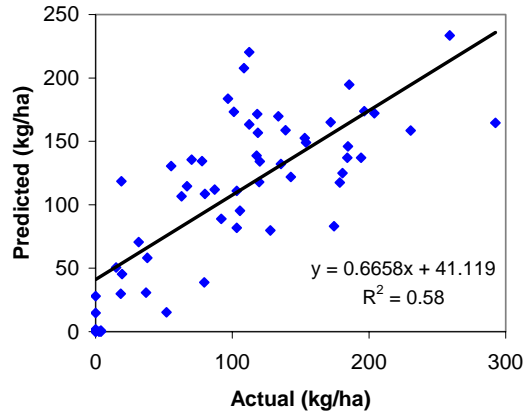


Figure 4.15. Plot of predicted versus actual application rates for field B.



**Figure 4.16. Plot of predicted versus actual application rates for field C.**

The actual versus predicted application rates for the validation points were plotted to determine the performance of the "as-applied" spatial data model (figs. 4.15 and 4.16). As can be observed, the model's performance was not extremely strong in predicting the actual application rates. A linear regression was fitted to the data (figs. 4.15 and 4.16), confirming this observation. Coefficients of determination ( $R^2$ ) equal to 0.45 (field B) and 0.58 (field C) along with slopes around 0.66 were computed, indicating a weak linear relationship. As can be seen, the model worked better on Field C. Although the model showed weak correlation with the actual application rates, it performed better than expected considering the current shortcomings of representing the application area with rectangular polygons.

Very poor correlations were found between the actual application rates and prescription maps for fields B and C ( $R^2$  values of 0.16 and 0.21, respectively; table 4.6). These values are much lower than those determined when comparing the actual and predicted application rates and are indicative of poor performance by the VR spinner spreader. The VRT spinner spreader was unable to apply what the prescription required. Possible explanations for the high deviations may include VRT hardware and software latency, operator error, and spreader setup and calibration.

**Table 4.6. Comparison of various layers.**

Comparison	$R^2$	
	Field B	Field C
Actual versus predicted	0.45	0.58
Actual versus prescription map	0.16	0.21

The low correlation observed also suggests that the "as-applied" spatial data model better estimates actual application rates than prescription maps. Application errors exist for both fixed- and VR application. The assumption that VRT application is consistent with prescription maps is misleading.

Further, these low correlations demonstrate that using prescription maps for analysis purposes is not appropriate. While the "as-applied" surfaces do not accurately predict actual application rates, they appear to be a better representation of actual application than the prescription maps. However, modifications to the current model are needed to improve "as-applied" map generation accuracy.

## **SUMMARY**

"As-applied" surfaces were generated in ArcView<sup>®</sup> 3.2 (ESRI, 1999) using distribution patterns characterized by Fulton et al. (2001) and an FAF. Avenue scripts were written to generate the "as-applied" surfaces by merging the distribution pattern information and the FAF within ArcView<sup>®</sup>. "As-applied" surfaces were compared to prescription maps to assess application errors and demonstrate the utility of "as-applied" surfaces. An  $R^2$  of 0.47 was calculated for field A, indicating poor performance by the VR spinner spreader. The resulting "as-applied" surface showed errors existed especially at the intersection of management zones where rate changes occurred. Variability also existed within zones requiring higher application rates. Zones requiring zero application received only a small amount of material proximal to the borders of zones requiring murate of potash. This illustrated the need to properly set the "look-ahead" time in software application packages to improve application during rate changes when moving between zones. A difference surface was also generated to provide a visual representation for the spread quality by showing areas receiving over- and under-application of murate of potash.

Validation studies showed that the current "as-applied" spatial data model did a reasonable job of estimating field application of murate of potash. Even though relatively weak relationships ( $R^2$  values of 0.45 and 0.58) were found between the predicted and actual application rates for fields B and C, respectively, the "as-applied" surface provided a better estimate of actual application rates than the prescription map. Very poor correlations ( $R^2$  values of 0.16 and 0.21) were determined between the actual application rates and prescription maps for field B and C. These results reveal the undesirable performance of the VRT applicator, as well as the inability of prescription maps to depict actual application of products. Ultimately, this lack of correlation could be indicative of escalated application errors when moving from fixed- to VR application.

Offsets of 5.5 m (field B) and 4.9 m (field C) were determined to produce the best results for generating the "as-applied" surfaces. The reason for this difference in offsets is unknown. The effect of offset on the "as-applied" results needs further investigation to determine if different offsets are needed on a field-by-field basis. However, the difference (0.6 m) for these results is small when considering the application area of granular products.

In conclusion, the significance of this "as-applied" spatial data model is that it represents how granular materials are distributed during field application using spinner spreaders. The "as-applied" spatial data

model developed provides important insight into understanding VRT application errors. Making the assumption that the prescription map represents field application and using it for analysis purposes is misleading. Without properly knowing how materials are distributed across fields, true evaluations cannot be made about VRT.



## **CHAPTER FIVE**

# **COMPARISON OF VARIABLE-RATE GRANULAR APPLICATION EQUIPMENT**

### **INTRODUCTION**

The popularity of variable-rate technology (VRT) is growing since the advent of precision agriculture (PA). One area farmers are tending to focus on is nutrient fertility management. Fertilizer dealers and custom applicators are providing VRT services to farmers, which usually come as an additional cost due to the added equipment and software required to perform variable-rate (VR) application. The notion behind VRT is only applying what is needed based on local soil conditions and crop requirements. This assumes that soil and fertility variability exists and the traditional uniform-rate (UR) application tends to over- and under-apply. Thus, VRT may provide a method to make better use of granular inputs. While VRT seems to be a viable option for managing granular inputs, an understanding of application errors associated with VRT equipment is essential. Quantification of these errors will help establish whether VRT offers an effective way to apply products when contrasted with UR application. There is also the concern as to whether this technology actually pays for itself.

The two main technologies for granular material application are spinner discs spreaders and pneumatic applicators. Spinner spreaders still tend to be the most popular type of granular applicators found in the Midwest since they require less of a capital investment. However, air-boom applicators are popular among custom applicators. One concern about granular materials is product variability in terms of material density, particle size, and moisture content. This variability poses a potential problem with regard to the uniformity of application across the width of the machine. Many believe that air-boom technology offers more uniform product distribution across the swath when compared with spinner spreaders. In either case, deposition variability exists due to the nature of granular products, especially with VRT equipment. Producers acknowledge the existence of deposition variability. However, they continue to utilize the equipment despite the errors.

### **SUB-OBJECTIVES**

The goal of this investigation was to quantify the variability of different VRT applicators in terms of distribution pattern characterization and rate change response. Pattern characterization is important not only to evaluate potential application errors but it provides the required distribution information for VRT

applicators for use in the “as-applied” spatial model developed by Fulton et al. (2003). The specific objectives were:

- To characterize the distribution patterns from various granular applicators for varying application rates,
- To evaluate the accuracy of the various applicators under field operation,
- To assess the consistency of the characterized distribution patterns from the various applicators, and
- To quantify the rate change characteristics for various VR control systems.

## OVERVIEW OF APPLICATORS

The four granular applicators tested for this research were a Newton Crouch spinner spreader (fig. 5.1), a New Leader L3020G4 spinner spreader (fig. 5.2), a Gandy Orbit-Air pneumatic applicator (fig. 5.3) and AgChem SoilEction AirMax 2000 pneumatic applicator (fig. 5.4). The first two applicators utilize spinner disc technology to distribute material (figs. 5.1b and 5.2b). The spinner spreaders rely on pattern overlap from adjacent passes to achieve uniform application. The Gandy-Orbit-Air and AgChem pneumatic applicators do not rely on overlap except for the extreme outside distributors. The theory behind pneumatic applicators is that material is being metered uniformly through the distributors along the length of the boom. Thus, little or no overlap is required as with spinner technology.

Fulton et al. (2001) provided a full description of the Newton Crouch applicator and VRT control system. However, the most current control system included a software upgrade to AgView by GIS Solutions (AgView, 1999) and use of a Trimble 132 DGPS receiver. All pattern application tests were run at a nominal ground speed of 20.3 km/hr (table 5.1).

**Table 5.1. Applicator characteristics.**

<b>Applicator</b>	<b>Type</b>	<b>Test Speed (km/hr)</b>	<b>Swath Spacing (m)</b>	<b>Control Valve</b>
Newton Crouch	Spinner	20.4	16.0	Source Fluid Power
New Leader L3020G4	Spinner	14.5	18.3	Rawson (G4)
Gandy Orbit-Air	Pneumatic	9.4	12.2	Rawson
AgChem AirMax 2000	Pneumatic	12.9	21.3	Falcon

The New Leader L3020G4 bed and control system had an 18.3 m effective spread width for fertilizer. The VRT control system included a simplified Rawson controller and hydraulic drive (fig. 5.2c) manufactured for New Leader’s spinner spreaders. A computer, the software package AgView (AgView,

1999), and a Trimble Ag132 DGPS receiver were used to implement the VR capabilities on this spreader. The truck was operated in first gear at 2300 rpm generating a nominal speed of 14.5 km/ha for all tests (table 5.1). Spreader bed settings were the spinner valve positioned at 6.25 generating a nominal spinner speed of 800 rpm, a gate height of 3.8 cm, and a spinner position of 3.25.



**Figure 5.1. Newton Crouch spinner disc applicator; a) isometric view of applicator b) rear view showing spinner discs, and c) hydraulic drive motor and source fluid power control valve for apron chain.**



**Figure 5.2. New Leader L3020G spinner disc applicator a) side view of applicator b) rear view showing spinner discs, and c) hydraulic drive motor and control valve for apron belt.**



**Figure 5.3. Gandy Orbit-Air pneumatic applicator; a) isometric view of applicator b) fluted metering rollers, c) centrifugal blower and Rawson hydraulic control system, and d) deflector plates.**

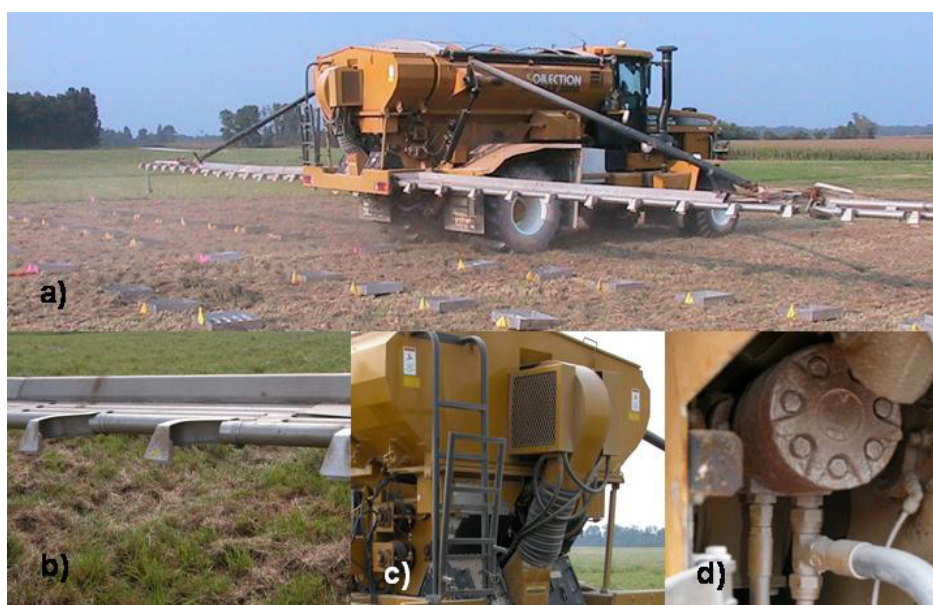


**Figure 5.4. AgChem AirMax 2000 pneumatic applicator; a) isometric view of applicator b) deflector plates, c) centrifugal blower, and d) hydraulic drive for apron chains.**

The AgChem SoilEction AirMax 2000 applicator contained a two compartment bed mounted on an AgChem 8104 Terra-Gator (fig. 5.1a) capable of applying two granular products simultaneously. The applicator has a 21.3 m effective spread width and was operated at a nominal speed of 12.9 km/hr (table 5.1). Material was conveyed from the metering system to the deflectors in 8.26 cm diameter stainless steel tubes (fig. 5.4b). The boom had 32 distributors spaced on 66.7 cm centers with deflectors turning material



90 degrees and targeting it downwards upon exit from the tube (fig. 5.4b). For the left and right booms, there are only eight tubes; thus each tube feeds two deflectors. Each half of the boom, right and left, is fed by separate 40.0 cm apron chains running the length of the bed. Dual 40.0 cm right and left apron chains exist for each of the two bins (4 total conveyors) to meter material out of each bin individually down onto the two main left and right apron chains feeding the booms. Thus, a total of six apron chains exist for metering material. The left and right sides are driven by hydraulic motors (fig. 4d) can be shut-off independently for half boom width spreading. A single 40.6 cm centrifugal fan driven with an axial-piston hydraulic motor generated the airflow for material conveyance from the metering conveyors to the deflectors (fig. 5.4c).

The AgChem applicator was fitted with a Falcon control system providing VR control for both compartments simultaneously. The Falcon system is a complete VR control system developed by AgChem utilizing a proprietary Controller Area Network (CAN) echelon for communications. It contains a computer mounted in the truck cab to run AgChem’s SGIS mapping software package. DGPS was provided by a Trimble 132 using the Coast Guard correction signal. The unique feature about AgChem’s SGIS software was that prescription maps are generated using contouring to smooth the transition at management zone boundaries (fig. 5.5).

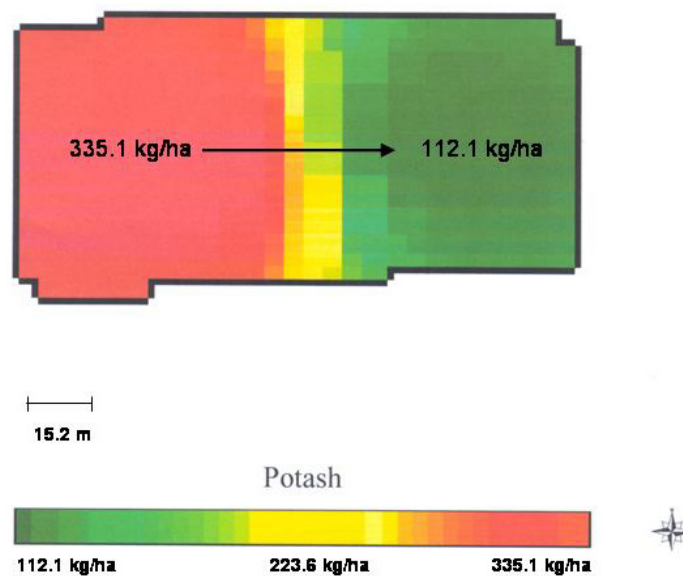


**Figure 5.5. AgChem prescription map generated by SGIS for the 336.2 to 112.1 kg/ha rate transition.**

## METHODOLOGY

Uniform-rate (UR) and VR pan tests for the New Leader L3020 and Gandy Orbit Air applicators were performed at the University of Kentucky’s Animal Research Center (ARC), in Woodford County,

Kentucky. Fulton et al. (2001) provides details for testing the Newton Crouch applicator. The AgChem AirMax 2000 pan tests were conducted in Christian County, Kentucky. For each applicator, a total of six tests were conducted: 4 at four different uniform rates and 2 VR transitions (one from low to high and another from high to low) using murate of potash (KCl). The tests were performed by modifying ASAE standard S341.2 (2000), using the same pans, and following the same test protocol as outline by Fulton et al. (2001). The test site was flagged to indicate collection pan positions and paths for the applicators to cover the test site (fig. 5.6).



**Figure 5.6. Material collection and test site layout.**

Several application rates were selected for performing the uniform-rate (UR) tests to characterize the distribution patterns for each of the applicators. The Newton Crouch was tested at 56.0 and 168.1 kg/ha (Fulton et al., 2001). The rates selected for the New Leader and Gandy were 56.0, 112.1, 224.2, and 336.2 kg/ha. The AgChem applicator was tested at 112.1, 224.2, 336.2, and 448.3 kg/ha. These application rates are based upon the maximum application rates for potassium from the University of Kentucky's Lime and Fertilizer Recommendations (AGR-1, 2002) along with the Tri-State Fertilizer Recommendations for Corn, Soybeans, Wheat, and Alfalfa (Tri-State, 2000). For murate of potash, there are instances where more than 336 kg/ha is recommended especially for alfalfa. Further, a high percentage of the granular fertilizer application in the Midwest occurs with blended products such as potassium and phosphorus. The low application rate of 56 kg/ha was chosen to determine if the New Leader and Gandy applicators would perform accurately at this low application rate and for comparison to the Newton Crouch results. Many spinner spreader manufacturers do not recommend applying fertilizers below 112 kg/ha. However, farmers implementing VRT on these applicators will apply under 112 kg/ha. The AgChem was not tested at the 56.0 kg/ha rate but rather at 448.3 kg/ha as requested by the owners of the applicator.

Two rate transition tests, representing a VR scenario, were performed for each applicator. Fulton et al. (2001) outlined the rate transition tests and analysis for the Newton Crouch. For the New Leader, Gandy,

and AgChem, rate transition tests performed were changing from 112.1 to 336.2 kg/ha and then 336.2 to 112.1 kg/ha.

All applicators were calibrated before performing any of the UR and VR tests using murate of potash. Calibration for the New Leader and Gandy consisted of following manufacturers' recommendations provided within the operator manuals. An average of 224 kg/ha (112 kg/ha and 336 kg/ha) was used for calibration. A single row of pans was used for calibration. Adjustments were made according to manufacturers' literature until the desired application rate (224 kg/ha) and distribution pattern were achieved. For the AgChem, the company (AgriChem, Hopkinsville, KY) supplying the applicator had already calibrated the applicator. Several pan tests (single-row) were conducted prior to the more extensive pattern testing to double-check the distribution pattern and ensure the machine was operating within specifications. Fulton et al. (2001) provided details about calibrating the Newton Crouch applicator.

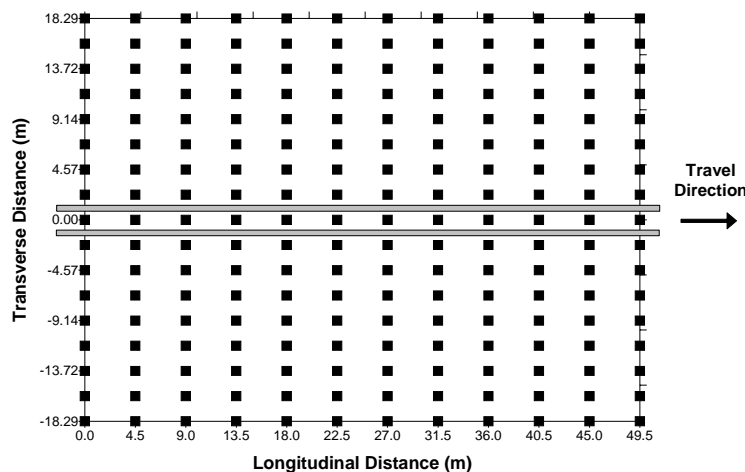


**Figure 5.7. New Leader UR collection pan matrix.**

The collection pan matrices for the New Leader, Gandy, and AgChem were developed based on the 2-D pan matrix used by Fulton et al. (2001). Figures 5.7, 5.8, and 5.9 present the UR pan matrices for the New Leader, Gandy, and AgChem, respectively. The width of the pan layouts was based upon the effective application and overlap widths for each applicator (table 5.1). The New Leader had an 18.2 m swath spacing therefore requiring a 36.6 m width or double the swath spacing (ASAE S341.2, 2000). ASAE standard S341.2 (ASAE S341.2, 2000) defines swath spacing as, “the lateral distance between spreader centerlines for overlapping broadcast applications” and effective swath width as, “the swath width that will produce acceptable field deposition uniformity for the intended application.” Swath spacing is interchangeably used with pass-to-pass-spacing. Since the Gandy and AgChem rely on application overlap at the outer ends of the boom, an additional row of pans was added to the AgChem

applicators pan matrix and two additional rows of pans were added to the Gandy pan matrix. These additional rows were added to determine if material was being applied beyond the effective spread width by the deflectors of these applicators. The 0-m transverse distance represents the pans that were straddled by each of the applicators during a test run. The applicators were permitted sufficient area to attain a steady ground speed before entering the test area.

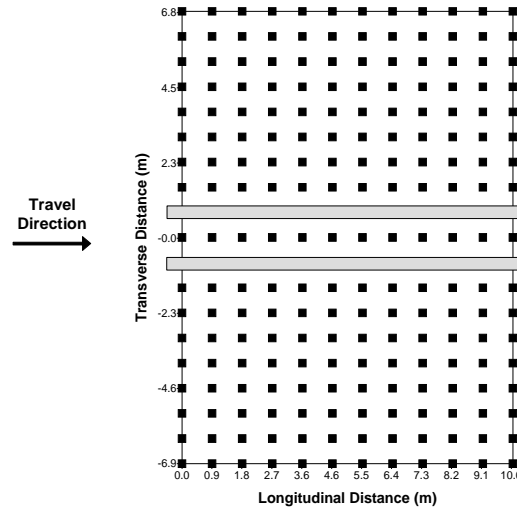


**Figure 5.8. Gandy UR collection pan matrix.**

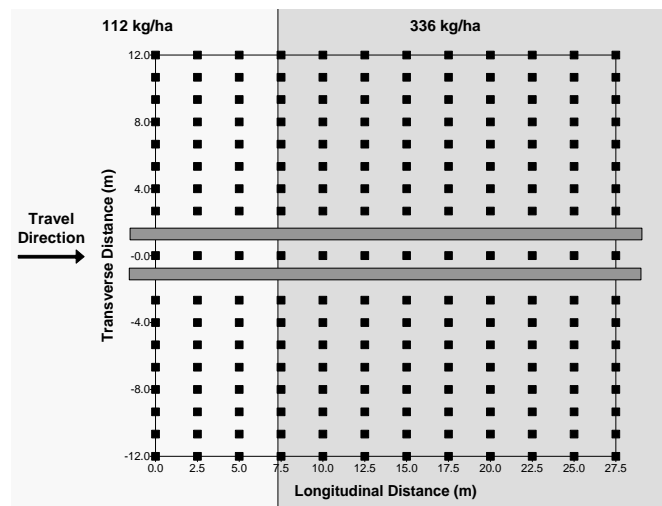


**Figure 5.9. AgChem collection pan matrix for single-pass UR and VR tests along with the desired rate transition line fed into SGIS.**

A total number of 255 pans were used for evaluating the New Leader, Gandy, and AgChem distribution patterns. Test pattern data were collected for the Newton crouch applicator using a fixed 13 by 13 matrix (169 total pans, Fulton et al., 2001). As the result of the earlier study (Fulton et al., 2001), it was decided that more transverse pans were required to better characterize the distribution patterns from



the applicators. The number of longitudinal rows was set at 12 to provide 12 replications for characterizing the distribution patterns at each of the 4 constant application rates. The number of transverse pans for each row was set at 225. Consideration had to be also taken to leave space for the applicator to drive through the test matrix and span at least one row of pans. The final number of pans for the UR tests was established at 204 for all three applicators.

The length of each test matrix was determined by estimating the time for making a rate change and the typical ground speed for each applicator. The time to make a rate change was obtained through discussions with experienced VRT equipment operators. The goal was to capture the rate change within the test matrix but keep the longitudinal pan spacing minimized and confine over several rows of pans. If the rate change happened between rows of pans, it would be hard to determine the start and end of the rate transition period. Longitudinal pan spacing was set at 4.5 m, 0.9 m, and 2.5 m for the New Leader, Gandy, and AgChem applicators, respectively (figs. 5.7, 5.8, and 5.9).

Preliminary testing concluded that the longitudinal pan spacing for the New Leader and Gandy needed to be adjusted plus a few rows added to capture the rate transitions during VR tests. Fourteen longitudinal rows were used spaced at 1.83 m for the New Leader and the desired rate line at 9.14 m (fig. 5.10). The outside two rows were removed for the VR tests since little or no material was collected in these pans during testing. The Gandy longitudinal spacing was not adjusted from the UR spacing but three rows were added with the rate change line set at 4.47 m (fig. 5.11). The two outside rows from the UR (a total of four transverse rows) were removed for the same reason as the New Leader to equal a total of 225 pans.

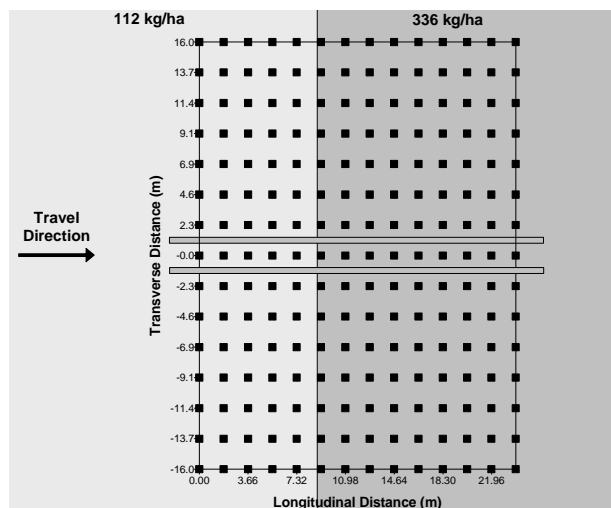


**Figure 5.10. New Leader collection pan matrix for single-pass, rate transition tests.**

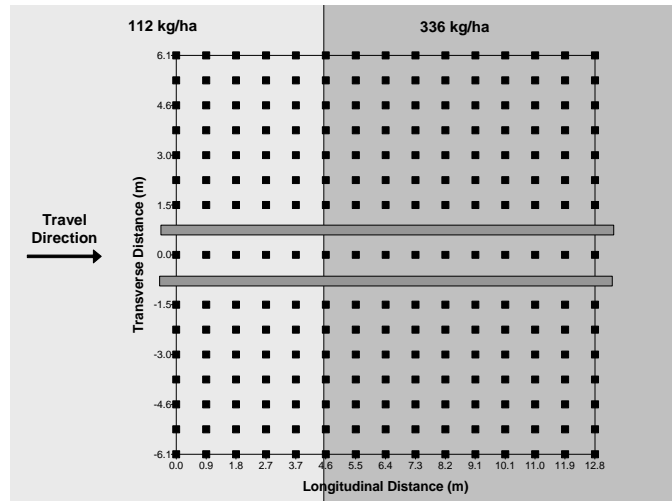


**Figure 5.11. Gandy collection pan matrix for single-pass, rate transition tests.**

The rate transition tests, 112 kg/ha to 336 kg/ha and 336 to 112 kg/ha, were conducted by developing two polygons with the intersection of these polygons representing the desired rate change line. The rate change location for the New Leader and Gandy was determined using a Trimble RTK system to mark the outer two pans at the desired longitudinal distance. A Trimble 132 DGPS receiver was used to locate the rate change line for the AgChem. These two polygons represent management zones and provide a means for characterizing rate transitions when moving between management zones. Two prescription maps were developed for each applicator: low to high and high to low. These prescription maps were loaded into AgView for the New Leader and Gandy. However, this information was imported into SGIS to generate the two prescriptions for the AgChem applicator. The process of contouring by SGIS introduces a difference from the Newton Crouch, New Leader, and Gandy tests thereby slowing the rate response of the AgChem applicator (fig. 5.5).

Upon completion of each distribution test run, the murate of potash particles in each pan were placed in individual plastic bags, sealed, and labeled according to location. A digital scale was used to measure the mass of each sample under laboratory conditions. The weights were recorded to establish the distribution patterns for the UR tests and rate transition data. The distribution pattern at each UR test was determined by computing the mean along each transverse pan position. The 95% confidence interval (CI) and CV was also computed for each transverse pan position for all UR tests.

The resulting single-pass distribution patterns were then used to generate the simulated overlap distribution patterns, using the progressive method outlined in ASAE S341.2 (2000) to assess application uniformity. The overlap patterns represent expected performance during field operation assuming the operator maintains the specified swath width for each applicator. Similarly, the three distribution patterns at 56.0, 112.1, and 168.1 kg/ha for the Newton Crouch applicator (Fulton et al., 2003) were used to

generate overlap distribution patterns. The mean application rate for the overlap patterns were computed by taking the mean of all points in each pattern. CVs were also computed to assess application variability for each of the applicators at each rate. The CVs were computed using two approaches: one to report accuracy ( $CV_{Acc}$ ) and the other to represent precision ( $CV_{Prec}$ ). For accuracy, the desired level was used as the mean when calculating the sample variance whereas the mean of the overlap pattern was used as the mean in the sample variance calculation for precision. Accuracy represents how the resulting distribution pattern deviates from the desired application rate. The  $CV_{Prec}$  relates to only pattern repeatability. There could be a case where the applicator has a small  $CV_{Prec}$  meaning that the overlap pattern was consistent but the  $CV_{Acc}$  could be large meaning that the mean of the overlap pattern deviated from the desired. Although only two of the rates used for the simulated overlap analysis for the Newton Crouch were equal to the four used for the other two applicators, the Newton Crouch results are indicative of trends and potential errors for this type of applicator.

Surface plots were generated using the software package Surfer (Surfer, 1996) for all UR and VR tests. These plots provide visual depictions of application variability and rate transition dynamics. The rate transition characteristics computed were the “transition time” and the “delay time.” The time required for a rate transition represents the time from start to finish of the transition. The delay time characterizes the time difference from when the rate change started to when it reached the desired rate. These features were calculated for each applicator under each of the two rate transition scenarios.

## **RESULTS AND DISCUSSION**

### **SINGLE-PASS ANALYSIS**

The single-pass UR statistics for the New Leader, Gandy, and AgChem are provided in tables 5.2, 5.3 and 5.4, respectively. These tables provide the mean distribution patterns for all four rates along with the standard deviation. As expected, the standard deviation for the outer couple of transverse pans tends to exceed the mean since these pans usually only capture a small amount of material, if any at times. Thus, a particle or two tends to increase the standard deviations for the outer pans. The  $\pm 7.62$  rows for the Gandy received no material for all four rates. The 224 and 336-kg/ha tests for the Gandy produced the highest standard deviations for all applicators. The New Leader tended to produce the lowest standard deviations. The general trend for all three applicators was that the standard deviation increased with application rate. Fulton et al. (2001) also saw an increase in standard deviation with an increase in application rate for the Newton Crouch. These results are expected since the magnitude of application rate increases, which should also increase the standard deviation.

**Table 5.2. Single-pass UR summary statistics for the New Leader applicator.**

Transverse Position (m)	56 kg/ha		112 kg/ha		224 kg/ha		336 kg/ha	
	Mean (kg/ha)	Std Dev	Mean (kg/ha)	Std Dev	Mean (kg/ha)	Std Dev	Mean (kg/ha)	Std Dev
-18.3	0.0	0.0	0.2	0.4	0.3	0.6	0.1	0.3
-16.0	0.0	0.0	2.1	4.1	0.7	1.3	2.1	2.7
-13.7	6.4	4.7	6.0	6.0	9.1	6.4	25.4	8.3
-11.4	17.5	6.3	30.0	10.6	52.2	21.1	121.7	20.7
-9.1	31.4	10.0	60.1	8.7	131.9	18.0	214.1	27.3
-6.9	33.4	5.7	75.8	16.8	150.2	17.6	217.2	29.8
-4.6	40.7	11.9	90.1	17.4	176.6	25.3	254.9	24.7
-2.3	51.0	13.4	114.6	24.1	193.4	29.7	267.0	20.5
0	52.0	11.7	100.9	21.0	226.1	24.1	327.7	25.8
2.3	44.7	12.8	94.3	22.2	181.0	16.7	254.5	22.4
4.6	38.9	5.8	79.6	15.8	167.1	15.4	247.5	30.0
6.9	30.1	7.2	59.3	13.7	142.1	17.6	199.5	17.0
9.1	30.4	8.5	55.7	8.9	114.8	19.2	174.8	17.5
11.4	25.8	9.0	41.2	4.9	88.0	13.8	118.4	23.5
13.7	15.4	7.7	21.2	9.9	40.4	13.1	43.4	9.1
16.0	7.3	4.0	5.9	7.0	6.2	4.2	9.5	5.8
18.3	0.9	2.1	2.0	3.5	2.0	3.9	0.9	1.5

**Table 5.3. Single-pass UR summary statistics for the Gandy applicator.**

Transverse Position (m)	56 kg/ha		112 kg/ha		224 kg/ha		336 kg/ha	
	Mean (kg/ha)	Std Dev	Mean (kg/ha)	Std Dev	Mean (kg/ha)	Std Dev	Mean (kg/ha)	Std Dev
-7.62	0.0	0.0	0.0	0.0	0.0	0.0	0.0	0.0
-6.86	0.2	0.5	0.0	0.0	0.1	0.2	0.1	0.2
-6.10	17.0	8.36	31.9	10.7	65.1	26.7	135.1	50.9
-5.33	65.0	22.1	127.0	29.7	257.4	64.8	372.9	123.6
-4.57	61.0	15.7	116.5	24.4	231.8	64.2	341.6	83.7
-3.81	59.3	14.5	120.1	33.4	231.9	44.5	307.3	71.2
-3.05	54.6	12.6	114.9	26.1	225.9	38.8	358.6	43.3
-2.29	60.4	7.4	115.8	19.1	217.9	29.5	332.5	50.4
-1.52	67.4	15.9	137.0	28.3	242.9	50.7	345.6	84.7
0.00	71.3	19.1	136.9	23.2	242.1	58.7	401.5	90.5
1.52	69.8	12.5	128.3	19.7	188.4	40.1	338.0	39.0
2.29	60.9	14.9	118.4	27.9	230.7	49.7	368.4	67.1
3.05	52.6	10.7	106.7	20.1	194.2	34.7	301.1	71.3
3.81	53.5	12.9	108.7	24.4	210.1	51.7	303.2	30.1
4.57	52.3	13.3	101.9	19.5	199.6	42.3	286.5	71.9
5.33	60.5	18.5	125.2	23.6	220.9	66.4	368.2	102.3
6.10	17.9	7.6	38.6	13.3	107.1	32.0	141.5	40.7
6.86	0.1	0.3	0.2	0.5	0.1	0.2	0.6	1.1
7.62	0.0	0.0	0.0	0.0	0.0	0.0	0.0	0.0

**Table 5.4. Single-pass UR summary statistics for the AgChem applicator.**

Transverse Position (m)	112 kg/ha		224 kg/ha		336 kg/ha		448 kg/ha	
	Mean (kg/ha)	Std Dev	Mean (kg/ha)	Std Dev	Mean (kg/ha)	Std Dev	Mean (kg/ha)	Std Dev
-12.00	1.3	3.8	0.0	0.1	0.3	0.7	0.6	1.3
-10.67	19.1	15.7	14.3	5.3	33.1	10.2	39.5	15.4
-9.33	93.2	14.2	228.8	19.8	348.8	34.9	487.0	34.9
-8.00	102.8	29.9	240.4	31.6	369.7	36.2	469.2	43.3
-6.67	105.8	19.2	218.4	19.8	359.9	27.2	474.0	34.5
-5.33	107.9	14.6	236.5	28.2	370.5	32.3	486.2	59.1
-4.00	102.7	14.0	216.7	23.2	345.9	31.9	445.7	20.0
-2.67	108.7	27.0	239.0	18.4	388.9	28.1	510.5	31.3
0.00	156.9	29.9	385.0	42.7	539.4	40.2	734.1	58.1
2.67	107.2	25.9	231.4	32.9	347.7	45.2	484.3	52.5
4.00	96.8	25.3	209.3	16.9	328.2	36.8	422.5	38.4
5.33	133.0	23.1	285.1	23.9	410.9	23.0	547.9	49.1
6.67	90.3	18.2	205.0	25.7	321.3	31.1	394.6	43.2
8.00	88.1	14.7	208.0	22.9	315.6	22.5	418.1	46.2
9.33	105.6	14.6	224.8	27.6	347.9	39.3	456.8	49.6
10.67	37.8	13.1	65.7	14.0	114.2	14.4	136.2	24.2
12.00	0.1	0.3	0.0	0.0	0.2	0.6	0.2	0.7

The New Leader distribution means indicate that the 0.0-m position produced the highest application rates with all but the 112 kg/ha test slightly lower than the desired application level (table 5.2). This could be indicative of under application by this applicator. For spinner disc spreaders, the highest application rates should occur at the center of the pattern with rates decreasing as one moves away from the center. Spinner disc applicators generally rely on around 50% overlap for adjacent passes to bring up the covered area to the desired application level.

The mean distribution patterns for the Gandy indicated that it was over applying at all four rates (table 5.3). Theoretically, the calculated means at all transverse locations between  $\pm 5.33$  m should be equivalent. The Gandy relies only on overlap at the end of the boom or at the  $\pm 6.10$  m pan positions. Therefore, the mean patterns between  $\pm 5.33$  m show variability in distribution along the boom. The same theory exists for the AgChem; all means between the  $\pm 10.67$  m positions for each pattern should be similar. However, similar to the Gandy, variability exists for each pattern along the boom.

The AgChem produces some interesting results when comparing the +10.67 and -10.67 m positions (table 5.4). The applicator applied more at the +10.67 position than at the left -10.67 m position; sometimes over twice as much. The left side of the boom between -10.67 m and -2.67 m seems to be rather uniform in application when compared to the center and right side. The centers of each pattern are well above the desired rates. The right side also produces two peaks in the distribution pattern at the 5.33-

m and 9.33-m positions. These results indicate a distribution problem at the center and with the right boom of this applicator.

An easier means for comparing the distribution patterns is to plot the mean patterns. Figures 5.12, 5.13, and 5.14 depict the distribution patterns along with the 95% CI's for the New Leader, Gandy, and AgChem, respectively. A unique feature in these figures is symmetry seems to exist about the center of the patterns for the New Leader and Gandy but not for the AgChem. Symmetry is a desirable feature in that similar distribution is occurring on both sides for the spinner applicators since they rely on overlap from adjacent passes. There does seem to be a slight shift in the pattern peak for the 112-kg/ha test where the maximum occurred at the -2.3-m position rather than at the center. The New Leader peak at the center becomes more prevalent as the application rate increases. The 56 and 112 kg/ha tests for the Gandy appear to be rather uniform with variability occurring at for the higher rate tests. But for the most part, the distribution patterns show consistency from side to side for the New Leader and Gandy which coincide with the results reported by Fulton et al. (2001) for the Newton Crouch applicator.

The mean patterns produced by the New Leader could be described as triangular in nature. This shape coupled with the correct swath spacing generates a uniform distribution of material. These results are different than the W- and M- shaped patterns observed for the Newton Crouch (Fulton et al., 2001).

Figure 5.14 demonstrates a definite distribution problem for the AgChem at the center and right boom. This problem was consistent from pattern to pattern and increased with application rate. The cause for this problem is unknown. It would appear to be a metering issue because the mean pattern results on either side of the peaks, at the center and 5.33 m positions, are similar to the results for the left boom. If it was a deflector or tube problem, then points on either side the peaks would not be the same. Therefore, more material is being conveyed into the tubes feeding the distributors at these locations causing these peaks. Correction of these peaks would result in consistent patterns for the AgChem.

The 95% confidence intervals reveal that the New Leader (fig. 5.12) and AgChem (fig. 5.14) are consistent applicators. Contrary to the New Leader and the AgChem results, the Gandy demonstrates quite bit of distribution pattern variability about the mean patterns especially at the 224 and 336 kg/ha rates (fig. 5.13). From these figures, the AgChem seems to have the tightest 95% CI indicating that is the most consistent applicator, or rather not much variability exists about the mean patterns. The New Leader is a close second with the Gandy being a distant third. The smaller CI's for the New Leader and AgChem are very desirable because this indicates that these applicators produce consistent patterns at each test rate. However, even though they are consistent with not much variability about the mean pattern, pattern problems from either a metering and/or distribution irregularities (metering or flow obstruction) have a profound effect on application accuracy. Therefore, proper calibration and maintenance could produce very desirable and repeatable results from either of these applicators.

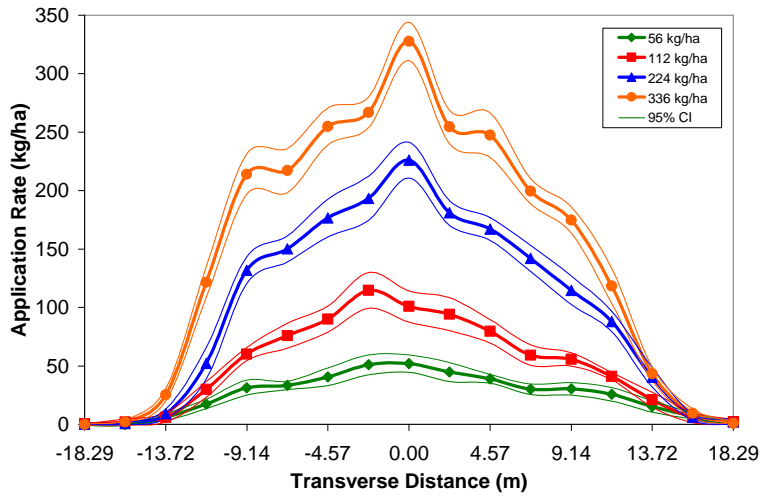


Figure 5.12. Characterized distribution patterns for the New Leader.

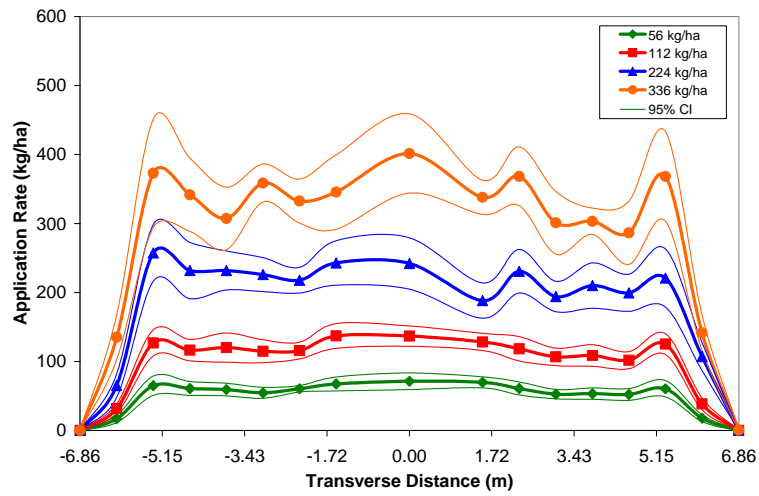


Figure 5.13. Characterized distribution patterns for the Gandy.

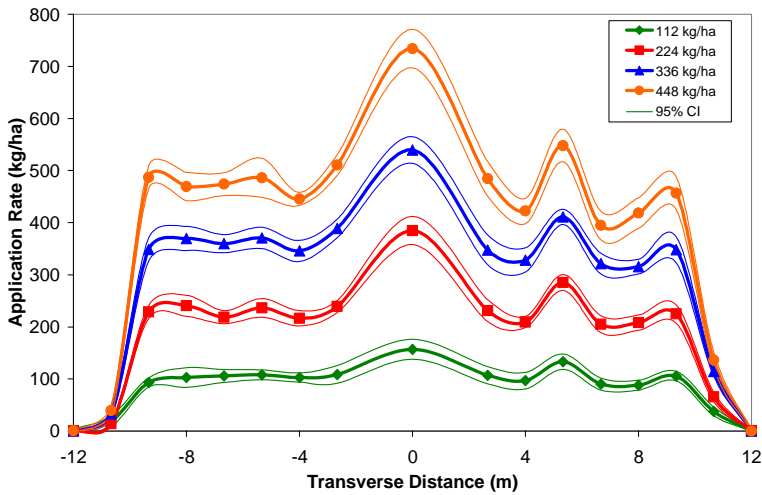
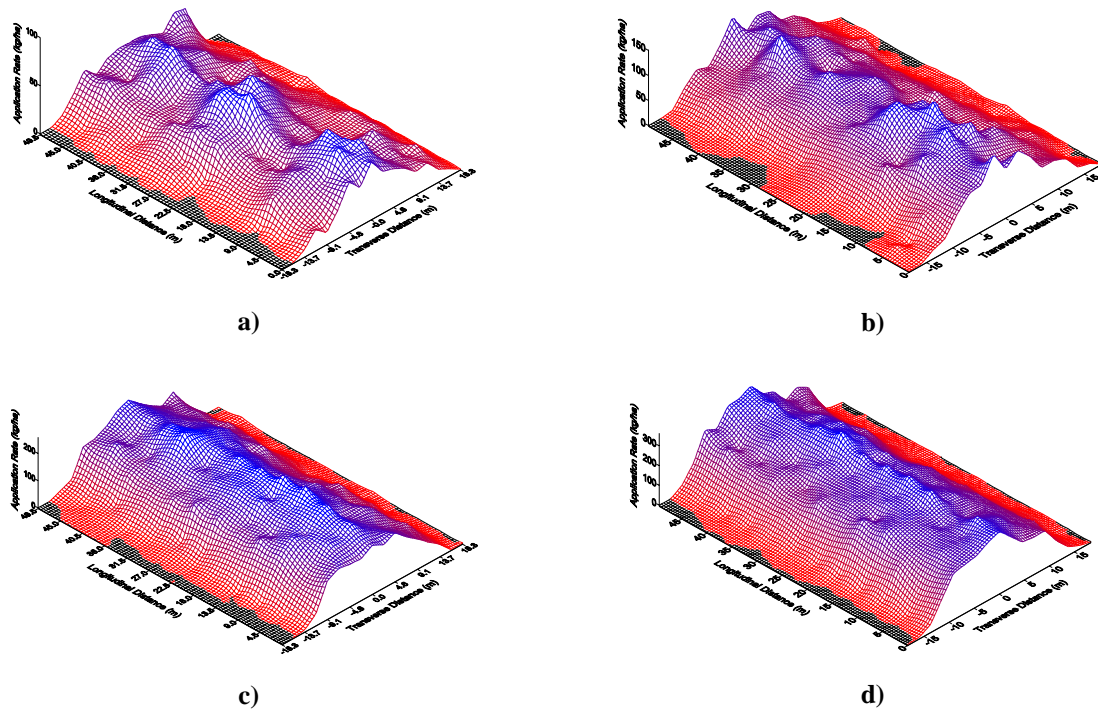


Figure 5.14. Characterized distribution patterns for the AgChem.

The causes for the variability in the Gandy at the UR tests are unknown. It would be recommended that this issue be investigated to improve its repeatability especially at the 224 and 336 kg/ha application rates. A deflector distribution or airflow problem seems to exist because during calibration, metering from the fluted rollers was consistent.

The distribution surfaces generated for all three applicators further demonstrates the above results. The surfaces for the New Leader show more variability in the lower two test rates (figs. 5.15a and 5.15b) with more consistency at the higher two test rates (figs. 5.15c and 5.15d). The Gandy surfaces demonstrate the most variability of the three applicators (fig. 5.16) with many peaks and depressions for all tests. The surfaces produced for the AgChem (fig. 5.17) show the repeatability of these patterns with the most variability occurring at the lowest test rate (fig. 5.17a).



**Figure 5.15. Uniform application surfaces for the New Leader - a) 56.0 kg/ha, b) 112.1 kg/ha, c) 224.2 kg/ha, and d) 336.2 kg/ha.**



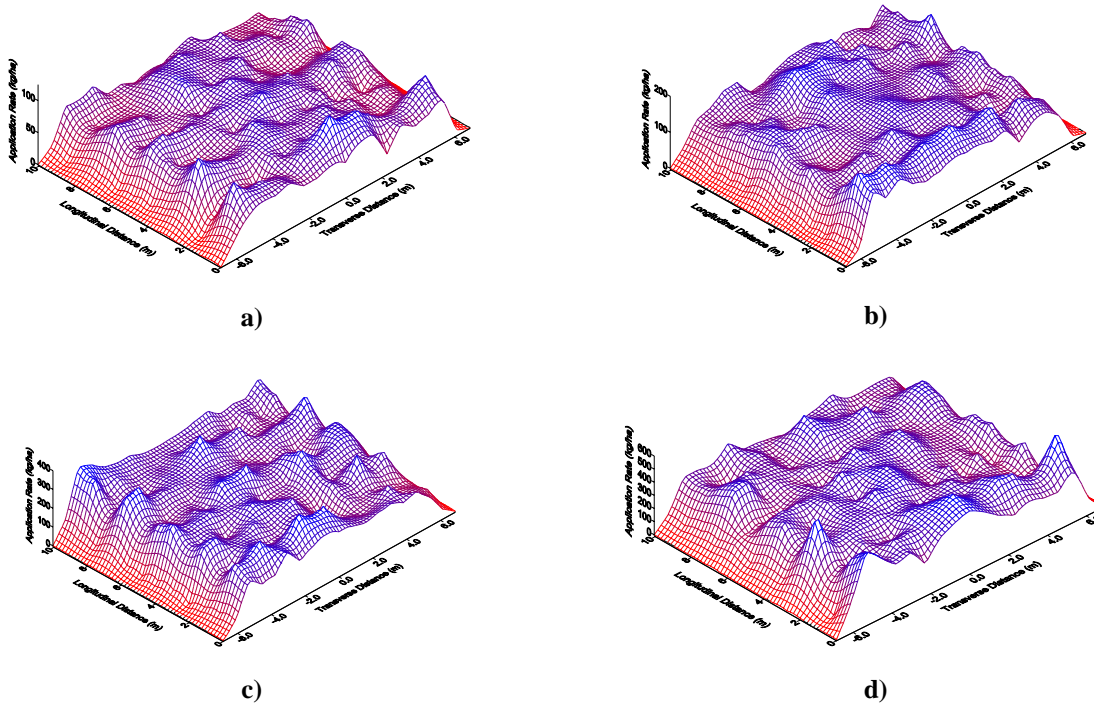


Figure 5.16. Uniform application surfaces for the Gandy - a) 56.0 kg/ha, b) 112.1 kg/ha, c) 224.2 kg/ha, and d) 336.2 kg/ha.

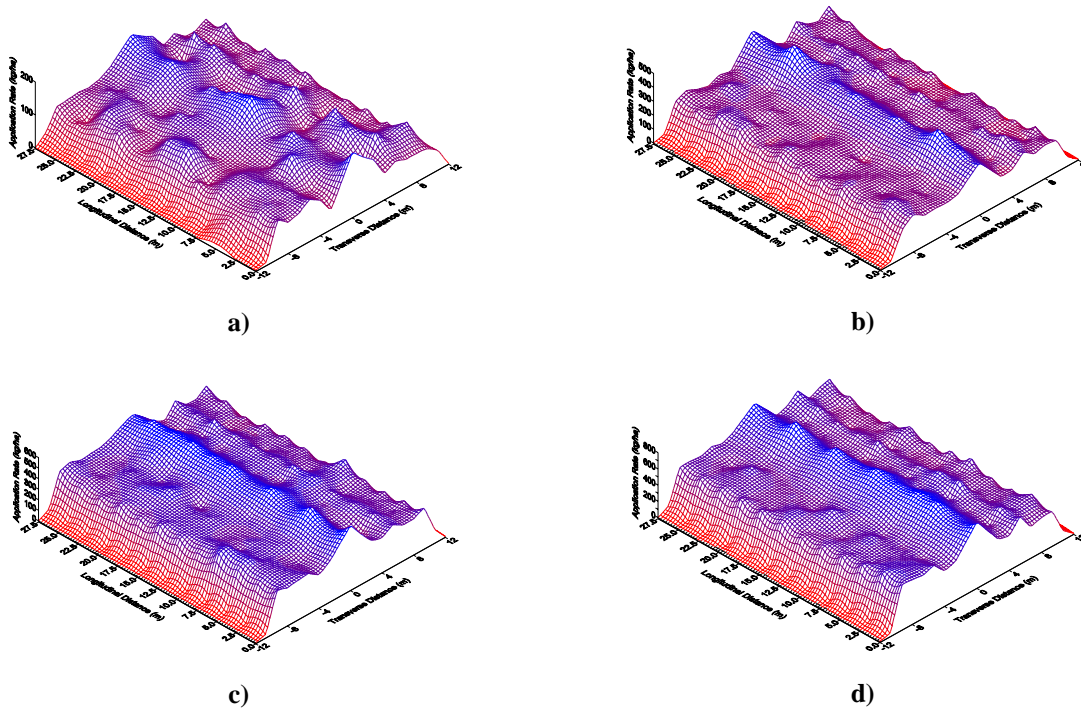


Figure 5.17. Uniform application surfaces for the AgChem – a) 112.1 kg/ha, b) 224.2 kg/ha, c) 336.2 kg/ha, and d) 448.3 kg/ha.

## OVERLAP ANALYSIS

The application accuracy for applicators can be assessed by generating the simulated overlap distribution patterns. These overlap patterns provide a means to estimate how single-pass distribution pattern variations affect field operation by accounting for overlap of parallel passes. These plots were created using the manufacturer recommended swath spacing reported for each applicator in table 5.1. In theory, the overlap data should produce a horizontal line indicating uniform distribution of material. The desired application levels are indicated with a dashed line in each figure to help show deviations in the estimated application.

Figure 5.18 presents the overlap results for the Newton Crouch. These estimated patterns were similar to those generated from the New Leader (fig. 5.19). Peaks formed in the middle with tails exceeding the desired level on the outside for the two higher rates. These results could indicate trends with spinner spreaders that need to be corrected to provide a more uniform distribution of material. An adjustment needs to be made by moving material from the outside of the pattern towards the center to fill in the valleys shown for the higher two application rates for both applicators. This distribution adjustment would generate a more uniform overlap pattern. The peaks occurring at the center of the pattern do meet or exceed the desired application levels for the higher two rate tests for the Newton Crouch unlike what was found with the New Leader. The trend appearing for these two applicators is that the patterns deviate more from the desired level with an increase in application rates. The 56-kg/ha test for the Newton Crouch and the 56 and 112-kg/ha tests for the New Leader produced the most uniform results with small deviations from the desired level and patterns being rather horizontal.

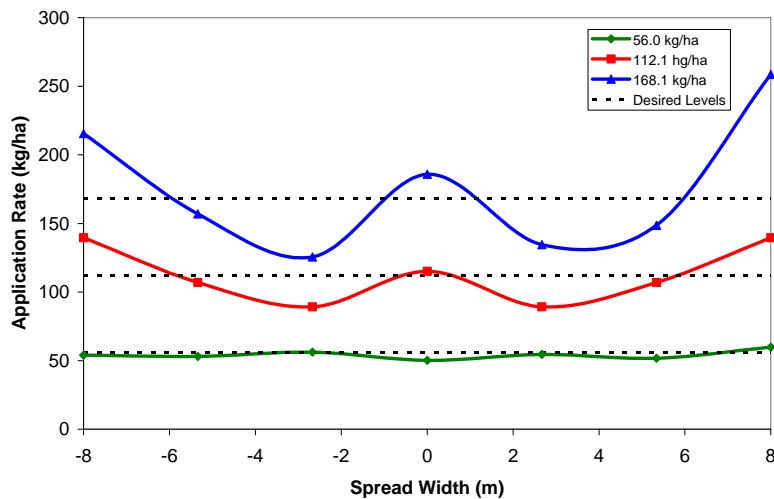
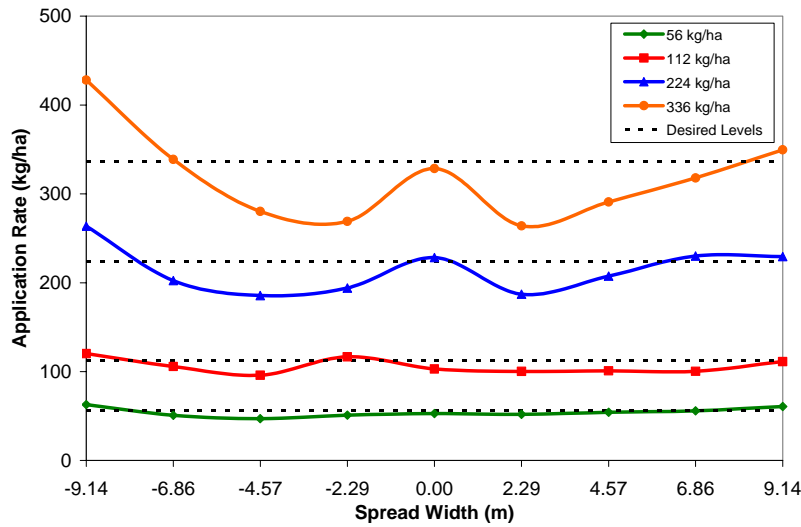
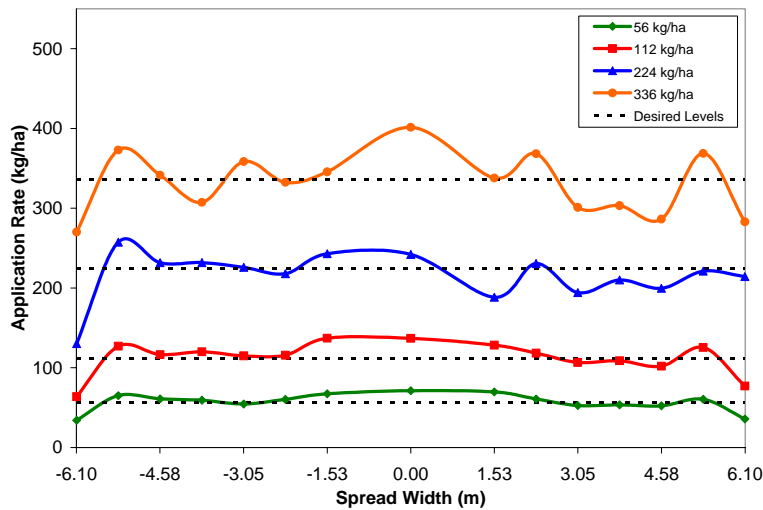


Figure 5.18. Simulated overlap distribution pattern for Newton Crouch.



**Figure 5.19. Simulated overlap distribution pattern for New Leader.**

The results for the Gandy show quite a bit of pattern irregularities about the desired level (fig. 5.20). The overlap pattern at all four rates fluctuates about the desired level except at either end of the pattern. As with the spinner spreader, more variability in the pattern occurred with an increase in application rate. A common feature with all four patterns is the under application at the tails ( $\pm 6.10$  m) and over application at the centers (0.0 m). Changes to the hardware of the Gandy to improve distribution could minimize the overlap variability. Overall, it appears on average that the Gandy applies close to the desired levels.



**Figure 5.20. Simulated overlap distribution pattern for the Gandy.**

The AgChem overlap patterns show quite of bit of variability as a result of pattern problems noted previously (fig. 5.21). The left boom seems to produce uniform distribution of material close to the

desired level. The center and the peak occurring at the 5.33 m position generate application errors. Similar to the Gandy, the tails on all the patterns under apply suggesting a smaller swath spacing to increase overlap. Correction of these under and over application issues could produce a uniform overlap pattern for the AgChem especially observing the consistency of the left boom. As with the other applicators, increasing the application rate increases pattern variability and distribution problems of the AgChem.

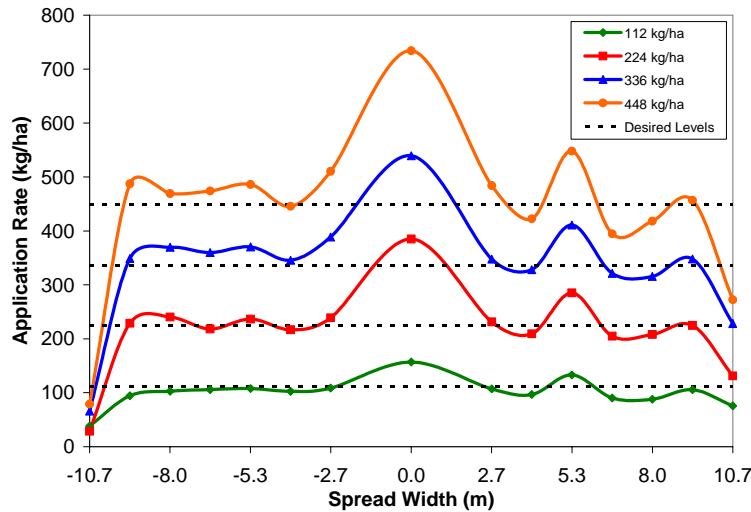


**Figure 5.21. Simulated overlap distribution pattern for the AgChem.**

The optimal swath spacing for each applicator was not investigated except for the Newton Crouch applicator (fig. 5.22). The over- and under-application occurring at the tails on the overlap patterns could possibly be corrected by adjusting the swath spacing for the applicators. The optimal swath spacing determinations for the Newton Crouch is difficult because of the distribution variability. The appropriate swath spacing should be selected by choosing the largest swath spacing which maintains CVs below 20%. Figure 5.22 indicates that the acceptable swath spacing would be 18.7 m for both 56 and 168 kg/ha application rates which are 2.7 m larger than the recommended 16.0 m swath spacing for the Newton Crouch applicator. However, the 168 kg/ha swath spacing illustrates the sensitivity in application variation with only a  $\pm 2.7$  m change from 18.7 m creating CVs greater than 20%. The 56 kg/ha curve generates CVs larger than 20% with a swath spacing greater than 18.7 m. Due to the high CVs ( $\geq 40\%$ ) for a swath spacing greater than 18.7 m, it is suggested a swath spacing of 16.0 m is appropriate and should continue to be used for the Newton Crouch applicator. This would provide a cushion for potential deviations in the swath spacing during application while keeping the CVs at somewhat of an acceptable level even though the 168 kg/ha curve produces CVs greater than 20% at 13.4 and 16.0 m spacings. The section of the optimal swath spacing needs to be fully thought out since it has a dramatic influence on the quality of spread adding another source of application error. Similar analysis could be performed for the

New Leader applicator to show that increasing the swath spacing could reduce the application rates at the margins for the overlap patterns while maintaining acceptable distribution.

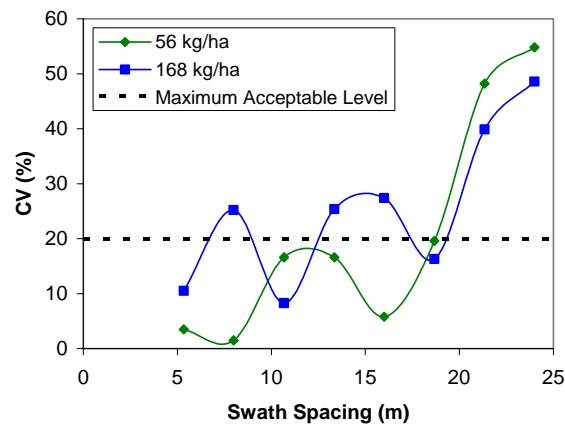


**Figure 5.22. The effect of swath spacing on the CV for the Newton Crouch applicator.**

The under-application occurring at the overlap pattern tails for the Gandy and AgChem applicators could be rectified by reducing the swath spacing thereby increasing overlap and the application rates at the tails. Increasing the swath spacing for the Newton Crouch and New Leader applicators would cause the opposite effect at the tails. Future analysis should be performed to establish the optimal swath spacing for each applicator and determine the influence of swath spacing on application variability.

Table 5.5 provides summary statistics for the simulated overlap patterns. The Gandy applied at slightly lower rates than the desired application level with the difference from the desired level increasing with an increase in rate. The CVs calculated for accuracy are a little higher than for precision but both decreased with an increase in application rate. All the computed CVs are within an acceptable range (< 20%) with the 336 kg/ha rate producing CVs below 15%. Though the Gandy performed satisfactorily, an adjustment to the controller to increase the application rate by approximately 5% would improve accuracy CVs. The under-application should have been determined and accounted for during calibration. The precision CVs represents pattern repeatability meaning setup variables other than a controller adjustment is needed to generate more uniform patterns.

The AgChem produced CVs between 25% and 34% which resulted from the identified distribution pattern issue. These CVs are above the acceptable value of 20%. The applicator did tend to under apply except for the 336-kg/ha test. Since the precision and accuracy CVs did not differ much, the pattern problem contributes most to the application errors and not deviation from the desired level. Rectifying the pattern problem would improve performance of the AgChem, producing CVs below 20%. In accordance with the observed consistency of this applicator, it would not be unreasonable to expect CVs around 15%.

The New Leader performed the best with all CVs below 20%, and three tests producing CVs less than 15%. The 56 and 112 kg/ha tests produced CVs less than 10%. However, since the accuracy CVs are slightly higher than those for precision, and the applicator tended to under apply for all tests, a slight improvement could be made by increasing the application rate by 5%. An adjustment of the controller would account for the under application.

**Table 5.5. Simulated multiple pass summary statistics (progressive method).**

Desired Rate (kg/ha)	Gandy				AgChem			
	Mean (kg/ha)	Diff. (kg/ha)	CV <sub>Prec</sub> <sup>1</sup> (%)	CV <sub>Acc</sub> <sup>2</sup> (%)	Mean (kg/ha)	Diff. (kg/ha)	CV <sub>Prec</sub> (%)	CV <sub>Acc</sub> (%)
56.0	55.2	-0.8	18.9	19.9	-	-	-	-
112.1	105.4	-6.7	17.9	19.7	100.9	-11.2	25.5	25.2
224.2	212.5	-11.7	14.0	17.9	219.2	-5.0	34.0	33.3
336.2	320.6	-15.6	11.6	12.0	339.3	3.1	29.3	29.6
448.3	-	-	-	-	445.5	-2.8	31.3	31.1
Desired Rate (kg/ha)	New Leader				Newton Crouch			
	Mean (kg/ha)	Diff. (kg/ha)	CV <sub>Prec</sub> (%)	CV <sub>Acc</sub> (%)	Mean (kg/ha)	Diff. (kg/ha)	CV <sub>Prec</sub> (%)	CV <sub>Acc</sub> (%)
56.0	54.2	-1.8	9.2	9.6	54.2	-1.8	5.8	6.6
112.1	106.1	-6.0	7.8	9.3	112.3	0.2	18.6	18.7
168.1	-	-	-	-	175.2	7.1	27.4	28.9
224.2	214.3	-9.9	12.0	12.4	-	-	-	-
336.2	318.6	-17.6	16.1	16.3	-	-	-	-

1. Precision of application represented by the CV computed using the mean simulated application rate for calculating the variance.
2. Accuracy of application represented by the CV computed using the desired application rate for calculating the variance.

The CVs for the Newton Crouch were good for the lower two rates but greater than 20% at 168-kg/ha. The 56 kg/ha test produced the best results for all the rates and applicators tested with a CV equal to 5.8%. The precision and accuracy CVs differed slightly but the main concern for this applicator is improving its performance at the 168.1 kg/ha level. A decrease in the mean application would help slightly but the main cause of error is the resulting W-shaped distribution pattern generating peaks at the center and tails of the overlap pattern (fig. 5.18). These peaks result in application rates in excess of the desired level. The overlap pattern also exhibits valleys between these peaks which are below the desired level. The desirable action would be to smooth this pattern out by depositing material from the peaks into the valleys. However, this could cause pattern problems at the lower application rates.

The Gandy, New Leader, and the Newton Crouch performed within the acceptable range at the lower two rates. The Newton Crouch at the higher rate and the AgChem at all rates require adjustments to

improve performance to within a desirable level. One note is that the overlap plots (figs. 5.18, 5.19, 5.20, and 5.21) tended to show more variation than the CVs, meaning that the CVs can be used to quantify distribution variability but overlap plots are needed to draw meaningful conclusions about the spread quality. Similarly, determination of precision and accuracy CVs are indicative of possible error sources.

Off target application can usually be corrected through calibration. Alternation of distribution patterns may require considerable effort up to and including design changes at the point of distribution. The existence of pattern shifts will require simultaneous adjustments of the hardware during rate transitions (Fulton et al., 2001 and Olieslagers et al., 1997). Such adjustments to the hardware, even if minor, could potentially generate additional sources of error. The goal is to strive for good precision and accuracy for this VRT equipment.

### DISTRIBUTION PATTERN COMPARISON

To compare the distribution patterns of the applicators tested and at different application rates, the data were standardized based on the mean application rate calculated using the simulated overlap analysis (table 5.5). For example, the New Leader pattern for the 56 kg/ha test was divided by 54.2 kg/ha. Figures 5.23, 5.24, 5.25, and 5.26 show the standardized patterns plotted for the Newton Crouch, New Leader, Gandy, and AgChem, respectively. These figures indicate that the AgChem patterns were the most consistent, with the New Leader and Gandy patterns being fairly consistent with minor deviations, and a noticeable shift was observed in the patterns of the Newton Crouch.

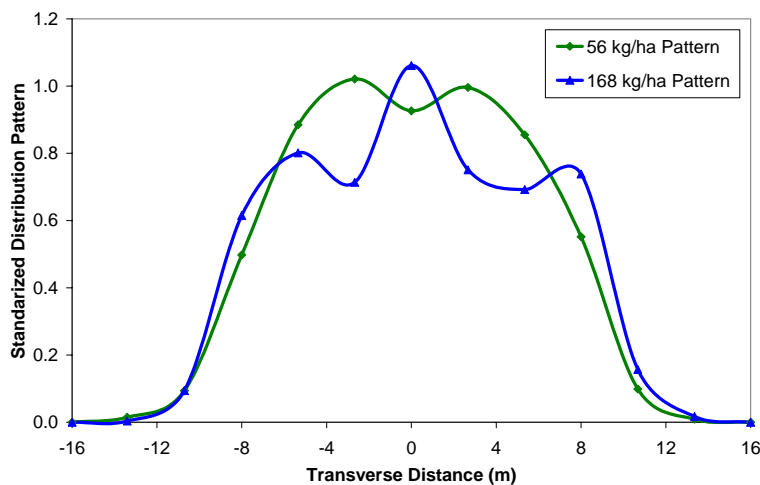


Figure 5.23. Standardized distribution patterns for the Newton Crouch.

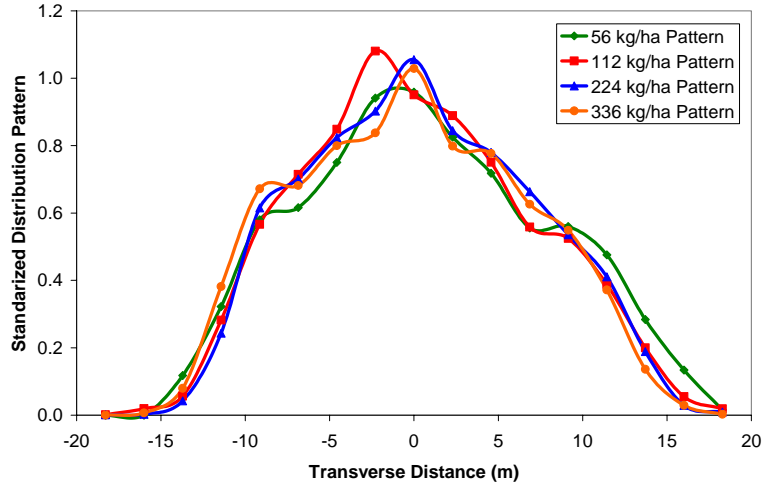


Figure 5.24. Standardized distribution patterns for the New Leader.

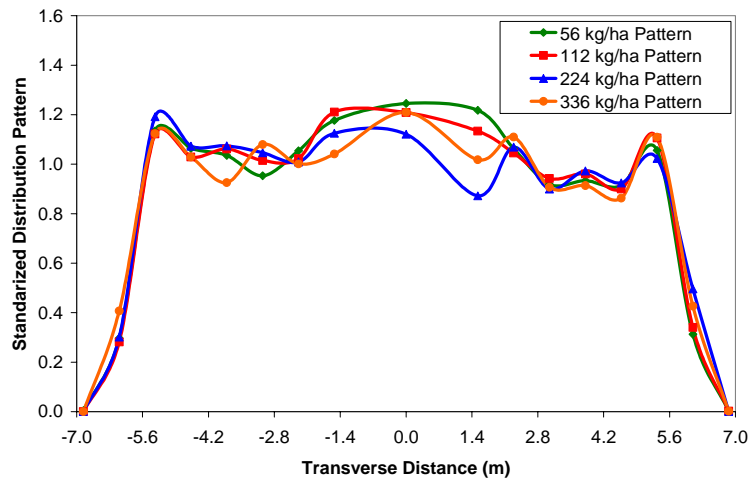


Figure 5.25. Standardized distribution patterns for the Gandy.

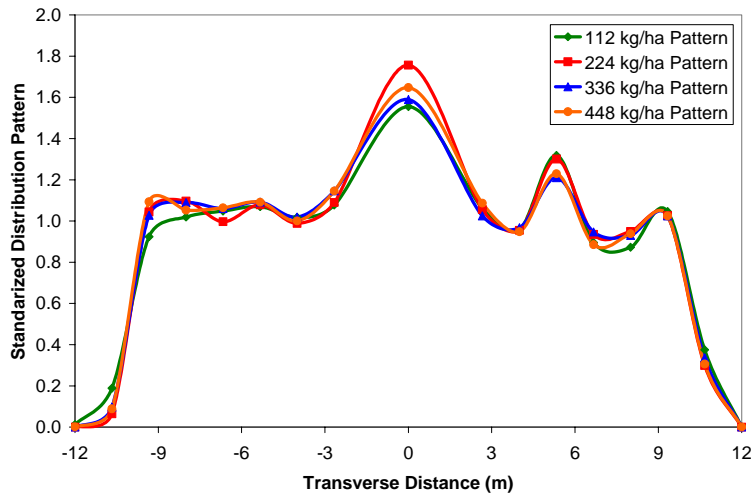


Figure 5.26. Standardized distribution patterns for the AgChem.



Pattern standardization also allows for quantifiable comparisons. An ANOVA was conducted using SAS's GLM procedure, enabling comparisons between rates across all positions (rate), transverse positions across all rates (position), and rates within each position (rate\*position) (table 5.6). The presence of pattern shifts is indicated by a significant interaction between rate and position.

**Table 5.6. ANOVA results for the various applicators.**

Applicator	Source	DF	SS	P-value
Newton Crouch	Rate	1	0.106	0.0092
	Position	12	63.46	<0.0001
	Rate by Position	12	2.08	<0.0001
	Error	312	4.8083	
New Leader	Rate	3	0.006	0.9250
	Position	16	95.245	<0.0001
	Rate by Position	48	1.340	<0.0001
	Error	748	9.0606	
Gandy	Rate	3	0.017	0.9440
	Position	16	120.554	<0.0001
	Rate by Position	48	1.9354	0.6773
	Error	748	33.6453	
AgChem	Rate	3	0.01573	0.8068
	Position	16	163.5132	<0.0001
	Rate by Position	48	0.9404	0.1537
	Error	748	12.0411	

For the application rates tested, there was a significant difference in the standardized amount applied by the Newton Crouch as judged by the interaction with rate ( $P=0.0092$ ) and position ( $P<0.0001$ ). The significant differences between the transverse positions are to be expected when evaluating the distribution pattern of a spinner disc spreader, since the pattern decreases with distance from the center. More importantly, however, a significant ( $P<0.0001$ ) pattern shift with rate change was confirmed for the Newton Crouch. The M-shaped pattern at the lower rate is in contrast to the W-shaped pattern at the higher rate.

In contrast, the New Leader did not show a significant ( $P>0.05$ ) pattern-rate interaction. However, as with the Newton Crouch, the New Leader demonstrated a highly significant ( $P<0.0001$ ) pattern-position interaction. These differences are again attributable to the characteristics of a spinner discs spreader. There was also a highly significant ( $P<0.0001$ ) interaction between application rate and position, indicating a possible pattern shift in the New Leader. Upon observation of the patterns, no discernable trend exists for this interaction in the New Leader patterns.

The apparent and significant pattern shift for the Newton Crouch implies that any calibration approach designed for this applicator should take into account these potential pattern shifts. Since no technology

currently exists to correct pattern shifts simultaneously with rate changes, this spreader should be calibrated at the median rate of the expected application range for which the applicator is predominately operated. Once an acceptable distribution is reached, then distribution tests should be performed at low and high rates within the anticipated operating range to quantify potential application errors. If the distribution patterns show deviations from one another, then it may be advisable to operate the spreader only within a specified range about the calibration rate. For example, if the spreader was calibrated at 200 kg/ha with desirable results, then additional pattern tests might conclude that the distribution pattern does not change between 150 to 250 kg/ha.

Though the New Leader exhibited a significant rate by position interaction ( $P < 0.0001$ ), observation of the standardized patterns showed no discernable trend that would necessitate separate calibration protocols in characterizing its patterns. Thus, a pattern test at an application rate within normal operating ranges would be sufficient to characterize the distribution pattern for the New Leader for a range of application rates.

The Newton Crouch is based on an older (circa 1980's) spinner disc, feed chain, and divider designs, whereas the New Leader is a newer system (2001). Advancements in the feed and distributing mechanisms may have helped to minimize pattern shifts; implying newer spinner disc technology may be void of pattern shifts under VR scenarios. This statement is made with caution as it is based on a sample size of one plus tests greater than 168.1 kg/ha were not conducted for the Newton Crouch.

Similar to the New Leader, the Gandy and AgChem pneumatic applicators showed no significant ( $P > 0.05$ ) rate effect. The pneumatic applicators also shared the spinner discs spreaders significant ( $P < 0.0001$ ) position effect. In contrast to the spinner discs spreaders, the Gandy and AgChem pneumatic applicators exhibited no significant ( $P > 0.05$ ) interaction between rate and position that would indicate pattern shifts.

The results from the pneumatic applicator tests indicate that application rate as a function of position varied ( $P < 0.0001$  for position). While this is to be expected in the spinner discs spreaders, such variability across the distribution pattern of pneumatic applicators is not desirable. For both pneumatic applicators, however, the standardized rate applied across all positions was very consistent ( $P > 0.05$  for rate). This suggests that minor design changes, hardware correction, or further calibration steps could correct differences across the transverse positions, resulting in applicators that are precise and accurate across the spread width. Furthermore, the absence of distribution pattern shifts can be expected within the rate ranges tested for each applicator. Such consistency in the distribution patterns of the pneumatic applicators is a desirable feature, as it implies that a single pattern test can be conducted for distribution pattern characterization. As a result, calibration time is reduced and applications could be more precise.

## RATE CHANGE RESPONSE

The rate transition surfaces are provided in figures 5.27, 5.28, and 5.29 for the New Leader, Gandy, and AgChem. The black line on each surface represents the desired rate transition line where the rate change should start (a delay time equal to zero). In most cases, a high percentage of the rate transition occurred within the tests areas. However, several of the transitions appear to either start or end outside the test area therefore the collection pan matrix did not fully capture the rate change (figs. 5.26b and 5.28b). Even though this occurred twice, a majority of the transition was captured for these particular tests, providing sufficient data to characterize the rate response.

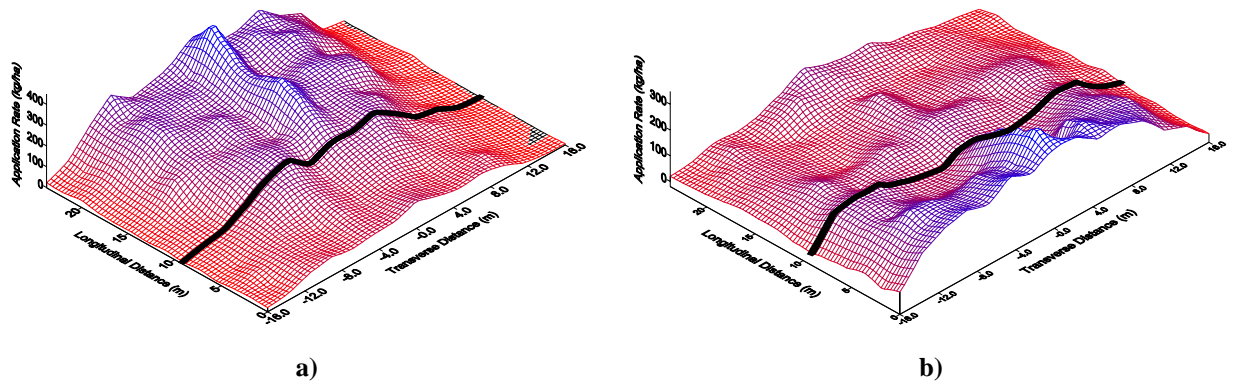


Figure 5.27. Rate transition surfaces for the New Leader; a) 112 to 336 kg/ha and b) 336 to 112 kg/ha.

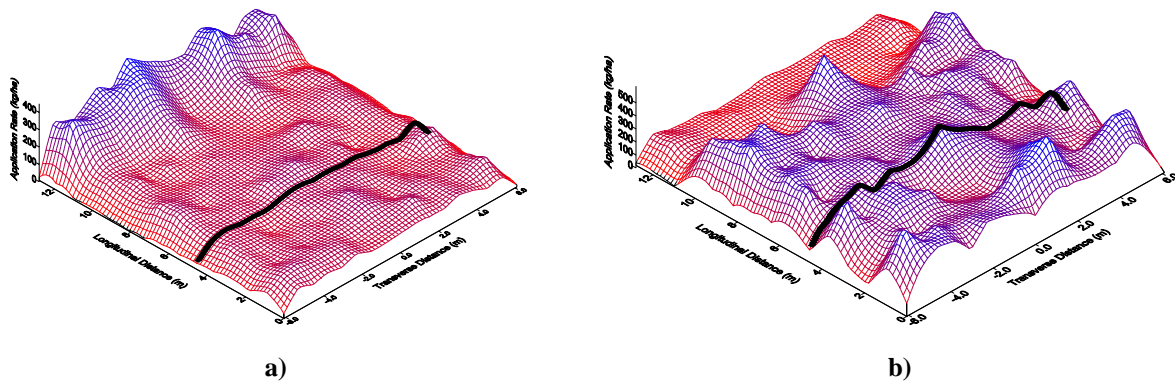
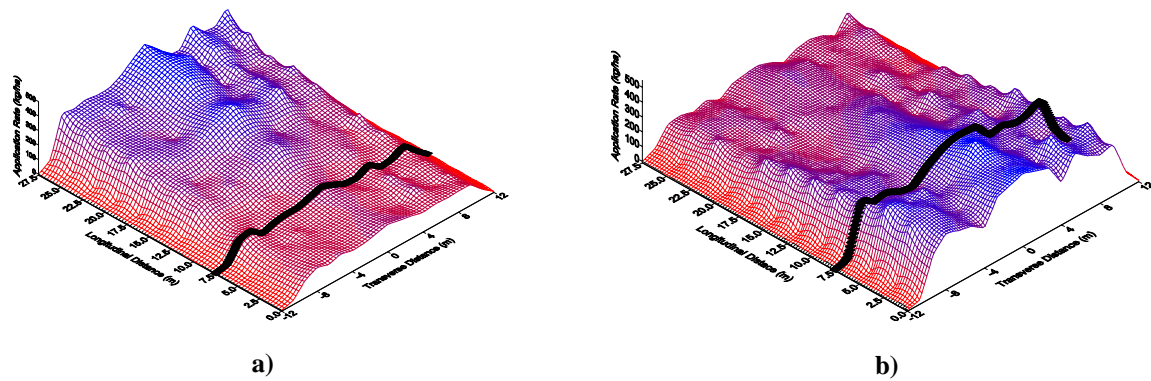


Figure 5.28. Rate transition surface for the Gandy; a) 112 to 336 kg/ha and b) 336 to 112 kg/ha.



**Figure 5.29. Rate transition surfaces for the AgChem; a) 112 to 336 kg/ha and b) 336 to 112 kg/ha.**

The New Leader surfaces indicate that the rate change started slightly before the desired rate transition line and occurred fairly quickly. However, the rate changes did not occur instantaneous. Thus, by adjusting the initiation time, rate transitions should occur at zone borders thereby reducing application errors by minimizing deviations from the desired rate. A majority of the 112 to 336 kg/ha transition for the New Leader appears to take place after transition to the next zone (fig. 5.27a). Conversely, a high percentage of the 336 to 112 kg/ha transition occurs ahead of the next zone. In theory, equivalent transition times for increasing or decreasing rate changes would be desired. There does appear to be a slight increase in deposition at the center of the applicator causing a distinct peak in the patterns at the higher rates for both tests.

The Gandy rate response occurred subsequent to crossing from one zone to the next (fig. 5.28). However, the rate transition occurred abruptly in both tests. The Gandy exhibited a much more rapid rate transition than the other applicators. The rate transition took about the same time in both tests and started around the same distance beyond transition to the next management zone. These results indicate that the VR system response was the same in both tests, a desirable characteristic for any VRT applicator. The delay in the rate response is a feature that most VRT software packages should be able to correct for with the operator entry of “look-ahead.” The proper “look-ahead” feature would shift the rate change in time to coincide with zone boundaries.

The rate transitions for the AgChem (fig. 5.29) were of longer duration than those for the New Leader and Gandy. Contouring of prescription maps for the AgChem was in part responsible for this delay. The rate transition started at different locations for each test. The 112 to 336 kg/ha rate transition started around the zone boundary whereas the 336 to 112 kg/ha transition started before the spreader boom crossed the boundary (fig. 5.29a). The high to low transition took longer than the low to high transition.

The start and end distances for the rate transitions were established by using the same four-parameter, sigmoidal regression function to model the rate change as outlined by Fulton et al. (2001). A sigmoidal fit best described both the increase and decrease rate transitions for the New Leader, Gandy, and AgChem unlike the linear response observed for the high to low transition for the Newton Crouch (Fulton et al., 2001). Several different types of regression functions were used to model the step rate change in application rate but the 1st order sigmoidal fit continually produced the best results. Sigma Plot 8.0 (Sigma Plot, 2001) was used to fit the sigmoidal functions to each transverse position of all rate transition tests for the New Leader, Gandy, and AgChem. Since little or no material was collected in the outer pans for the applicators, the two outer rows of pans for the New Leader and AgChem and the three outer rows of pans for the Gandy were omitted from this analysis. Tables 5.7, 5.8, and 5.9 provide the  $R^2$  values for all the sigmoidal fits for the New Leader, Gandy, and AgChem. A majority of the  $R^2$  values were in the 0.87 to 0.94 range indicating a good regression fit. The Gandy 336 to 112 kg/ha transition produced the worst fits with several  $R^2$  below 0.87 (table 5.8) which is expected when looking at the application variability during this test (figure 5.28b).

**Table 5.7. Sigmoidal regression results for New Leader rate transitions.**

Transverse Position (m)	112 to 336 kg/ha Transition	336 to 112 kg/ha Transition
	$R^2$	$R^2$
-13.7	0.81	0.95
-11.4	0.92	0.92
-9.1	0.93	0.97
-6.9	0.94	0.92
-4.6	0.95	0.90
-2.3	0.94	0.86
0	0.92	0.95
2.3	0.90	0.92
4.6	0.95	0.93
6.9	0.92	0.95
9.1	0.84	0.97
11.4	0.93	0.85
13.7	0.71	0.87

**Table 5.8. Sigmoidal regression results for Gandy rate transitions.**

Transverse Position (m)	112 to 336 kg/ha Transition	336 to 112 kg/ha Transition
	R <sup>2</sup>	R <sup>2</sup>
-5.33	0.91	0.74
-4.57	0.93	0.72
-3.81	0.93	0.84
-3.05	0.93	0.79
-2.29	0.95	0.88
-1.52	0.96	0.82
0.00	0.73	0.44
1.52	0.83	0.95
2.29	0.91	0.85
3.05	0.91	0.87
3.81	0.97	0.74
4.57	0.82	0.63
5.33	0.84	0.56

**Table 5.9. Sigmoidal regression results for the AgChem rate transitions.**

Transverse Position (m)	112 to 336 kg/ha Transition	336 to 112 kg/ha Transition
	R <sup>2</sup>	R <sup>2</sup>
-9.3	0.93	0.81
-8.0	0.94	0.93
-6.7	0.90	0.92
-5.3	0.87	0.78
-2.7	0.93	0.92
0	0.94	0.90
2.7	0.89	0.93
5.3	0.92	0.92
6.7	0.94	0.89
8.0	0.91	0.87
9.3	0.97	0.89

Figure 5.30 illustrates the procedure for defining the start and end distance for the rate transitions. The start and end points were defined by using a 5% settling time. This corresponds to a 5% and 95% change in the overall rate transition defined by the sigmoidal regression minimum and maximum rates on the asymptotic tails. A 5% settling time was chosen because of the variability in the observed data. The minimum and maximum rates estimated for the 0.0-m New Leader transverse position were 16.9 kg/ha and 335.5 kg/ha, respectively (fig. 5.30). Therefore, 5% and 95% of this range were 119.3 kg/ha at 5.8 m

and 343.1 kg/ha occurring at 15.0 m, respectively. In return, the delay distance can be calculated by subtracting the desired from the start distance. Similarly, the distance for a rate transition equals the end distance minus the start distance. These distances can then be converted into time using the applicator ground speed (table 5.1) thereby estimating the “delay time” and “rate transition time.” The delay and transition times determined for each transverse position were averaged to calculating these times for the low to high and high to low tests for each applicator.

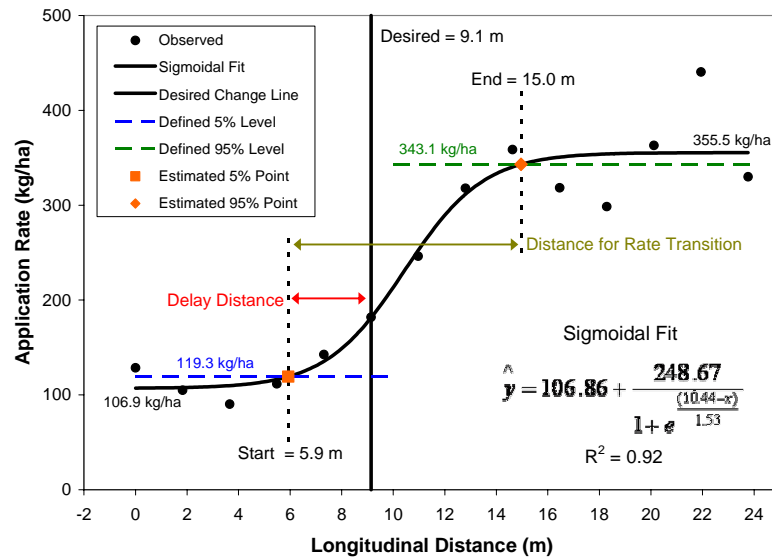


**Figure 5.30. Example illustration for characterizing rate change dynamics (New Leader 0.0 m transverse position).**

The transition and delay times for the Newton Crouch’s 56 to 168-kg/ha test were computed in the same manner as for the other applicators since sigmoidal in nature. The characterization method was slightly modified for the 168 to 56 kg/ha transition to account for the linear makeup of the transition identified by Fulton et al. (2001). In this case, it is hard to determine from the rate transition surface whether the complete transition was captured within the pan matrix. The mean 56 and 168-kg/ha pattern data were used to define the upper and lower limits of the transition. A 5% settling time was again utilized to define the start and end positions to maintain similarity between analyses. The outer three rows of pans ( $\pm 16.0$  m,  $\pm 13.4$  m, and  $\pm 10.7$  m) were omitted from these analyses for the same reasons as with the sigmoidal analysis. For the  $\pm 10.68$  transverse positions, these two rows of pans did receive material but a linear fit generated a slope equal to or near zero. Thus, these two rows did not reflect the rate transition. The  $R^2$  values from the regression analysis for the Newton Crouch are presented in table 5.10.

**Table 5.10. Regression results for the Newton Crouch rate transitions.**

Regression Transverse Position (m)	Sigmoidal	Linear
	56 to 168 kg/ha Transition R <sup>2</sup>	168 to 56 kg/ha Transition R <sup>2</sup>
-8	0.95	0.82
-5.3	0.83	0.76
-2.7	0.94	0.63
0	0.88	0.91
2.7	0.97	0.79
5.3	0.83	0.82
8	0.71	0.76

The rate response characteristics were different for the New Leader for increasing versus decreasing rate changes (table 5.11). The rate transition time nearly doubled for the 336 to 112-kg/ha transition. The delay time for both tests were negative meaning that the rate change started before zone transition but the delay started 2.6 seconds sooner with decreasing rates.

**Table 5.11. Rate transition characteristics.**

Applicator	Test	Transition Time (sec)	Delay Time (sec)
New Leader	112 to 336 kg/ha	3.6	-0.9
	336 to 112 kg/ha	7.1	-3.5
Gandy	112 to 336 kg/ha	0.4	1.5
	336 to 112 kg/ha	0.3	1.2
AgChem	112 to 336 kg/ha	6.6	0.1
	336 to 112 kg/ha	12.4	-4.3
Newton Crouch	56 to 168 kg/ha	6.7	3.3
	168 to 56 kg/ha	10.6	1.6

The Gandy demonstrated the most consistency with nearly the same rate transition and delay times (table 5.11). This is a desirable feature of the Gandy VR system since a single, proper delay time could adjust the rate change to occur at the proper time. The VR control system of the Gandy also produced the quickest rate transition time. The transitions times were under 0.5 seconds.

The contouring effect of the prescription maps (AgChem) resulted in longer response times (table 5.11). The rate transition time nearly doubled when decreasing the rate. A similar trend observed with the



New Leader for decreasing rate transition. The delay time for the 112 to 336 kg/ha rate change was close to zero whereas the rate transition started about four seconds ahead of the zone boundary. Due to the magnitude of the rate transition times, it would be desirable to have the rate transition be split between management zones. This could be the reason SGIS contours prescription maps to help minimize errors at zone boundaries. It was difficult to determine whether the contouring effect or the Falcon control system had a significant impact on the transition times.

The transition tests for the Newton Crouch were performed between 56 and 168 kg/ha (Fulton et al., 2001). Similar to the New Leader, and AgChem, the calculated times for the Newton Crouch are different for the two tests. The transition time took almost four seconds longer for the 168 to 56-kg/ha test but the transition started 1.7 seconds before the 56 to 168-kg/ha test. These results show inconsistency in rate response for this VR control system. While the magnitude and rates for the transitions differed from the other applicators, it would be expected that the transition time would be longer. In general, the VR control systems response for the Gandy and New Leader are faster than that of the Newton Crouch's. This could be attributed to the control valve style (Rawson system) on the New Leader and Gandy. These results indicate that appropriate valve technologies can minimize rate transition times.

One similarity between the New Leader, AgChem, and Newton Crouch VR systems was that the transition time took longer when decreasing the rate than increasing it. In theory, it would be desirable for the transition times to be similar if not equivalent. In two cases, this time nearly doubled. The delay time also occurred earlier for the decreasing rate changes in contrast to the increasing rate changes. For the New Leader and AgChem, this delay occurred 4.0 seconds shorter.

The rate response characteristics are important parameters to be considered by VR software developers and users of VRT equipment. While the equipment tested in this investigation varied from applicator to applicator, some important characteristics resulted that could have implications for future system designs and calibration of VRT equipment. These results also emphasize the need for the development of a standard pertaining to VRT systems plus re-visitation to the current UR standard.

Ideal rate transition times of zero would result in an instantaneous transition or perfect step response. In reality, delay times between 0.0 and 1.0 seconds or even up to 1.5 seconds would be highly desirable for a VR control systems. In some cases where the rate transition time is large, applicator ground speed may need to be limited to minimize application errors. For the AgChem, SGIS software always contours the prescription map which alters rate transition time for this equipment. The transition times for rate changes dictates management zone resolution especially if they become large. For example, the 10.6 second transition time for the Newton Crouch when decreasing the application rate calculates into 60 m when driving at the test speed of 20.4 km/hr (table 5.1). A 0.40 ha zone equates to 63.4 m by 63.4 m

square indicating that this rate change would occur almost over the entire length of the zone. Therefore, the rate transition time can influence the selection of management zone dimensions.

Varying delay times can be accommodated in software using the “look-ahead” feature. The proper delay or “look-ahead” time would ensure rate changes occur at the appropriate time. This assumes that delay times for rate increases and decreases are the same for a VR system. For example, a single rate delay time could be used for the Gandy to shift the rate transition to the appropriate point in time. On the other hand, differences in the delay times with the other applicators indicates that two “look-ahead” times made be needed to correctly adjust the rate transition timing. Currently this is not an option in most VR software packages. It is important to note that differences in the delay time would be expected depending on the magnitude of the rate transition, adding more complexity to the proper selection of delay times. Further research is required to address these questions and improve application accuracy.

## **SUMMARY**

Distribution patterns were characterized from various VR granular applicators to assess application precision and accuracy. The New Leader produced consistent triangular shaped patterns at all test rates unlike the pattern shifts observed from the Newton Crouch (Fulton et al., 2001) during VR testing. The Gandy, a pneumatic applicator, produced a consistent pattern at all test rates but exhibited high variability within each pattern for a particular rate. The AgChem, another pneumatic applicator, produced the most consistent pattern from test to test but exhibited distribution problems with the right and center boom sections on the applicator. All the distribution patterns were symmetric about their center with greater pattern variability occurring at higher application rates.

Simulated multiple-pass overlap distribution patterns were developed to better assess spread quality. The patterns reported by Fulton et al. (2000) were incorporated into this analysis for the Newton Crouch applicator. The New Leader produced desirable results with CVs less than 20% with the three lower rate tests having CVs below 15%. This applicator did under apply by around 5% for all tests. The Newton Crouch performed well at the 56 and 112-kg/ha levels with the 56-kg/ha test having the lowest CV around 6% for any of the tests conducted. However, for the 168-kg/ha test, the Newton Crouch had a CV near 30% indicating poor performance as a result of the W-shaped distribution pattern. This applicator under applied by 3% at the 56-kg/ha rate and over applied by 4% at the 168-kg/ha rate. The Gandy performed within acceptable limitations with CVs under 20% for all tests. The CVs did decrease with an increase in application rate but the applicator was under applying by about 5% at all rates. The overlap patterns highlighted the distribution pattern problem for the AgChem with CVs between 25% and 34%. These CVs are well above the accepted 20% level. However, because of the consistency of this applicator, the CVs would be expected to fall below the acceptable level if the pattern irregularities are resolved.

The simulated overlap plots illustrated similar spread patterns for the New Leader and Newton Crouch. Both applicators produced uniform patterns at the lower test rates but produced peaks at the center and on the tails of the overlap patterns. Adjustments are needed to each applicator to generate more uniform overlap patterns as observed at the lower rates. The Gandy overlap plot showed that the distribution occurred about the desired level with under application at the margins of the boom where overlap occurs. The Gandy also seemed to have less distribution variability at the lower rates when compared with the higher rates which contradicts the CV results. The overlap plots for the AgChem show the magnitude of the pattern problem and under application at the boom margins suggesting a reduced swath spacing. Hence, distribution plots should accompany the calculated CVs to assess application quality during calibration and any field tests. Additionally, CVs should be computed for both accuracy and precision to help identify possible sources of error. These results suggest that spread quality could be improved for all three applicators.

The standardized, single-pass distribution patterns were individually compared statistically. These comparisons supported no difference existed in the patterns produced by either pneumatic applicator (Gandy and AgChem). The consistency in distribution patterns by each of these applicators means that a single-pass pan test may be sufficient to represent the patterns at all rates. The New Leader analysis also supported no difference in its four patterns, but the analysis did show that rates within some transverse positions were significantly different. However, similar to the pneumatic applicators, one distribution test could be performed to characterize the expected patterns. For the other spinner disc spreader (Newton Crouch), a significant difference was found between patterns verifying a pattern shift occurred between 56 and 168-kg/ha as suggested by Fulton et al. (2001). Pattern shifts are undesirable and indicate that several tests would be required for characterizing distribution patterns at different rates. Caution should be taken when calibrating an applicator exhibiting this attribute in order to minimize errors. However, these results suggest that one test can characterize the distribution patterns for pneumatic applicators while more intensive testing might be required for spinner spreader pattern characterizations. Specifying only one test for pneumatic applicators reduces testing and simplifies the number of patterns used within the “as-applied” data model.

Rate response tests demonstrated that VR system for the Gandy was quick and consistent for both the increasing and decreasing rate transitions. While the time for a rate transition was quick, the Gandy did have around a 1.2 to 1.5 second delay time for the rate change to start. The other applicators were inconsistent in their rate responses producing differing delayed transition times when comparing low to high transitions with high to low. The transition and delay times were different for both tests. The rate transition for the AgChem occurred over a longer period of time compared to the New Leader and Gandy probably due to the contouring of management zone boundaries during creation of prescription maps. The

Newton Crouch transition times for both tests were lengthy considering only a change of 112.1 kg/ha when compared with a 224.2 kg/ha change for the other applicators. Based on these results, the rate transition for the Newton Crouch took longer than those for the New Leader and Gandy. One possible reason for the quicker response time could be control valve styles used on the New Leader and Gandy.

The “look-ahead” feature of most software applications can be utilized to correct for consistent delay times (low to high and high to low). Differing delay times whether increasing or decreasing, could mean that two “look-ahead” times are required to minimize application errors. Accounting for both rate transition and delay times is not a current feature provided by VRT software developers. However, if the industry expects to produce accurate VRT systems, then consideration of both rate transition and delay times are needed. In conclusion, the results of this investigation can help equipment and software manufacturers develop more accurate products and assist users in properly calibrating VRT equipment. This work highlights the need for precise and accurate applications and consistent transition and delay times from VRT equipment.

## **CHAPTER SIX**

# **AS-APPLIED SPATIAL DATA MODEL FOR EVALUATION OF VARIABLE-RATE FERTILIZER APPLICATION ACCURACY**

### **INTRODUCTION**

Computers, the Global Positioning System (GPS), geographic information systems (GIS), sensors, and other electronic devices are typical tools used on the modern day farm. Electronics have revolutionized the way farmers cultivate the land today. Precision agriculture (PA) is the term used to describe the spatial management of within field variability. Technology, competition, and environmental concerns along with public policies are the three driving forces bringing PA to North America (Lowenberg-DeBoer and Swinton, 1997). PA offers farmers the opportunity to improve profitability through spatial management while promoting good stewardship of the land. One of the drawbacks to PA has been the rapid evolution of new technology without proper assessment and understanding for its use. Most of the technology is well intentioned but the quality of performance in terms of spatial management is poor in terms of actual variability.

The growth of variable-rate technology (VRT) has led to site-specific management (SSM) of fertilizers, pesticides, herbicides, and other inputs on the farm. Variable-rate (VR) fertilization was one of the first areas where VRT was implemented since many believed this was where potential profits could be captured. This notion was based on factors such as redistribution of fertilizer inputs for more efficient use by crops while minimizing over- and under- application. While VRT is being used by farmers, few have the ability to evaluate its performance to help determine whether there is a positive benefit to their operation. Currently, only a few ad hoc procedures exist to speculate on the performance of the equipment but none provide feedback about the spatial distribution of material during field application.

An initial attempt with some success was made by Fulton et al. (2003) to create “as-applied” maps depicting the distribution of granular fertilizer. These maps were generated using a spatial data model using GIS functionality but shortcomings of the methodology were noted. This investigation serves to incorporate these pattern characterizations of Chapter Five plus make modifications to the “as-applied” spatial data model. Field data were collected to validate the revised spatial model. The model was used to generate “as-applied” surfaces as a means of quantifying the performance of VRT applicators.

## **SUB-OBJECTIVES**

The goal of this investigation was to improve and evaluate the “as-applied” spatial data model developed by Fulton et al. (2003). The specific objectives were:

- To refine the “as-applied” spatial data model,
- To validate the revised spatial model using various types VRT applicators under field operation, and
- To assess VRT errors using the generated “as-applied” surfaces.

## **METHODOLOGY**

Several features of the original “as-applied” spatial model were maintained. Model code development was continued by using Avenue Script in ESRI’s ArcView<sup>®</sup> 3.X (ESRI, 2001) environment. Users must input an offset to compensate for VR system latency and GPS antenna offset (fig 6.1a). Fulton et al. (2003) provided details on the function of the offset distance and its implementation within code. The process of converting the accumulated mass to an application rate was preserved for the Newton Crouch. The code and process for specifying the “as-applied” surface using a grid point file was not altered. Changes to the spatial model included incorporating the characterized distribution patterns and applicator features reported in Chapter 5, a new method for defining the area associated with an application point, a new graphical user interface (GUI), and automation of re-projecting the FAFs.

## **APPLICATOR DESCRIPTION FILE**

A unique applicator description file (ADF) was built for each of the applicators (AgChem, Gandy, and New Leader) based on the results of Chapter 5. An ADF provides the distribution patterns and particular features for an applicator. ADF’s are also unique to the material applied.

The results in Chapter Five suggest a single pattern characterization test could be performed for pneumatic applicators but multiple patterns would be required for spinner spreaders to accommodate patterns shifts with rate changes. An applicator exhibiting a consistent triangular or Gaussian pattern shape over all rates would simplify the ADF as only one pattern is required. A more extensive ADF would be required for an applicator exhibiting pattern shifts such as the Newton Crouch. Minor setup changes to an applicator or different products would warrant new ADF’s that reflect the altered patterns. For this investigation, multiple ADF’s were generated for the New Leader, Gandy, and AgChem to simulate various pattern strategies where a series of patterns for differing application rates were considered similar in shape. Selection of single patterns was performed in two ways. First, by randomly selecting one of the four patterns from each applicator and secondly, averaging the four standardized patterns to generate a single pattern. The random selection of a single pattern was performed using

Microsoft Excel to generate a pseudorandom whole number between 1 and 4. This resulted in the 112.1 kg/ha standardized pattern being selected for the Gandy and the 224.2 kg/ha standardized pattern for the New Leader. Initial validation was performed by using all patterns with the additional ADF files used to determine if the results changed.

The standardized patterns defined in Chapter 5 for the New Leader (fig. 5.23), Gandy (fig. 5.24), and AgChem (fig. 5.25) are the main features of the ADF. A specified range was defined by for each pattern (table 6.1). The Newton Crouch standardized patterns and ranges (table 4.2) were reported by Fulton et al. (2003). The format of these patterns was modified to fit the new ADF. Table 6.2 contains additional important features of each applicator. An acronym was developed for each applicator and was used in the ADF name. The number of sub-polygons differs for the applicators and is based on the number of pans used during the uniform-rate (UR) single-pass test (Fulton et al., 2001 and Chapter 5). The spread width represents the total application width used when performing the UR, single-pass tests for each applicator. Each pan represents an area specified by the pan spacing, 2.29 m for the New Leader; the product of pan spacing and the number of transverse pans (number of sub-polygons) determines the spread width: 38.9 m for the New Leader. The spread width is unique for each applicator and defines the outer sub-polygon borders for each FAF data point.

**Table 6.1. Application ranges.**

<b>New Leader and Gandy</b>		<b>AgChem</b>	
<b>Test Rate (kg/ha)</b>	<b>Range (kg/ha)</b>	<b>Test Rate (kg/ha)</b>	<b>Range (kg/ha)</b>
56.0	0.0 to 84.1	112.1	0.0 to 168.1
112.1	84.2 to 168.1	224.2	168.2 to 280.2
224.2	168.2 to 280.2	336.2	280.3 to 392.3
448.3	280.3 to 672.5	448.3	392.4 to 672.5

The ADF's were developed as database files (.dbf). The first row of each file contains column headings with subsequent rows corresponding to characterized standardized pattern. The first two columns were labeled as "low" and "high" representing the minimum and maximum of the ranges presented in table 6.1. The number of succeeding columns was based on the total number of sub-polygons for each applicator. These columns were labeled consecutively starting at one and concluding with the number of sub-polygons for an applicator (table 6.2). Column one represents the far left sub-polygon with the largest number representing the outside right sub-polygon. Each number was also tagged with the applicator's acronym (table 6.3). Appendix A contains the ADF's for the Gandy, New Leader, and

AgChem applicators. Currently, the other applicator characteristics (table 6.2) are contained in a separate ADF named “applicator characteristics.dbf.” This file includes three columns: applicator type (Aptype), number of zones or sub-polygons (Numzones), and spread width (Width). This file can be easily incorporated into the other ADF’s to create a single ADF for describing the features of an applicator.

**Table 6.2. Applicator characteristics.**

<b>Applicator</b>	<b>Acronym</b>	<b>No. of Sub-Polygons</b>	<b>Spread Width (m)</b>	<b>GPS Antenna Offset (m)</b>
AgChem AirMax 2000	AC	19	25.3	5.5
Gandy Orbit-Air	G	19	14.5	2.4
New Leader L3020G4	NL	17	38.9	4.9
Newton Crouch	NC	13	34.7	4.9

**Table 6.3. Example ADF for the New Leader: NL.dbf (only left half of file shown).**

<b>LOW</b>	<b>HIGH</b>	<b>NL1<sup>1</sup></b>	<b>NL2</b>	<b>NL3</b>	<b>NL4</b>	<b>NL5</b>	<b>NL6</b>	<b>NL7</b>	<b>NL8</b>	<b>NL9</b>	<b>NL10<sup>2</sup></b>
0.0	84.1	0.00	0.00	0.12	0.32	0.58	0.62	0.75	0.94	0.96	0.83
84.2	168.1	0.00	0.02	0.06	0.28	0.57	0.71	0.85	1.08	0.95	0.89
168.2	280.2	0.00	0.00	0.04	0.24	0.62	0.70	0.82	0.90	1.06	0.84
280.3	672.5	0.00	0.01	0.08	0.38	0.67	0.68	0.80	0.84	1.03	0.80

1. NL1 represents the far left of the patterns.
2. NL10 represents the center of the patterns.

## AREA DEFINITION

A noted shortcoming of the “as-applied” spatial model developed by Fulton et al. (2003) was representation of curvilinear travel by an applicator. Rectangular polygons were used to represent the area of application for each data point within the field application file (FAF). Thus, open areas and exaggeration of polygon overlap towards the inside turning radius result thereby misrepresenting the actual application area (fig. 4.6). To remedy this oversight, a new procedure was developed for better area definition of each data point contained in a FAF. Rather than defining one large rectangular polygon for each point and then sub-dividing it, lines or transects were defined perpendicular to each point’s bearing (fig. 6.1b). The length of each transect was defined by the spread width of the applicator (table 6.1). These transects were then sub-divided into equal length sections based upon the pan spacing (spread width divided by number of polygons) of each applicator with nodes consecutively labeled from one, representing the far left of the spread area, to the number of polygons plus one, representing the far right border line of the spread area (fig. 6.2).



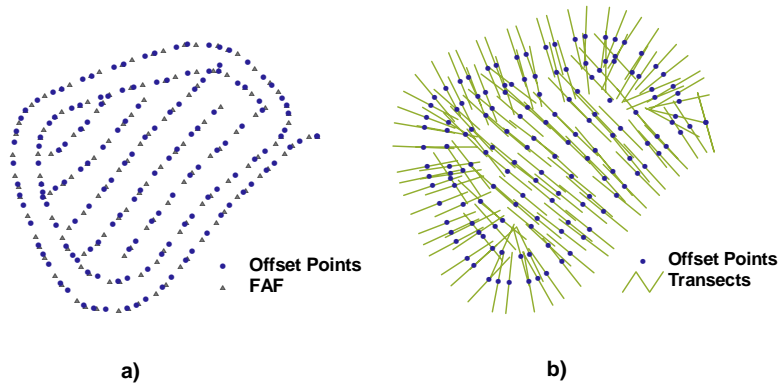


**Figure 6.1. Application of offset and definition of transects.**

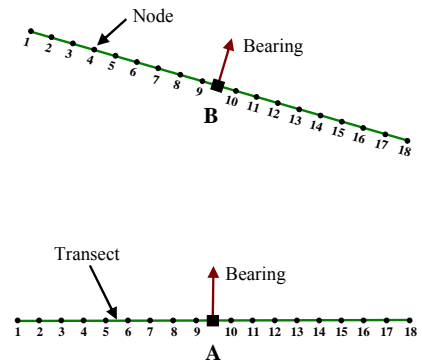


**Figure 6.2. Transect designation and delineation into equal length sections (New Leader example with 19 sub-polygons).**

Sub-polygons are generated by connecting similar numbered nodes (1 to 1, 2 to 2, etc) between consecutive points (fig. 6.2). All sub-polygons are defined to generate the distribution pattern polygon layer (fig 6.3a). The sub-polygon rate assignment is established by determining what range the application rate for a particular point in a FAF falls within based on the ADF and then multiplying this application rate by each of the standardized multipliers. For example, the New Leader FAF specify 155.2 kg/ha for a particular point. This rate falls within the 84.2 to 168.1 kg/ha range (table 6.3) thereby indicating that the far left sub-polygon receives 0.0 kg/ha ( $0.00 \times 155.2$  kg/ha), the second sub-polygon receives 3.1 kg/ha ( $0.02 \times 155.2$  kg/ha), the third sub-polygon receives 9.3 kg/ha ( $0.06 \times 155.2$  kg/ha) and similarly repeated for each sub-polygon up to 19 for this FAF data point.

Application rate adjustments are made for sub-polygon area differences. These rate adjustments are computed by first selecting the center sub-polygon area. Then for each sub-polygon, an area ratio is computed, center sub-polygon area divided by the sub-polygon area, and the assigned rate is multiplied by this ratio. The center sub-polygon ratio equals 1, signifying that the assigned rate does not change.

Thus, during curvilinear travel, the inner sub-polygons will receive more material (over-application) while the outer, larger sub-polygons receive less material (under-application).

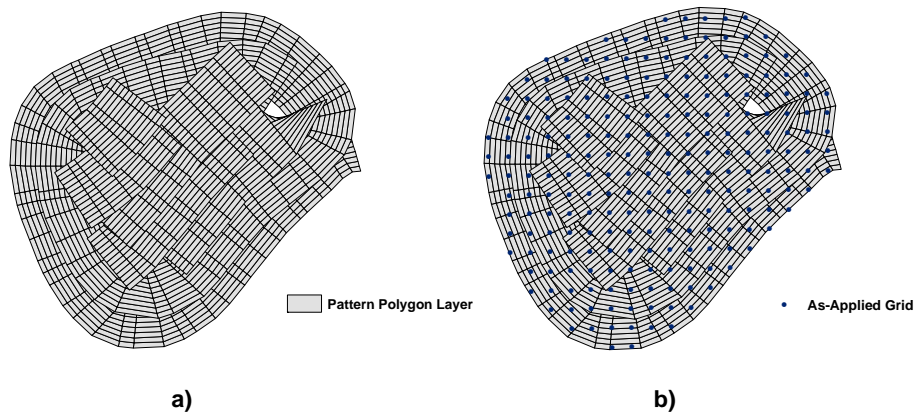


**Figure 6.3. Resulting pattern polygon layer and grid overlay for specification of the “as-applied” surface.**

## PROJECTION AUTOMATION AND GUI

The Kentucky North, State Plane coordinate system was used for initial development (Fulton et al., 2003). To make the spatial model more versatile, re-projection into Universal Transverse Mercator (UTM) coordinate system was used and automated within the code. Most spatial data collected by agricultural software packages are stored in geographic coordinates (WGS84). Therefore, the shape files (FAFs) are kept in WGS 84 geographic coordinates rather than re-projected before processing. Eliminating and automating this step reduced FAF preprocessing. Projection into UTM used the North American Datum 1927 (NAD 27) within the spatial model but NAD 83 can also be easily used.

An improved GUI was added to better guide users when inputting information. The GUI allows the user to select the applicator of choice (Newton Crouch, New Leader, Gandy, or AgChem), the working directory to store temporary files and the generated “as-applied” file, the type of material applying (currently only potash), the location of the FAF file to process, the offset distance, and the UTM zone. All FAFs were collected in zone 16 for this investigation. Once these parameters are set, the user initiates processing by clicking the ‘START’ icon. The code runs creating the pattern polygon layer containing the sub-polygons and their associated application rate. The user is then prompted for the location of the grid shape file used in developing the “as-applied” surface. The code spears through the pattern polygons layer, summing the application rates at intersecting sub-polygons for each grid point to create the “as-applied” surface (fig. 6.3b). A 10-m by 10-m grid was used in creating the “as-applied” surfaces. The Avenue Script for the spatial model is presented in Appendix B.

## FIELD DATA COLLECTION

The methodology for validating the “as-applied” spatial model was similar to that described by Fulton et al. (2003). Field collection of the validation data was conducted in Shelby County, Kentucky. Ten fields were selected to apply murate of potash (KCl) using the New Leader and Gandy applicators. In addition, the FAF data for fields B and C applied using the Newton Crouch (Fulton et al., 2003) was processed with the revised spatial model.

The fields were subdivided into 0.4 ha square management zones. A few zones in each field were larger or smaller than 0.4 ha due to the irregular field shapes. Prescription maps were generated for each field using the software packages SSToolbox (SST, 1999) and ArcView 3.3<sup>®</sup> (ESRI, 2001). Table 6.4 contains the field areas and prescription map summary statistics for each of the ten fields. The summary statistics demonstrate that there were several management zones in each field requiring a zero rate of murate of potash, and in some cases the zero rate extended to more than one half of a the field. The maximum prescribed (desired) rates ranged from 174.6 to 334.2 kg for the various fields. Figures 6.4, 6.5, and 6.6 present the prescription maps for the fields 11 and 230, applied with the New Leader applicator, and field 12, applied using the Gandy applicator, respectively.

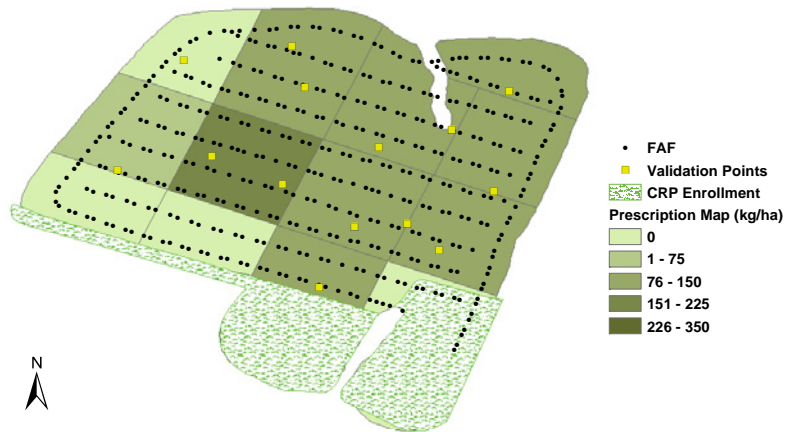


**Figure 6.4. The application prescription map, FAF, and validation points for field 11 (Applied using New Leader).**

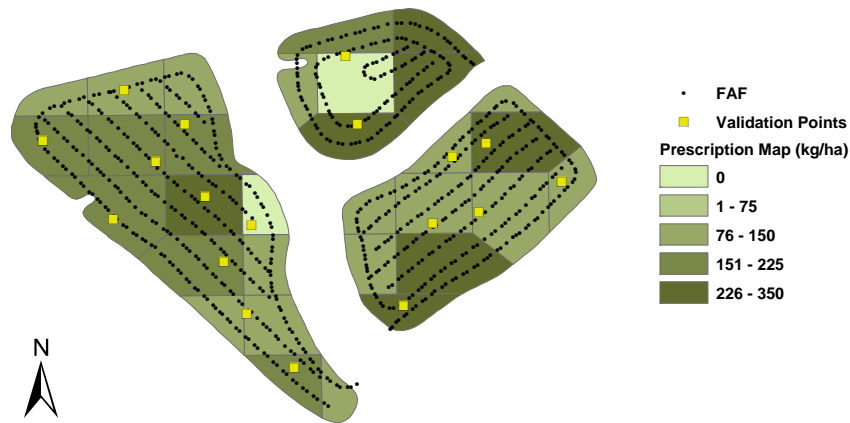


**Figure 6.5. The application prescription map, FAF, and validation points for field 230 (Applied using New Leader).**

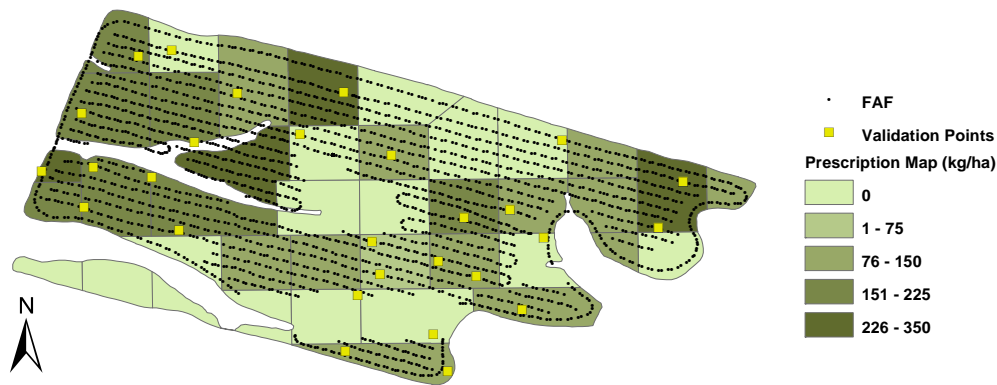


**Figure 6.6. The application prescription map, FAF, and validation points for field 12 (Applied using Gandy).**

Applicators were assigned randomly to each field. Field numbering was consistent with the field identification scheme used by the farmer. The random assignment included sorting the fields in ascending order by total area. They were then grouped into pairs by field area: the two smallest up to the two largest. The Gandy was assigned the number one and the New Leader number two. Selecting each pair of fields, Microsoft Excel was used to randomly generate a one or two. The pseudorandom number generated indicated which applicator was assigned to the smallest field of the pair. The process was repeated for each pair. This method of assigning applicators was intended to produce comparable areas covered by each applicator. Two fields intended for application by the Gandy were not used due to wet field conditions. Therefore, six field tests were conducted with the New Leader while only four with the Gandy.

Validation data sets were collected on each field. Collection pans were randomly assigned to each field before being placed within the fields. The number of pans and their random locations was

determined by using the boundary and prescription maps. The procedure included limiting the minimum number of pans at 15 for any field regardless of size. Other constraints imposed were applying pans at a rate of 2.0 pans per hectare and only 25% of the pans could be in zones requiring zero application. Further, those pans specified in a 0.0 kg/ha zone had to be within three spread widths of a zone requiring application. This stipulation removed pans in areas potentially never covered by an applicator but kept pans within a defined distance of where the applicator would be applying to find out if potash was applied in zones requiring no material. Lastly, pans could not be within 7.6 m of one another

The assignment of collection pans was performed by first determining the field boundary extents which can be obtained from the prescription shape file in ArcView 3.3<sup>®</sup>. The extents of a shape file are four spatial points which define the extents of the field boundary file. Using Microsoft Excel, three hundred pseudorandom spatial points were generated between the extents to ensure enough were generated to meet the constraints. These points were imported into ArcView 3.3<sup>®</sup> along with the field boundaries and prescription maps. The boundary map was used to clip the points preserving only points within the field boundary using the Geoprocessing Extension. The prescription map was then buffered using twice the spread width for an applicator. All points that were located in a 0.0 kg/ha zone but not within the buffer were deleted. The points themselves were then buffered at 7.6 m. If points were contained within the buffer of one another, one was deleted. The remaining points represented potential pan locations. The final selection involved starting at the top of the processed file and selecting the pre-calculated total number of pans for a field (field area\*2.0) and making sure that no more than 25% of the pans were located in 0.0 kg/ha zones. A shape field containing pan locations was then generated for each field.

The previously generated point shape files were used to place pans in the field by navigating to desired locations using an All-Terrain Vehicle (ATV), Trimble<sup>®</sup> Ag132 DGPS receiver and a PDA running the software package ArcPad by ESRI (ESRI, 2003). Pans were placed at the desired locations along with numbered flags. Figures 6.4, 6.5, and 6.6 illustrate pan locations for three fields.

The prescription maps were uploaded into the AgView software of each applicator. An attribute of Rawson VR controllers is that rates are defined in 6<sup>2</sup>/<sub>3</sub>% increments from the preset nominal rate. The nominal rate was set at 168.1 kg/ha for both the New Leader and Gandy applicators. Thus, the Rawson application rates were adjusted to the nearest 11.2 kg/ha increment from 168.1 kg/ha when communicated from AgView to the Rawson controller (fig. 6.7). Operators were instructed to apply as normal ignoring the pans. The applicator setup and operation was the same as outlined in Chapter Five (table 5.1) for the pan tests. A Trimble<sup>®</sup> Lightbar using a 10 Hz, Ag132 receiver was used for guidance.

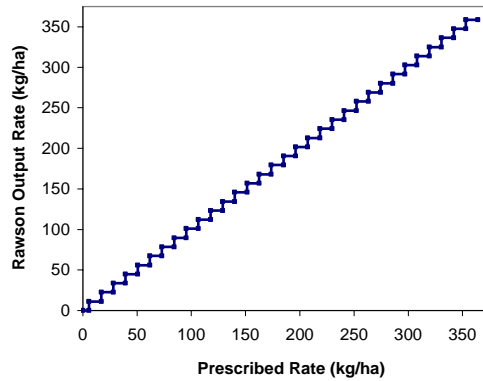


**Figure 6.7. Rawson controller output versus the prescribed application rate.**

Figures 6.4, 6.5, and 6.6 show example FAFs generated by AgView. Some areas of the fields requiring zero application were not covered to reduce application time. One difference in the FAFs generated for these two applicators compared to those for the Newton Crouch is that an actual application rate is fed back from the Rawson and stored. This is in contrast to the accumulated mass echoed back from the TASC 6200 controller (Fulton et al., 2003).

Upon completion of a field, the particles collected within a pan were bagged, numbered according to location, and weighed to compute the actual application rate. The validation points (actual) were compared to the prescription map (desired) and predicted values generated by the “as-applied” spatial model to evaluate performance. A comparison was also made between the actual and desired (prescription map) rates. The same procedure was used as outlined by Fulton et al. (2003). Different offsets were also used to evaluate its effect on the predicted values.

## **RESULTS AND DISCUSSION**

Table 6.5 contains a summary for the validation data (actual) and “as-applied” spatial model application rates for each field. The number of validation data points for each field varied from 15 to 58. There were a few instances where material was lost during the collection process, a couple pans tipped over, and in field 33 the control system was not turned in one area. For these cases, the points in question were omitted. The spatial model tended to under predict the maximum validation application rates for all the fields except field 45. The maximum predicted application rates for fields B and C were about 50% less than the actual application rates indicating a potential coding problem when assigning a rate to each sub-polygon.

**Table 6.5. Summary data for validation comparisons.**

Applicator	Field	No. Points	Actual		Predicted	
			Minimum Rate (kg/ha)	Maximum Rate (kg/ha)	Minimum Rate (kg/ha)	Maximum Rate (kg/ha)
New Leader	8	20	8.2	289.5	0.0	197.7
Gandy	10	15	0.0	323.4	0.0	223.1
New Leader	11	14	10.2	202.4	0.0	157.8
Gandy	12	28	0.0	392.7	0.0	390.9
Gandy	13	15	0.0	239.2	0.0	203.4
New Leader	33	18	0.0	234.3	0.0	147.1
New Leader	45	25	0.0	296.3	0.0	302.6
New Leader	230	18	9.7	299.7	0.0	376.4
Newton Crouch	B	29	0.0	133.3	0.0	63.8
Newton Crouch	C	58	0.0	292.4	0.0	154.6

**SPATIAL MODEL VALIDATION**

Comparison of model predictions to the validation test data are presented in table 6.6. The  $R^2$  values are reported for all tests. Since a pattern shift occurred for the Newton Crouch, all three standardized patterns were used as reported by Fulton et al. (2003). For the Gandy and New Leader, three different pattern scenarios were considered for the analysis. Various GPS antenna offset distances were used in the spatial model with the primary ones being 0.0-m, the actual antenna offset distance, and half of the antenna offset (table 6.2). Other offsets were used to observe how much effect this distance had on the predictive performance of the “as-applied” spatial model for selected fields.

The validation comparisons produced a wide variety of results. The  $R^2$  values ranged from 0.03 for field 13, using all patterns and a 0.0-m offset, up to 0.77 for several offsets and pattern scenarios in field 11. The lowest correlations were found in field 13 using the Gandy applicator with no relationship (all  $R^2 < 0.24$ ) existing between the actual and predicted. Inspection of the applicator revealed that three tubes were plugged. The problem was discovered and corrected after completing field 13 but before applying to fields 10 and 12.

**Table 6.6. Validation results for various offsets and patterns.**

Applicator	Field	Offset (m)	R <sup>2</sup>			
			All Patterns <sup>1</sup>	Single Pattern <sup>2</sup>	AVG Pattern <sup>3</sup>	
<b>Gandy</b>	10	0.0	0.58	0.60	0.59	
		1.2	0.43	0.43	0.43	
		2.4	0.43	0.44	0.44	
	12	0.0	0.48	0.64	0.66	
		2.4	0.51	0.51	0.51	
	13	0.0	0.03	0.07	0.05	
		1.2	0.16	0.24	0.20	
		2.4	0.12	0.12	0.09	
		3.7	0.08	0.08	0.05	
	<b>New Leader</b>	8	0	0.58	0.58	0.59
			2.4	0.63	0.63	0.65
			4.9	0.70	0.71	0.71
11		-2.4	0.75	0.73	0.74	
		0.0	0.76	0.73	0.76	
		2.4	0.77	0.73	0.76	
		3.7	0.77	0.73	0.76	
		4.9	0.77	0.73	0.77	
		6.1	0.77	0.73	0.77	
33		-2.4	0.54	0.57	0.55	
		0.0	0.32	0.36	0.33	
		2.4	0.16	0.16	0.15	
		4.9	0.38	0.40	0.39	
45		0.0	0.43	0.42	0.45	
		2.4	0.43	0.42	0.45	
		4.9	0.57	0.54	0.57	
230		0.0	0.65	0.68	0.68	
		2.4	0.64	0.73	0.69	
		4.9	0.72	0.76	0.76	
<b>Newton Crouch</b>		B	0.0	0.24	-	-
			3.0	0.31	-	-
	3.7		0.40	-	-	
	4.3		0.43	-	-	
	4.9		0.21	-	-	
	5.5		0.18	-	-	
	6.1		0.16	-	-	
	C	0.0	0.45	-	-	
		2.4	0.47	-	-	
		4.9	0.49	-	-	

1. Represents using all standard patterns for each applicator.
2. Uses only the 224.2 kg/ha New Leader and 112.1 kg/ha Gandy standardized patterns.
3. Uses the average of the four standardized patterns for the Gandy and New Leader.



The Gandy and New Leader results show little difference among the pattern scenarios investigated (table 6.6). The  $R^2$  values were nearly identical with all being within a couple hundredths of one another except for field 13 where the range was slightly higher. While not much difference existed, the trends seem to be that the randomly selected pattern for both applicators produced slightly better results. The single pattern for the Gandy produced better results for fields 10 and 13. Comparable results were found in field 12 for the single and average patterns. For the New Leader applicator, the relationships in field 8 were very similar at each offset distance. Nearly the same was true for field 11 except that the randomly selected pattern produced slightly worse relationships over the other two scenarios. The randomly selected pattern generated a little better relationship for field 33. The single and average standardized pattern correlations were similar and tended to perform better in field 45. The single and average pattern scenarios for each offset were comparable except for the 2.4-m offset where the single pattern produced a  $R^2$  of 0.73 compared to  $R^2$  of 0.69 for the average pattern.

The analogous results between the three different pattern scenarios for the Gandy and New Leader were expected based on the conclusions drawn in Chapter Five. The statistical analysis in Chapter Five suggested that the standardized distribution patterns were statistically the same for both applicators. Thus, a single pattern is sufficient for generating the ADF for use in the spatial model.

Antenna offset distance influenced the validity of the “as-applied” spatial model. The most consistency with offset distance was in field 11 where the spatial model performed well with  $R^2 > 0.73$ . The within pattern scenario  $R^2$  variance was very small for field 11 and was unchanged for the single pattern. All the other fields produced varying correlations with offset distance. For example, a 4.9-m offset distance in field 45 produced a better relationship ( $R^2 = 0.57$ ) over the 0.0 m ( $R^2 = 0.45$ ) and 2.4 m ( $R^2$  of 0.45) offset when looking at the average pattern correlations.

A 0.0-m offset worked the best for the Gandy except for field 13 where a 1.2-m offset produced the highest  $R^2$ . However, neglecting field 13 because of the blocked tubes at application, a 0.0-m offset distance is recommended for generating “as-applied” surface using the spatial model for the Gandy.

A 4.9-m offset produced the best performance of the spatial model for the New Leader applicator. Only in field 33 did a different offset work better where a -2.4-m offset produced the highest  $R^2$  values (0.57) with the 4.9-m offset providing the second best correlations ( $R^2$  of 0.40). The cause for the anomalous offset for field 33 is unidentified when compared to the consistent 4.9-m offset found for the other four fields. Therefore, a 4.9-m offset is recommended when using the spatial model for the New Leader applicator. Further, the 4.9-m offset corresponds to the measured GPS antenna offset for this applicator.

The spatial model did not perform well for the Newton Crouch applicator with the best  $R^2$  values computed of 0.43 for field B and 0.49 for field C (table 6.6). These  $R^2$  values were lower than those

computed by Fulton et al. (2003) for these fields using the same data. The area representation from rectangular to trapezoidal polygons hoped to improve the results for the Newton Crouch. The reason for the lower correlations is unknown since the assignment of the mass per sub-polygon is the same as described by Fulton et al. (2003). One possibility could be the calculation of the mass per sub-polygon is incorrect. The maximum predicted values for this applicator were approximately 50% smaller than the maximum actual application rates (table 6.5) and the comparable maximum application rates for the actual and validation data reported previously (table 4.3) (Fulton et al., 2003).

The single and averaged standardize pattern scenarios were not investigated for the Newton Crouch applicator since pattern shifts were observed. Better consistency was observed for the range of  $R^2$  values for field C when contrasted with field B. Therefore, the offset distance had more of an effect in field B than field C. An offset distance change from 3.7 and 4.3 m produced lower correlations in field B. An offset of 4.9 m produced the highest correlation ( $R^2 = 0.49$ ) in field C which equaled the measured GPS antenna offset distance for this applicator and which is identical to the best offset determined by Fulton et al. (2003). The highest correlation ( $R^2 = 0.43$ ) in field B was found at an offset of 4.3 m with the 4.9 m offset producing a lower correlation ( $R^2 = 0.21$ ). A recommended offset for this applicator is more difficult to specify because of the varying results in B and C. Additional studies are needed to determine if a consistent offset distance exists for the Newton Crouch.

The best validation results for the “as-applied” spatial model occurred with the New Leader applicator. For three fields (8, 11, and 230), the computed  $R^2$  values were greater than 0.70. These high correlations indicated good performance of the spatial model. Figure 6.8 shows the spatial model predicted values plotted against the actual application rates for fields 11 and 8. The spatial model performed well for field 11 with a linear fit almost equivalent to the 1:1 line with a slope of one and y-intercept near zero (fig. 6.8a). The linear fit for field 10 also illustrated a good fit ( $R^2 = 0.71$ ) but the slope ( $m = 0.686$ ) and intercept (12.4) varied from the 1:1 line (fig. 6.8b) indicating that the model tended to under-predict for this field. In fields 33 and 45, the spatial model did not perform as well ( $R^2 = 0.57$ ) when using the New Leader applicator.

The Gandy validation results suggested good performance by the spatial model for fields 10 and 12 with moderate relationships ( $R^2$  of 0.60 and 0.66, respectively). A poor relationship ( $R^2$  of 0.24) was found for field 13 and was expected as a result of plugged tubes on the applicator. Figure 6.9 plots the spatial model predicted values versus the actual application rates for field 10 and 12, respectively. In field 10, the spatial model did not perform as well for the higher actual application rates, over 300 kg/ha (fig. 6.9a). This conclusion was drawn since a majority of the points are located below the 1:1 line and a slope of 0.587 was computed for the linear regression line. The linear regression line for field 12 appears to be somewhat parallel to the 1:1 line within the 0.0 to 350.0 kg/ha application range (fig. 6.9b). The slope of

1.11 was computed along with a y-intercept of 7.2 kg/ha signifying that the spatial model slightly over-predicted for this field.

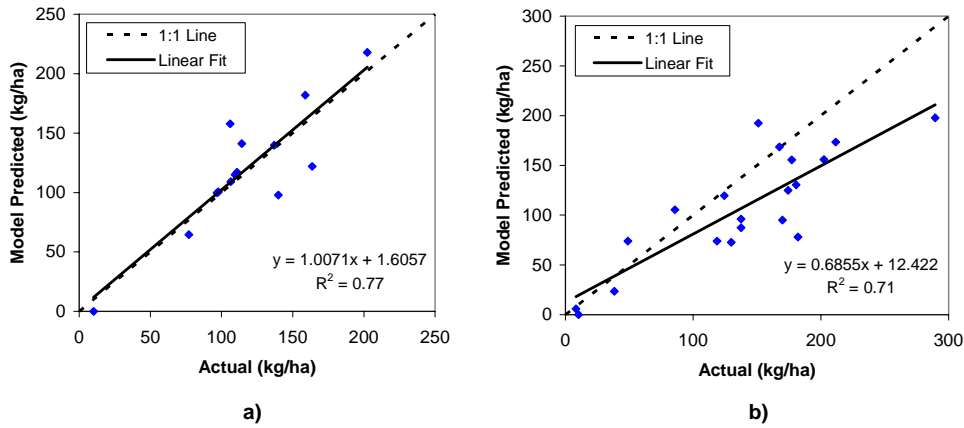


**Figure 6.8. Plot of predicted versus actual application rate: a) field 11 and b) field 8 (New Leader).**

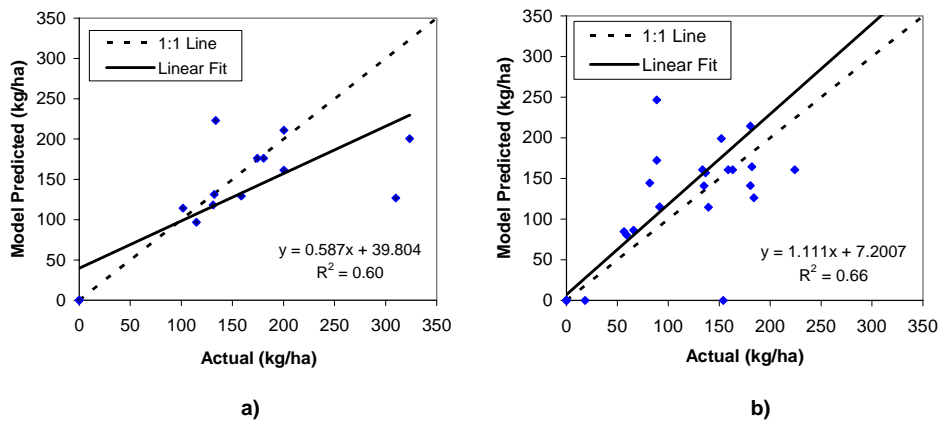


**Figure 6.9. Plot of predicted versus actual application rate: a) field 10 and b) field 12 (Gandy).**

The performance of the “as-applied” spatial model was consistent for the New Leader and Gandy applicators (table 6.6). Three of five fields for the New Leader produced similar correlations ( $R^2 > 0.70$ ), with two having poor relationships ( $R^2$  of 0.57). Further, a 4.9-m offset distance produced the best results in four of five fields for the New Leader. Data from three fields were used for validating the spatial model for the Gandy applicator, compared with five for the New Leader applicator. The validation results for the Gandy were acceptable with two fields producing  $R^2 \geq 0.60$ . One reason for slightly lower correlations could be the distribution pattern inconsistency observed with the Gandy during the UR tests (fig. 5.13 and 5.16). The Gandy produced the largest confidence intervals indicating the most pattern variability, possibly causing more unevenness of spread during the field tests. Overall, the spatial model performed

well for the Gandy and New Leader applicators when contrasted with the performance reported by Fulton et al. (2003).

Several factors are ignored by the “as-applied” spatial model which could have influenced the validation results. Variables affecting granular material application include wind, terrain irregularities (which includes slope variations within fields), and material variability. Occasionally, gusts of wind occurred during field application, especially during the afternoon hours. However, the magnitude of the wind speed was deemed acceptable to continue application. Both applicators were operated on fields with varying terrain attributes which can affect the performance of lightbars or guidance systems. GPS antennas are usually mounted at the highest point on equipment and therefore position determinations can be influenced by vehicle pitch and roll on hillsides. Failure to compensate for equipment pitch and roll affects GPS position determinations adding to the errors in the FAF. The lightbar used for this investigation did not contain terrain compensation for the GPS receiver. Further, it is plausible that the distribution pattern had been altered even though the applicators’ setups were the same. Variations in the murate of potash product (particle size, density, or shape) could have altered the distribution pattern(s) and nominal application rate. It is difficult to explain the difference in the spatial model performance between the New Leader and Gandy applicators.

### **AS-APPLIED SURFACES**

As-applied surfaces were generated for fields 10 (fig. 6.10), 8 (fig. 6.11), and 11 (fig. 6.12). Areas labeled as Conservation Reserve Program (CRP) enrollment have been taken out of production and were not covered during field application. The legends for the “as-applied” and prescription maps are equivalent; therefore the existence of points indicates deviation from the desired application rate. All three maps show application deviations from the prescription maps.

The Gandy applicator demonstrated significant errors in the northwest corner of field 10 (fig. 6.10). The four management zones requiring potash in this area show almost all the “as-applied” points (fig. 6.10a). Further, these points indicate over-application by the Gandy applicator since most of the points are darker than the management zone defined color. This over-application could be indicative of narrow pass-to-pass spacing by the operator causing over-application in these areas (fig. 6.10a). Random measurements of parallel pass spacing using the measurement tool in ArcView 3.3 (ESRI, 2001) indicated that the operator maintained narrower pass-to-pass spacing in these areas creating application errors. The other management zones requiring potash do not exhibit as much application variability. The variability in application could be a result of the distribution pattern variability observed in Chapter Five for the Gandy applicator. There does appear to be a few instances where application occurred in zones requiring zero potash. The “as-applied” maps generated for the Newton Crouch by Fulton et al. (2003) illustrated

more application deviations from the prescription maps at the boundaries of 0.0 kg/ha zones. These results could be indicative of the VR system response of the Gandy applicator. In Chapter Five, this VR system responded quickly when making rates changes and the “as-applied” surface for field 10 illustrates this point. Overall, the Gandy applicator performed well in field 10 but consistent pass-to-pass spacing may reduce application errors in some zones.

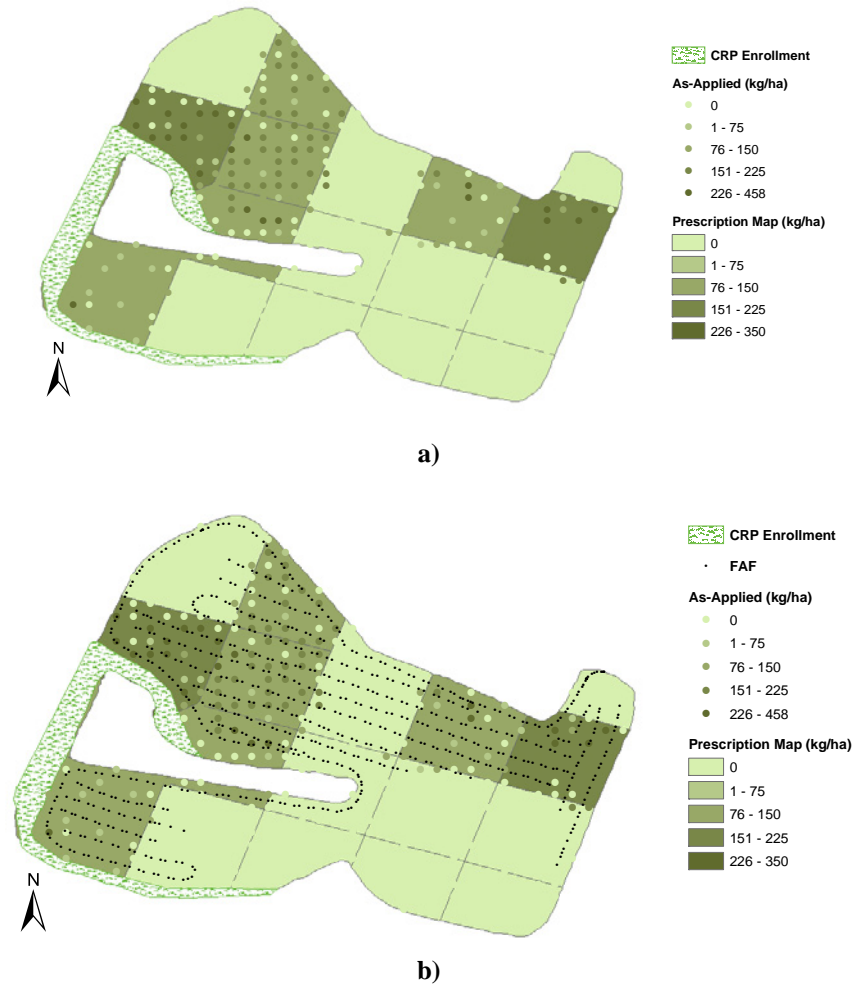


**Figure 6.10. “As-applied surface superimposed on the prescription map for field 10 (Gandy).**

The “as-applied” surface for field 8 illustrates significant deviation from the prescription map (fig. 6.11). Unlike the application results for the Gandy applicator, management zones requiring zero application tended to receive potash at zone borders (fig. 6.11a). The slower VR system response and inconsistently for the New Leader applicator could contribute to these application errors at the 0.0 kg/ha zone boundaries. However, the third pass from the North points out how an applicator trip close to and parallel to zone boundaries create application errors (area A, fig. 6.11b). This pass occurs in the first row of management zones from the North and near zone boundaries thereby depositing material in a zone

requiring zero potash, under-applying in an adjacent zone requiring potash since the applicator was in a 0.0 kg/ha zone, and then over-applying in a zone requiring less than the zone just North of it. These results show how the limitations of VRT equipment should be considered when defining the size of management zones, and the driver's choice for navigating the field. The management zones are 0.4 ha (63.6 by 63.6 m) square zones with many zones less than 0.4 ha adjacent to the field boundary. The New Leader has an 18.3 m spread spacing meaning that when traversing parallel to zone orientations, it would require 3.5 passes to cover a zone thereby causing over- and under-application to adjacent zones when completing the fourth pass. In many cases, this would be hard to resolve because of irregular shaped fields, but the probability of minimizing this type of application error would require selecting zone sizes that are a multiple of the applicator's effective spread width.

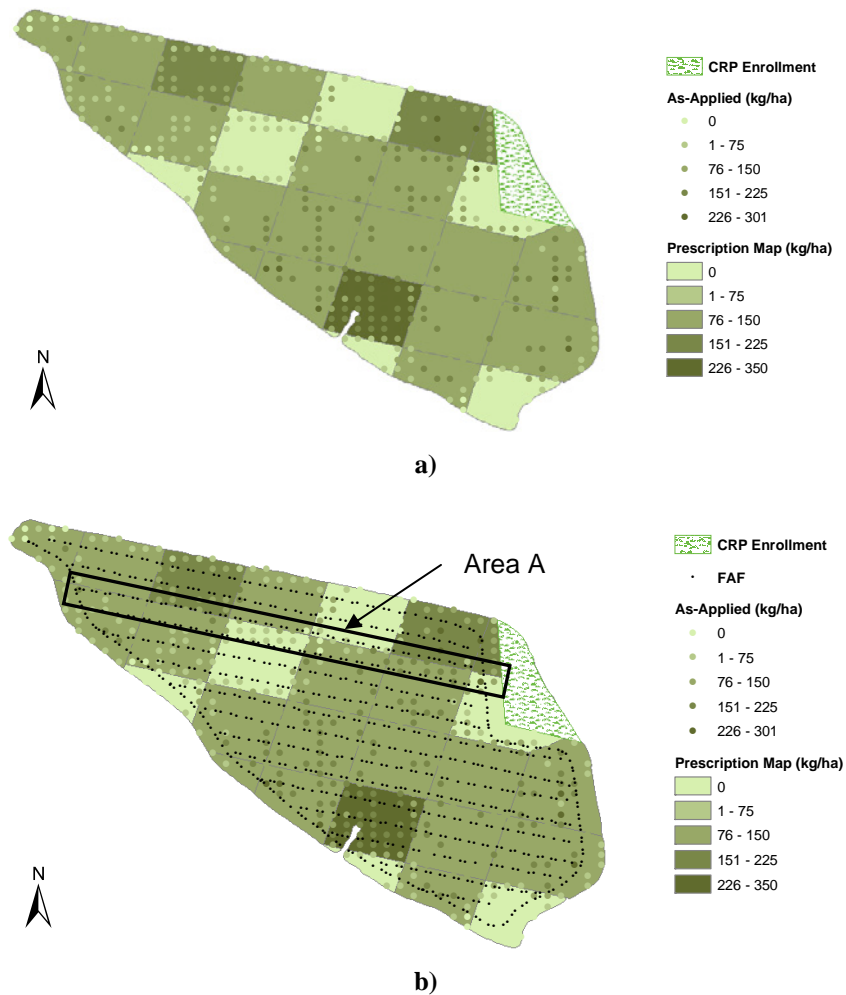


**Figure 6.11. “As-applied surface superimposed on the prescription map for field 8: a) “as-applied” surface and prescription map only, and b) FAF included (New Leader).**

The majority zones requiring potash in field 8 showed better application accuracy over the Gandy applicator in field 10 with fewer points being visible (fig. 6.11a). The driver was very consistent with the pass-to-pass spacing in field 8 (fig. 6.11b) thereby reducing application errors in these zones. The “as-applied map demonstrates one pitfall of spinner spreaders that has not been rectified. The outside pass around the periphery results in under-application (fig. 6.11a). VRT applicator performance in field 8 was acceptable considering some of the application errors in this field.

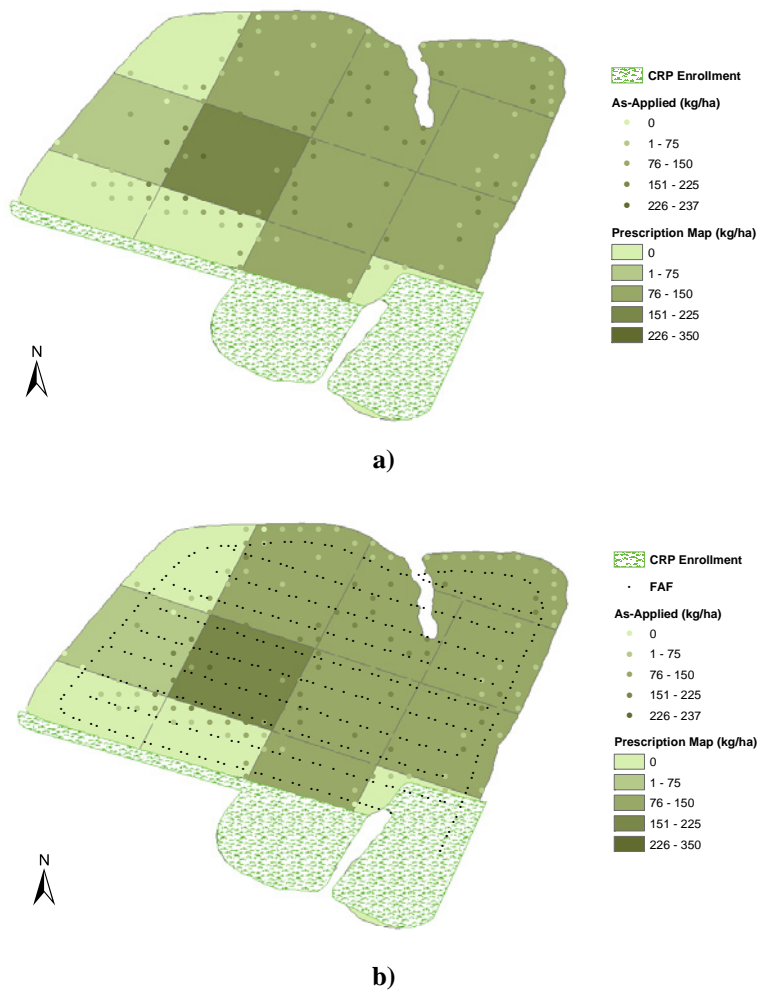


**Figure 6.12. “As-applied surface superimposed on the prescription map for field 11: a) “as-applied” surface and prescription map only, and b) FAF included (New Leader).**

The New Leader applicator performed exceptionally well in field 11 with few points appearing on the “as-applied” surface overlaid on the prescription maps (fig. 6.12). This field also exhibited the best validation results. Most of the applications errors within field 11 occur for the same reasons as for field 8. Zone boundaries show deviations from the prescription map which can be attributed to rate response characteristics of this applicator. However, fewer deviations occurred at the zone boundaries. The “as-

applied” surface at the field borders demonstrates under-application; as would be expected with spinner technology (fig. 6.12a). Application in the two 0.0 kg/ha zones in the southwest corner resulted from a close pass when traversing the zones just North of these two which required potash (fig. 6.12b). The parallel passes for this field were established based on the first trip across the southern border of this field causing the third pass from the South to be near the two 0.0 kg/ha zones in the southwest corner. Neglecting this over-application area and the outside first pass, this VRT applicator performed as well as could be expected.

The “as-applied” surfaces generated with the new model illustrated better VRT performance than those depicted for the Newton Crouch (figs. 4.9 and 4.10). The “as-applied” surfaces demonstrated potential errors associated with VRT application thereby showing the importance of “as-applied” surfaces for representing the actual application of material.

Difference maps were created for fields 10 (fig. 6.13), 8 (fig. 6.14), and 11 (fig. 6.15) comparing the “as-applied” surfaces and prescription maps. These maps provide a depiction of under- and over-application of murate of potash. Larger symbols represent larger deviations from the prescription maps while small triangles represent little variation in application. The difference maps support the conclusions discussed previously about VRT application in each of these fields. The application errors in field 10 occur within the management zones requiring potash whereas the majority of application errors in fields 8 and 11 occur at the fields’ peripheries and zone boundaries. A good feature of difference maps is that they provide an easier method to identify under- and over-application of inputs.

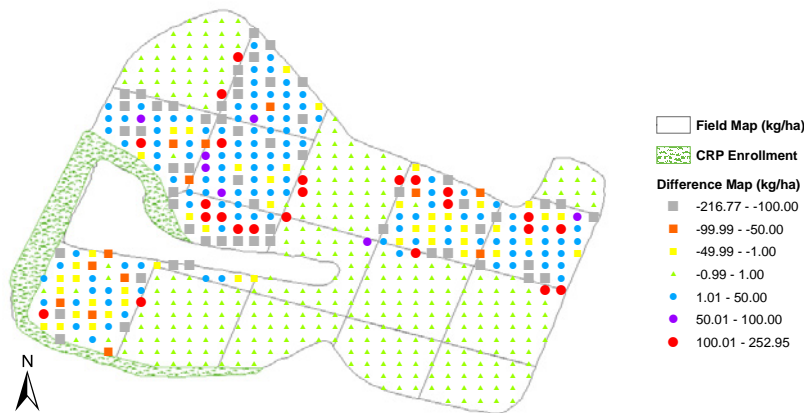


**Figure 6.13. Difference between the “as-applied” surface and prescription map for field 10.**



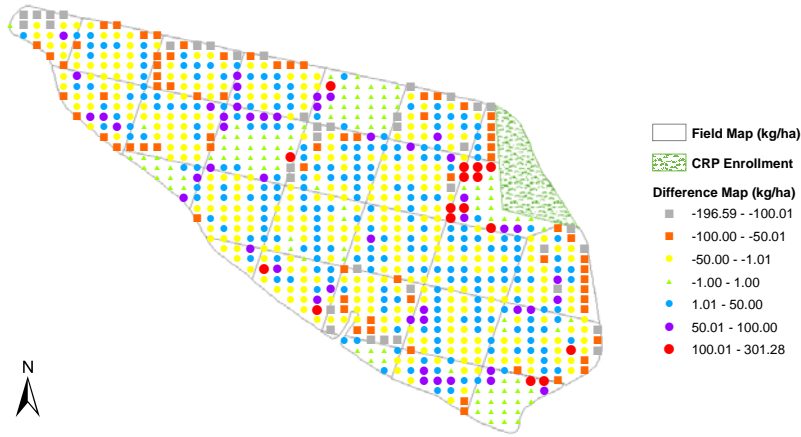


**Figure 6.14. Difference between the “as-applied” surface and prescription map for field 8.**

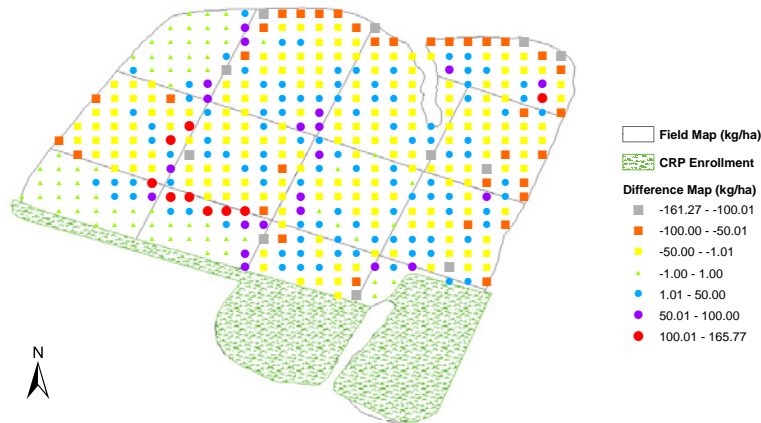


**Figure 6.15. Difference between the “as-applied” surface and prescription map for field 11.**

Summary statistics for the “as-applied” surfaces and difference maps are presented in table 6.7. These layers contained 607, 867, and 433 points for fields 10, 8, and 11, respectively. The difference map application means ranged from -7.7 to -5.0 kg/ha indicating possibly slight under-application in of these fields. However, the maximum values for the difference maps deviated more from zero than did the minimum values. The statistics provided are difficult to draw substantial conclusions from since application did not occur in several of the 0.0 kg/ha management zones and the “as-applied” points representing these zones were used when computing these statistics.

**Table 6.7. Statistics for the “as-applied” surfaces and difference maps.**

<b>As-Applied Surface</b>	<b>Field 10</b>	<b>Field 8</b>	<b>Field 11</b>
Number of Points	607	867	433
Mean (kg/ha)	56.5	102.9	93.9
Standard Deviation (kg/ha)	83.5	60.3	58.9
Minimum (kg/ha)	0.0	0.0	0.0
Maximum (kg/ha)	458.1	301.3	236.8
<b>Difference Map</b>			
Mean (kg/ha)	-5.0	-7.7	-5.5
Standard Deviation (kg/ha)	56.6	46.1	39.8
Minimum (kg/ha)	-216.8	-196.6	-161.3
Maximum (kg/ha)	253.0	301.3	165.8

Table 6.8 provides several rate categorizations for the difference maps. The majority of the difference points fall between -50.0 and 50 kg/ha for each field. In field 10, 16% of the points fall outside this range while 20.0% and 17.3% occur beyond this range for fields 8 and 11, respectively. Over-application occurred in field 10 using the Gandy applicator with 75.7% of the points ranging from -1.0 to 50.0 kg/ha possibly due to the narrow pass-to-pass spacing maintained by the operator. For fields 8 and 11, the majority of points (52% and 53.6%, respectively) are less than -1.0 kg/ha indicating slight under-application. However, the percentages are more uniformly distributed about the -1.0 to 1.0 kg/ha range for fields 8 and 11 when compared to those of field 10. These percentage categorizations should accompany difference maps to help quantify under- and over-application.

**Table 6.8. Rate difference categorization between the “as-applied” surface and prescription map.**

<b>Rate Difference Range (kg/ha)</b>	<b>Percent (%)</b>		
	<b>Field 10</b>	<b>Field 8</b>	<b>Field 11</b>
-220.0 to -100.1	9.3	4.4	2.5
-100.0 to -50.1	2.1	8.3	7.9
-50.0 to -1.1	7.6	39.3	43.2
-1.0 to 1.0	55.8	12.9	15.5
1.1 to 50.0	19.9	27.7	24.0
50.1 to 100.0	1.2	5.5	4.8
100.1 to 302.0	4.0	1.8	2.1

## SPATIAL MODEL PREDICTED VERSUS ACTUAL APPLICATION

A comparison was conducted between the actual application rates and prescription maps (table 6.9). The  $R^2$  values computed ranged from 0.24 for field 13 to 0.81 for field 10. These  $R^2$  values are much higher than those reported by Fulton et al. (2003). In several cases, both the Gandy and New Leader performed well ( $R^2 > 0.60$ ). On the other hand, the performance of these applicators was poor ( $R^2 < 0.50$ ) for several fields. Figure 6.16 demonstrates the consistency of the Gandy applicator for field 10 with a small scatter in the data points. It appears that the Gandy tended to over-apply potash since all points fall below the 1:1 line; especially at the higher application rates. A narrower pass-to-pass spacing produces over-application of material which is apparent when viewing the “as-applied” surface for field 10 (fig. 6.10).

**Table 6.9. Comparison of the actual applications versus the prescription map.**

Field	Applicator	$R^2$
		Actual vs prescription map
7	Gandy	0.68
8	New Leader	0.49
10	Gandy	0.81
11	New Leader	0.75
12	Gandy	0.49
13	Gandy	0.24
33	New Leader	0.50
34	New Leader	0.51
45	New Leader	0.45
230	New Leader	0.65

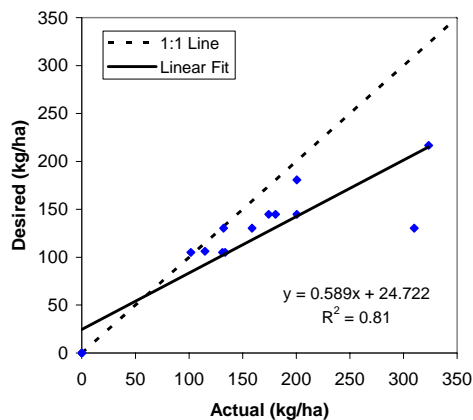


**Figure 6.16. Plot of desired versus actual application rates for field 10.**

Similar to the Gandy applicator in field 10, the New Leader data demonstrated over-application in field 8 but that the applicator tended to over-apply in a predictable manner with the majority of data points falling beneath the 1:1 line (fig. 6.17b). Field 11 results indicated that the New Leader performed well with a slope near 1 and y-intercept of 8.75 kg/ha (fig. 6.17a). The outcomes for these fields show how VRT can be inconsistent from field-to-field. Further research is required to determine the reasons for field-to field variability. Perhaps the single greatest effect on VRT application accuracy is the equipment operator. These factors include maintaining the specified pass-to-pass distance but possibility equipment speed during application can have an affect on model performance and should be incorporated as a variable into the model.

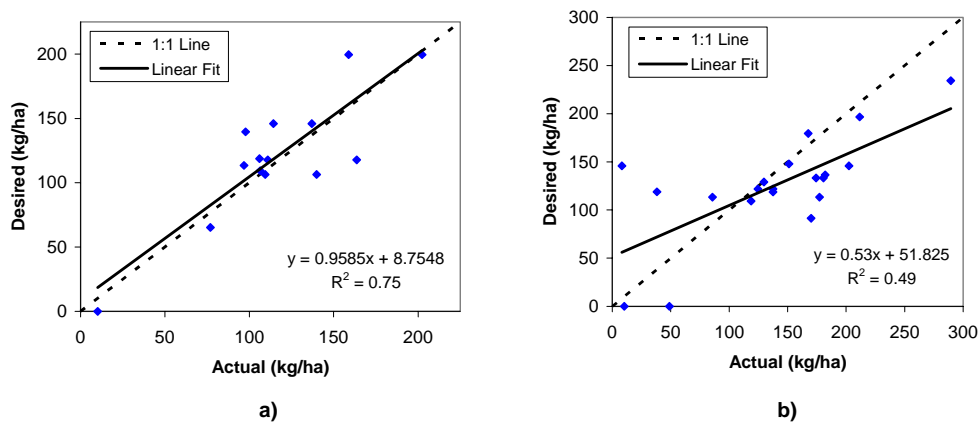


**Figure 6.17. Plot of desired versus actual application rates: a) field 11 and b) field 8 (New Leader).**

An interesting note is that the  $R^2$  values reported in table 6.9 account for operator performance. While the Gandy applicator produced the highest correlation ( $R^2 = 0.81$ ), it produced the largest range of  $R^2$  values (0.24 to 0.81) whereas the New Leader  $R^2$  range was much smaller (0.49 to 0.75). These varying ranges could indicate that the operator of the New Leader was more consistent by maintaining the correct pass-to-pass spacing in contrast to the Gandy’s operator. Figures 6.11b and 6.12b show how consistent the driver of the New Leader was consistent with pass-to-pass spacing. Even though the applicators did perform well at times, these results demonstrate potential differences existing between prescription maps and actual field application.

## SUMMARY

Modifications to the “as-applied” spatial model included using trapezoidal polygons rather than rectangular polygons to represent the area of each point within the FAF. This modification was made to improve the spatial model for representing application in turns. Other new features including automation of re-projecting the FAF file into the UTM coordinate system and a GUI to better assist the user in

uploading data. The concept of an ADF file was developed to describe an applicators pattern and spread characteristics for input to the spatial model.

Field validation data were collected on several fields using the Gandy and New Leader applicators to evaluate the performance of the “as-applied” spatial model. Similarly, two fields for the Newton Crouch used by Fulton et al. (2003) were also incorporated into this analysis. The actual application rates were compared to those predicted using the “as-applied” spatial model. The “as-applied” model performed well and rather consistently for the New Leader applicator with  $R^2$  values above 0.70 for three fields but only moderately ( $R^2 = 0.57$ ) for the other two fields. The highest  $R^2$  values computed was 0.77 using the New Leader with a linear fit slope of one and y-intercept near zero for this particular field’s validation data. Moderate relationships ( $R^2 = 0.67$  and  $0.66$ ) were found for two fields using the Gandy applicator with a poor relationship ( $R^2 = 0.24$ ) existing for another field. However, plugged distribution tubes were identified as the cause for this low correlation, demonstrating the influence of applicator setup or maintenance problems on application errors. The spatial model produced poor correlations ( $R^2$  of 0.43 and 0.49) for the fields applied using the Newton Crouch. These results were lower than those reported using the previous version of the “as-applied” spatial model (Fulton et al., 2003). The cause for these lower correlations for the Newton Crouch was not identified. One observation was that the spatial model under-predicted the maximum rates by 50% for the Newton Crouch.

A study of three different standardized pattern scenarios demonstrated no advantage to using the multiple patterns over a single pattern for the New Leader and Gandy applicators. These results were expected since no difference existed in the standard patterns for either applicator. However, offset affected the results when comparing the actual application rates those predicted by the “as-applied” spatial model. In all cases, except for one field, different offset distances produced varying  $R^2$  values. A 4.9-m offset consistently produced better correlations than other offsets for the New Leader applicator and was recommended when processing FAFs with the “as-applied” spatial model. The 4.9 m offset corresponded well with the physical GPS antenna offset distance measured on the New Leader applicator. A 0.0-m offset was recommended to for the Gandy applicator. For the Newton Crouch, no trend was observed in determining the appropriate offset for this applicator.

Generated “as-applied” surface for three fields demonstrated potential application errors associated with VRT equipment. These included errors at zone boundaries for the New Leader illustrating the effect of delay and transition times on application accuracy. The absence of overlap for the outer pass by the New Leader applicator caused under-application errors which were apparent in the “as-applied” surfaces. The effect of zone dimensions not being a multiple of the spread spacing was observed for the New Leader applicator. The Gandy applicator showed application deviations in zones requiring potash but appeared to be a result of the narrower pass-to-pass spacing maintained by the driver. However, the “as-

applied” surfaces showed deviations from the prescribed application rates pointing out the importance of “as-applied” surfaces when performing any type of analyses for VR application.

The actual application rates were compared to the prescription maps for the fields applied using the Gandy and New Leader applicators. The  $R^2$  values computed for this comparison ranged from 0.24 to 0.81 which were higher than those reported by Fulton et al. (2003). For four of the ten fields, moderate to strong relationships ( $R^2 > 0.60$ ) were observed with six other fields showing poor relationships ( $R^2 < 0.51$ ) and indicate how VRT application can vary from field-to-field.

# CHAPTER SEVEN

## CONCLUSION

### CONCLUSIONS

Objective 1 of this research was addressed by developing a test procedure, a modification of ASAE Standard S341.2 (ASAE Standards, 2000), to capture distribution patterns and rate response characteristics from VRT granular applicators. A two-dimensional collection pan layout was used in place of the traditional one-dimensional pan array. The modified test procedure permitted the characterization of distribution patterns from two VRT spinner spreaders and two VRT pneumatic applicators for UR and VR tests.

Distribution patterns from all four applicators highlighted importance of proper setup and calibration. These tests also summarize the tribulations of achieving accurate application of a variable product. Some applicators produce consistent distributions with variations in material properties suggesting one distribution patterns to be sufficient to characterize an applicator performance over a range of application rates. This was the case for three of the applicators with the fourth applicator exhibiting a pattern shift. A plot of the overlap pattern with CVs for both accuracy and precision are required to properly assess the field performance of applicators. The CVs are a useful tool for assessing the quality of spread but do not provide enough feedback on potential distribution problems.

Only one of the VR systems produced consistent delay and transition times with the other three exhibiting varying delay and transition times during increasing and decreasing rate changes. The quantification of these response characteristics revealed a major source of VRT application errors when moving between management zones requiring different applications rates. Both positive and negative delay times were calculated and the time to make a rate transition could be in the range of 4 to 10 seconds depending upon the VR control system. These rate response considerations are important for VRT equipment manufacturers, software developers, and users to help minimize the application errors. Those developing software for conducting VR application need information about the response characteristics of applicators. VR software packages should be modified to include different “look-ahead” times to account for these delays. These results support the development a VRT standard encompassing the performance of VR systems.

Objective 2 was accomplished by developing a spatial model for creating “as-applied” surfaces by through GIS functionality. The “as-applied” spatial model was developed using the ArcView 3.X product and Avenue script. Applicator description files (ADFs) were generated using the distribution pattern

characterizations for all four granular applicators. This information was then merged with field application files (FAF), point files containing spatial points tagged with application amounts, to produce the “as-applied” surfaces (point files) representing the distribution of fertilizer across fields. The “as-applied” surfaces can then be used as a feedback tool to assess VRT application by illustrating application deviations from the prescription map.

Work conducted under Objective 3 demonstrated the “as-applied” spatial model performed with success producing  $R^2$  values ranging from 0.43 to 0.77 when comparing the actual and predicted distribution rates for all fields except one. Validation analyses showed the spatial model performed well with good correlations ( $R^2 > 0.66$ ). These results demonstrated that the “as-applied” methodology can accurately model the spatial distribution of granular fertilizers. Antenna offset distances affected the performance of the “as-applied” spatial model with offsets of 4.9 m and 0.0 m recommended for the New Leader and Gandy applicators, respectively. The development of ADF’s could help VRT software developers and users to minimize application errors during applicator setup and for generating “as-applied” surfaces. The “as-applied” surfaces provide insight into understanding sources of VRT application errors, assist in calibrating VRT equipment, and selecting the appropriate “look-ahead” time. Prescription maps do not necessary represent the actual application of material as observed with the range of correlations ( $0.16 < R^2 < 0.81$ ) found between actual application rates and the prescription maps. “As-applied” surfaces offer the potential to extract site-specific fertility response curves when used in combination with fertility and yield maps.

In conclusion, the research presented in this dissertation presents an approach for identification and quantification of the application errors associated with VRT. Several sources of error were identified using the “as-applied” surfaces and array pan tests. Careful calibration and setup is required when using VRT equipment to minimize application errors. Operators, farm managers, and researchers must understand the limitations to VRT equipment to use it effectively. Further, the results of this investigation suggest opportunities with future improvements in VRT. Development of a VRT standard test methodology is essential for the future refinement of VRT. The development of the spatial model for generating “as-applied” surfaces provides a means to assess VRT application accuracy. Additionally, “as-applied” surfaces supply one on the missing links for proper economic and agronomic analyses of VRT investigations. Ultimately, agricultural machinery manufacturers should strive to improve the precision, accuracy, and rate response of VRT equipment to accurately manage the spatial variability of soil fertility.

## **SUGGESTIONS FOR FUTURE WORK**

The low correlations found between the spatial model and actual application rates indicate that improvements are needed to the "as-applied" model. The incorporation of a simulation technique to



account for distribution pattern variability could help characterize the stochastic nature of granular fertilizer application, and better help represent field application by granular applicators. Another modification consists of investigating the possibility of modeling the distribution pattern in two dimensions instead of one dimension. Other variables such as equipment speed, terrain attributes, and wind speed need to be investigated on their influence on the model. Additional data is required to ensure the efficacy of the approach for use with multiple granular products and different classes of application equipment.

A method to correct pattern shifts for the Newton Crouch applicator is needed to maintain the desired distribution pattern. Investigating adjustable on-the go pitch vanes on the spinner discs and an electric motor on the rear divider could be possible solutions to correction of pattern shifts during rate changes. Another potential resolution could be adjusting the spinner disc speeds to properly regulate the desired distribution pattern.

Various combinations of rate changes (56 to 112, 112 to 56, 112 to 336 kg/ha, etc.) need to be examined to determine how VRT systems respond. Investigating rate changes using other granular products is essential in understanding if they affect the distribution of an applicator. This research would answer the question if the expected rate of change and delay times is similar for 56 to 112-kg/ha, 112 to 224-kg/ha and other increasing and decreasing combinations for the different applicators. Information of this type will aid VRT software developers and users in improving application accuracy of VRT equipment.

Research is required to determine the largest contributor to application errors responsible for the lengthy delay and varying transition times for several of the applicators tested. Identifying the largest source of VRT application error would assist hardware and software developers in helping address the root cause and move toward minimizing it while improving application accuracy. While the exact cause of inconsistency was not identified, software and hardware all have an influence on application accuracy of VRT applicators. For the VRT AgChem applicators, generation of the contoured prescription maps with the SGIS software influences transition times. Research is needed to focus on producing consistent rate transition times for applicators on a complete system level.

## **APPENDIX A**

### **APPLICATOR DESCRIPTION FILES (ADF'S)**

**Gandy ADF (All Patterns)**

LOW	HIGH	G1	G2	G3	G4	G5	G6	G7	G8	G9	G10	G11	G12	G13	G14	G15	G16	G17	G18	G19
0.0	84.1	0.00	0.30	1.13	1.06	1.04	0.95	1.05	1.18	1.21	1.25	1.85	1.22	1.06	0.92	0.93	0.91	1.06	0.31	0.00
84.2	168.1	0.00	0.28	1.12	1.03	1.06	1.02	1.02	1.21	1.21	1.21	1.17	1.13	1.05	0.94	0.96	0.90	1.11	0.34	0.00
168.2	280.2	0.00	0.30	1.19	1.07	1.07	1.05	1.01	1.13	1.12	1.12	1.00	0.87	1.07	0.90	0.97	0.93	1.02	0.50	0.00
280.3	448.3	0.00	0.41	1.12	1.03	0.93	1.08	1.00	1.04	1.13	1.21	1.11	1.02	1.11	0.91	0.91	0.86	1.11	0.43	0.00

**New Leader ADF (All Patterns)**

LOW	HIGH	NL1	NL2	NL3	NL4	NL5	NL6	NL7	NL8	NL9	NL10	NL11	NL12	NL13	NL14	NL15	NL16	NL17
0.0	84.1	0.00	0.00	0.12	0.32	0.58	0.62	0.75	0.94	0.96	0.83	0.72	0.56	0.56	0.48	0.28	0.13	0.02
84.2	168.1	0.00	0.02	0.06	0.28	0.57	0.71	0.85	1.08	0.95	0.89	0.75	0.56	0.52	0.39	0.20	0.06	0.02
168.2	280.2	0.00	0.00	0.04	0.24	0.62	0.70	0.82	0.90	1.06	0.84	0.78	0.66	0.54	0.41	0.19	0.03	0.01
280.3	448.3	0.00	0.01	0.08	0.38	0.67	0.68	0.80	0.84	1.03	0.80	0.78	0.63	0.55	0.37	0.14	0.03	0.00

**AgChem ADF (All Patterns)**

LOW	HIGH	AC1	AC2	AC3	AC4	AC5	AC6	AC7	AC8	AC9	AC10	AC11	AC12	AC13	AC14	AC15	AC16	AC17	AC18	AC19
0.0	168.1	0.01	0.19	0.92	1.02	1.05	1.07	1.02	1.08	1.32	1.56	1.31	1.06	0.96	1.32	0.90	0.87	1.05	0.38	0.00
168.2	280.2	0.00	0.07	1.04	1.10	1.00	1.08	0.99	1.09	1.42	1.76	1.41	1.06	0.96	1.30	0.94	0.95	1.03	0.30	0.00
280.3	392.3	0.00	0.10	1.03	1.09	1.06	1.09	1.02	1.15	1.37	1.59	1.31	1.03	0.97	1.21	0.95	0.93	1.03	0.34	0.00
392.4	504.4	0.00	0.09	1.09	1.05	1.06	1.09	1.00	1.15	1.40	1.65	1.37	1.09	0.95	1.23	0.89	0.94	1.03	0.31	0.00

**Gandy ADF (Average Pattern)**

LOW	HIGH	G1	G2	G3	G4	G5	G6	G7	G8	G9	G10	G11	G12	G13	G14	G15	G16	G17	G18	G19
0.0	448.3	0.00	0.32	1.14	1.05	1.02	1.02	1.02	1.14	1.17	1.20	1.28	1.06	1.07	0.92	0.95	0.90	1.07	0.39	0.00

**New Leader ADF (Average Pattern)**

LOW	HIGH	NL1	NL2	NL3	NL4	NL5	NL6	NL7	NL8	NL9	NL10	NL11	NL12	NL13	NL14	NL15	NL16	NL17
0.0	448.3	0.00	0.01	0.08	0.31	0.61	0.68	0.81	0.94	1.00	0.84	0.76	0.60	0.54	0.41	0.20	0.06	0.01

**APPENDIX B**

**SPATIAL MODEL AVENUE SCRIPT**

## Startup - maximizes the window, resets project title, opens analysis view window, and opens initial dialog box

```
'-- Maximize application window size
av.Maximize
'-- Set project title
av.SetName("UK BAE As-Applied Surface Generator Application")
'-- Open the project in the Data Overview document
dView = av.GetProject.FindDoc("As Applied Data")
dView.GetWin.Open
'-- Identify the startup dialog and center it in the application
theDlg = av.FindDialog("StartupDlog")

avUpperLeft = av.ReturnOrigin
avCenter = avUpperLeft + (av.ReturnExtent / (2@2))
halfDialogWidthHeight = theDlg.ReturnExtent.ReturnSize / (2@2)
movePoint = avCenter - halfDialogWidthHeight
theDlg.MoveTo(movePoint.GetX, movePoint.GetY)
'-- Initialize dialog elements & set initial values
theProj = theDlg.FindByName("txtProjName").SetText("")
oldDir = av.GetProject.GetWorkDir.AsString
wrkDir = theDlg.FindByName("txtWorkDir").SetText(oldDir)
fertType = theDlg.FindByName("txtFertType").SetText("")
offsetDist = theDlg.FindByName("txtOffsetDist").SetText("")
unitsList = {"feet", "meters"}
theUnits = theDlg.FindByName("lbUnits").DefineFromList(unitsList)
addData = theDlg.FindByName("cbRawData").SetSelected(False)
apType = theDlg.FindByName("lbApType")
apVTab = av.GetProject.FindDoc("App_Char.dbf").GetVTab
apFields = apVTab.GetFields
apType.DefineFromVTab(apVTab, apFields, false)
apType.SetSelectionStyle(#LISTBOX_SELECTION_SINGLEROW)
cancelBtn = theDlg.FindByName("btnCancel")
helpBtn = theDlg.FindByName("btnHelp")
goBtn = theDlg.FindByName("btnContinue")
'-- Open the dialog box
theDlg.Open
```

## Adds new ID field to FAF for comparison purposes in subsequent processing steps

```
'-- Initialize view and get view's themes
theView = av.GetActiveDoc
theThemes = theView.GetThemes
if (theThemes.Count > 1) then
  ptTheme = msgbox.choice(theThemes, "Select raw point theme", "Choose")
else
  ptTheme = theThemes.Get(0)
end
'-- Make the theme editable
ptFTab = ptTheme.GetFTab
ptFTab.SetEditable(True)
'-- Create new ID field
idField = Field.Make("Pt_ID", #FIELD_LONG, 5,0)
'-- Add the new fields to the FTab table
ptFTab.AddFields({idField})
'-- Add sequential ID to recordset
idNum = 0
for each rec in ptFTab
  idNum = idNum + 1
  ptFTab.SetValue(idField, rec, idNum)
end
'-- Close FTab and save changes
ptFTab.SetEditable(False)
```

**Make a copy of the raw FAF shape file for preprocessing, leaving the original FAF unchanged.**

```
'-- Retrieve the raw data file to be processed
theView = av.GetActiveDoc
theThemes = theView.GetThemes
if (theThemes.Count = 0) then
  msgbox.error("No data files are in the view." + NL +
  "Please load raw data.", "Processing Error")
elseif (theThemes.Count > 1) then
  t = msgbox.choice(theThemes, "Select raw input point Theme", "Choose")
else
  t = theView.GetThemes.Get(0)
end
p = FALSE
'-- Check to see if theme is exportable
if (t.Is( FTHEME ).Not) then
  if (t.CanExportToFtab.Not) then
    MsgBox.Info("Error in export", "ERROR")
  end
  def = av.GetProject.MakeFileName("theme", "shp")
  def = FileDialog.Put(def, "*.shp", "Convert " + t.getName)
  if (def = NIL) then return NIL end
  anFTab = t.ExportToFtab(def)
' For Database themes, which can return a nil FTab sometimes
if (anFTab=nil) then
  MsgBox.Warning("Error occurred while converting to shapefile." + NL +
  "Shapefile was not created.", "Convert " + t.getName)
end
shpfld = anFTab.FindField("Shape")
else
  tbl = t.GetFTab
  attribVis = FALSE
  for each f in tbl.GetFields
    if ((f.IsVisible) and not (f.IsTypeShape)) then
      attribVis = TRUE
      break
    end
  end
  shapeVis = tbl.FindField("Shape").IsVisible
  def = av.GetProject.MakeFileName("theme", "shp")
  def = FileDialog.Put(def, "*.shp", "Convert " + t.getName)
  if (def = NIL) then return nil end
  shpfld = (tbl.FindField("Shape"))
  if (shpfld.IsVisible.Not) then
    shpfld.SetVisible(shpfld.IsVisible.Not)
    WasNotVisible = TRUE
  else
    WasNotVisible = FALSE
  end
end
' see if the view is projected
thePrj = theView.GetProjection
if (thePrj.IsNull.Not) then
  p = MsgBox.YesNoCancel("ArcView has detected that your view is projected." ++
  "Do you want the new shapefile to be saved in the projected units?",
  "Convert", FALSE)
  if (p = Nil) then return nil end
end
' Does the user want to project the shape file, use ExportProjected
if (p) then
  anFTab = tbl.ExportProjected(def, thePrj, tbl.GetSelection.Count > 0)
else
```

```

    anFTab = tbl.Export(def, Shape, tbl.GetSelection.Count > 0)
end
if (anFTab.HasError) then
    if (anFTab.HasLockError) then
        MsgBox.Error("Unable to acquire Write Lock for file " +
            def.GetBaseName, "")
    else
        MsgBox.Error("Unable to create " + def.GetBaseName, "")
    end
    return nil
end
if (WasNotVisible) then
    shpflD.SetVisible(FALSE)
end
end
end
'-- Build the spatial index
anFTab.CreateIndex(shpflD)
'-- Create a theme and add it to the View
fthm = FTheme.Make(anFTab)
theView.AddTheme(fthm)
'-- Bring the View to the front
theView.GetWin.Activate
'-- Open and Close Attribute Table
fthm.EditTable
theTable = av.GetActiveDoc
theTable.GetWin.Close
'-- Make new point theme copy the active theme
theView = av.GetActiveDoc
theThemeList = theView.GetThemes.AsList
theThemeName = theThemeList.Get(0).AsString
for each t in theView.GetThemes
    if (t.GetName = theThemeName) then
        t.SetActive(True)
    else
        t.SetActive(False)
    end
end
end
end

```

#### **Add longitude and latitude coordinates to the temporary point shape file**

```

'-- Gather initial project information
theProject = av.GetProject
theView = av.GetActiveDoc
theTheme = theView.GetActiveThemes.Get(0)
'-- Make sure theme is a shapefile by searching for an FTab
if (theTheme.Is(FTheme).NOT) then
    MsgBox.Info("This theme is not a shapefile.", "Theme:" ++ theTheme.GetName)
    exit
end
'-- Make sure that the selected theme is a point theme
if (theTheme.GetFTab.GetShapeClass.GetClassName <> "Point") then
    MsgBox.Info("The theme is not a point theme.", "Theme: " ++ theTheme.GetName)
    exit
end
'-- Make sure that the selected theme is editable by checking FTab
if ((theTheme.GetFTab.CanEdit).NOT) then
    MsgBox.Info("This theme cannot be edited.", "Theme:" ++ theTheme.GetName)
    exit
end
'-- Set the theme editable
theFTab = theTheme.GetFTab
if (theFTab.IsEditable) then

```

```

    alreadyOpen = TRUE
else
    alreadyOpen = FALSE
end
theFTab.SetEditable(TRUE)
'-- Add X and Y Fields to FTab to receive output
xField = Field.Make("X",#FIELD_FLOAT,18,5)
yField = Field.Make("Y",#FIELD_FLOAT,18,5)
if(theFTab.FindField("X-coord") = NIL) then
    theFTab.AddFields({xField})
else
    xField = theFTab.FindField("X")
end
if(theFTab.FindField("Y-coord") = NIL) then
    theFTab.AddFields({yField})
else
    yField = theFTab.FindField("Y")
end
'-- Loop through point records and add the actual X & Y field values
shpField = theFTab.FindField("Shape")
for each rec in theFTab
    theShape = theFTab.ReturnValue(shpField, rec)
    x = theShape.GetX
    y = theShape.GetY
    theFTab.SetValue(xField,rec,x)
    theFTab.SetValue(yField,rec,y)
end
'-- Close the FTab
if ((alreadyOpen = TRUE).NOT) then
    theFTab.SetEditable(FALSE)
end
end

```

**Takes the longitude and latitude (decimal degrees) and projects them into UTM coordinates for a user-defined zone.**

```

'-- Get initial rectangle
myRect = Rect.Make(0@0,1000000@1000000)
myUTM = Trnmerc.Make(myRect)
'-- Retrieve UTM Zone from global variable --
a = _UTMZone
if (a = nil) then
    return nil
end
'-- Conversion factor to turn a UTM Zone into its Central Meridian --
b = ((a * 6) - 183)
'-- Set up other parameters --
myUTM.SetCentralMeridian(b)
myUTM.SetFalseEasting(500000)
myUTM.SetFalseNorthing(0)
myUTM.SetReferenceLatitude(0)
myUTM.SetScale(0.9996)
'-- Determine the XY Fields for the current dataset --
theView = av.GetActiveDoc
theTheme = theView.GetActiveThemes.Get(0)
theFTab = theTheme.GetFTab
theFields = theFTab.GetFields
theDDXfld = theFTab.FindField("X")
theDDYfld = theFTab.FindField("Y")
'-- Add New Latitude and Longitude fields to receive the UTM readings --
theNewUTMXfld=Field.Make("Longitude",#FIELD_DECIMAL,16,2)
theNewUTMYfld=Field.Make("Latitude",#FIELD_DECIMAL,16,2)
theNewFldList={theNewUTMXfld,theNewUTMYfld}
theFTab.SetEditable(True)

```



```

theFTab.AddFields(theNewFldList)
'-- Make the conversion and record the values to the FTab --
for each rec in theFTab
  theDDXval=theFTab.ReturnValue(theDDXfld,rec)
  theDDYval=theFTab.ReturnValue(theDDYfld,rec)
  theDDpoint=Point.Make(theDDXval,theDDYval)
  myUTM.ProjectPt(theDDpoint)
  theUTMXval=theDDpoint.GetX
  theUTMYval=theDDpoint.GetY
  theFTab.SetValue(theNewUTMXfld,rec,theUTMXval)
  theFTab.SetValue(theNewUTMYfld,rec,theUTMYval)
end
'-- Delete the current X and Y fields
currentField = theFTab.FindField("X")
theFTab.RemoveFields({currentField})
currentField = theFTab.FindField("Y")
theFTab.RemoveFields({currentField})
theFTab.SetEditable(False)
theFTab.Refresh
'-- Delete the temp shape file
theView.CutThemes
av.PurgeObjects
'-- Add an event theme based on remaining data table
theFTab = EventDialog.Show(theView)
if (theFTab <> nil) then
  theView.AddTheme(FTheme.Make(theFTab))
  av.GetProject.SetModified(true)
end
'-- Rename Event Theme
theThemes = theView.GetThemes
evTheme = theThemes.Get(0)
evTheme.SetName("Event Temp")
evTheme.SetActive(True)
'-- Create projected shapefile from event theme based on system script View.Export
for each t in theView.GetActiveThemes
  p = FALSE
  if (t.Is( FTHEME ).Not) then
    if (t.CanExportToFtab.Not) then
      continue
    end
    def = av.GetProject.MakeFileName("theme", "shp")
    def = FileDialog.Put(def, "*.shp", "Convert " + t.getName)
    if (def = NIL) then
      return NIL
    end
    anFTab = t.ExportToFtab(def)
'-- For Database themes, which can return a nil FTab sometimes
    if (anFTab=nil) then
      MsgBox.Warning("Error occurred while converting to shapefile."+NL+
        "Shapefile was not created.", "Convert " + t.getName)
      continue
    end
    shpfld = anFTab.FindField("Shape")
    else
    tbl = t.GetFTab
    attribVis = FALSE
    for each f in tbl.GetFields
      if ((f.IsVisible) and not (f.IsTypeShape)) then
        attribVis = TRUE
        break
      end
    end
  end
end

```

```

shapeVis = tbl.FindField("Shape").IsVisible
if ((attribVis and shapeVis).Not) then
    continue
end
def = av.GetProject.MakeFileName("theme", "shp")
def = FileDialog.Put(def, "*.shp", "Convert " + t.getName)
if (def = NIL) then return nil end
shpfld = (tbl.FindField("Shape"))
if (shpfld.IsVisible.Not) then
    shpfld.SetVisible(shpfld.IsVisible.Not)
    WasNotVisible = TRUE
else
    WasNotVisible = FALSE
end
'-- see if the view is projected
thePrj = theView.GetProjection
if (thePrj.IsNull.Not) then
    p = MsgBox.YesNoCancel("ArcView has detected that your view is projected."++
        "Do you want the new shapefile to be saved in the projected units?",
        "Convert", FALSE)
    if (p = Nil) then return nil end
end
'-- Determine if the user wants to project the shape, use ExportProjected
if (p) then
    anFTab = tbl.ExportProjected(def, thePrj, tbl.GetSelection.Count > 0)
else
    anFTab = tbl.Export(def, Shape, tbl.GetSelection.Count > 0)
end
if (anFTab.HasError) then
    if (anFTab.HasLockError) then
        MsgBox.Error("Unable to acquire Write Lock for file " +
            def.GetBaseName,"")
    else
        MsgBox.Error("Unable to create " + def.GetBaseName,"")
    end
    return nil
end
if (WasNotVisible) then
    shpfld.SetVisible(FALSE)
end
'-- Build the spatial index
anFTab.CreateIndex(shpfld)
'-- Create a theme and add it to the View
fthm = FTheme.Make(anFTab)
theView.AddTheme(fthm)
'-- Bring the View to the front
theView.GetWin.Activate
end
'-- Remove event theme
for each t in theView.GetThemes
    if (t.GetName = "Event Temp") then
        t.SetActive(True)
    else
        t.SetActive(False)
    end
end
theView.CutThemes
'-- Remove old temporary data table
theDocs = av.GetProject.GetSelectedDocs
for each d in theDocs
    if (d.Is(Table)) then

```

```

        if (d.GetName.Contains("Attributes of")) then
            av.GetProject.RemoveDoc(d)
            av.PurgeObjects
        end
    end
end
end
'-- Activate the new working shapefile
theTheme = theView.GetThemes.Get(0)
theTheme.SetActive(True)
'-- Set the active theme visible
theTheme.SetVisible(True)
'-- Zoom to Offset_UTM theme
av.Run("View.ZoomToThemes", {})

```

**Remove unnecessary fields and add new fields. Then, rearrange all fields for output to the working point shape file.**

```

'-- Let user choose point theme for calculations
theView = av.GetActiveDoc
theThemes = theView.GetThemes
for each t in theThemes
    if (t.GetName = "Theme2.shp") then
        ptTheme = t
    end
end
ptTheme = MsgBox.Choice(theThemes, "Select working Point Theme to be formatted.", "Choose")
'-- Make the theme editable
ptFTab = PtTheme.GetFTab
ptFTab.SetEditable(True)
'-- Check to see which applicator type is being used.
ptFields = ptFTab.GetFields
'-- If Newton Crouch applicator type chosen at startup
if (_appType = "NC") then
    appField = ptFTab.FindField("CC_App")
else
    appField = ptFTab.FindField("App_Rate")
end
'-- Create the new fields to accept calculated values
areaField = Field.Make("Area", #FIELD_DECIMAL, 10, 3)
acreField = Field.Make("Acres", #FIELD_DECIMAL, 10, 3)
lbsPtField = Field.Make("LbsPerPt", #FIELD_DECIMAL, 10, 3) 'nc only
lbsAcreField = Field.Make("LbsAcre", #FIELD_DECIMAL, 10, 0)
bearingField = Field.Make("Bearing", #FIELD_DECIMAL, 8, 4)
distanceField = Field.Make("Distance", #FIELD_DECIMAL, 10, 3)
flagField = Field.Make("SpFlag", #FIELD_BYTE, 1, 0)
'-- Delete the old fields to the FTab table
if (_appType = "NC") then
    areaField = ptFTab.FindField("Field_Area") 'nc only
    totAreaField = ptFTab.FindField("Total_Area") 'nc only
    distField = ptFTab.FindField("Distance") 'nc only
end
pdField = ptFTab.FindField("Pdop")
fixField = ptFTab.FindField("Fix_type")
qualField = ptFTab.FindField("Quality")
if (_appType = "NC") then
    ptFTab.RemoveFields({areaField, totAreaField, pdField, fixField, qualField, distField})
else
    ptFTab.RemoveFields({pdField, fixField, qualField})
end
'-- Add the new fields to the FTab table
if (_appType = "NC") then
    ptFTab.AddFields({bearingField, distanceField, flagField, areaField, acreField, lbsPtField, lbsAcreField})
else

```

```

    ptFTab.AddFields({bearingField,distanceField,flagField,areaField,acreField,lbsAcreField})
end
'-- Get the number of records in the dataset
numRecs = ptFTab.GetNumRecords
'-- remember numbering starts at zero, so actual number is one less than value returned...make adjustment
numRecs = numRecs -1
'-- Cycle through recordset one record at a time
if (_appType = "NC") then
  for each rec in ptFTab
    CumValue = ptFTab.ReturnValue(AppField, rec)
    nextRec = rec + 1
    if (nextRec > numRecs) then
      return nil
    end
    nextValue = ptFTab.ReturnValue(AppField, nextRec)
    ptValue = nextValue - CumValue
    ptFTab.SetValue(lbsPtField, rec, ptValue)
  end
else
  for each rec in ptFTab
    lbsPerAcre = ptFTab.ReturnValue(appField, rec)
    ptFTab.SetValue(lbsAcreField,rec, lbsPerAcre)
  end
end
end
ptFTab.SetEditable(False)

```

#### Calculate bearing for each point and length between points

```

'-- Select the working theme and get the FTab
theView = av.GetActiveDoc
workTheme = theView.GetActiveThemes.Get(0)
'-- Make the FTab editable
theFTab = workTheme.GetFTab
theFTab.SetEditable(True)
'-- Determine the number of records in FTab
numRecs = theFTab.GetNumRecords
'--less than value returned...make adjustment
numRecs = numRecs -1
'-- Select all records
if (theFTab.GetSelection..Count = 0) then
  theFTab.GetSelection.SetAll
end
'-- Initialize previous bearing variable
prevBearing = 0
'-- For each point to the next point
for each i in 0 .. (numRecs)
  X1 = theFTab.ReturnValue(theFTab.FindField("Longitude"), i )
  If (i < (numRecs)) then
    X2 = theFTab.ReturnValue(theFTab.FindField("Longitude"), i + 1)
  else
    X2 = theFTab.returnValue(theFTab.FindField("Longitude"), 0)
  end
  Y1 = theFTab.returnValue(theFTab.FindField("Latitude"), i )
  If (i < (numRecs)) then
    Y2 = theFTab.ReturnValue(theFTab.FindField("Latitude"), i + 1)
  else
    Y2 = theFTab.ReturnValue(theFTab.FindField("Latitude"), 0 )
  end
  pt1 = point.make(x1,y1)
  pt2 = point.make(x2,y2)
'-- Calculate the hypotenuse (distance between the 2 points)
h = pt1.distance(pt2)

```

```

dX = (X2 - X1)
dY = (Y2 - Y1)
a = 90 - (( dX /h).ACos.AsDegrees)
if (dX < 0) then
  if (dY < 0) then
    a = 180 + a.Negate
  else
    a = 360 + a
  end
else
  if (dY < 0) then
    a = 180 - a
  end
end
'-- Record the value of the distance in the FTab
theFTab.SetValue(theFTab.FindField("Distance"),i, h )
'-- Record the value of the bearing in the FTab
theFTab.SetValue(theFTab.FindField("Bearing"),i, a )
'-- Compare bearing value to previous bearing
if ((i = 0) or (i = numRecs))then
  prevBearing = a
else
  splitCheck = (a-prevBearing).abs
  if (splitCheck > 40) then
    '-- Make sure difference doesn't involve 360 vs small number
    if (splitCheck > 280) then
      theFTab.SetValue(theFTab.FindField("SpFlag"),i,2)
    else
      theFTab.SetValue(theFTab.FindField("SpFlag"),i,1)
    end
  end
  prevBearing = a
end
'-- Check for distance between points as split points
if (h>(50/3.281)) then
  theFTab.SetValue(theFTab.FindField("SpFlag"), i,3)
end
end 'each i in 0 .. (numRecs)
'-- Stop editing, save edits and refresh the view
theFTab.SetEditable(False)
theFTab.GetSelection.ClearAll
theFTab.UpdateSelection
theView.Invalidate

```

### Apply the user offset distance

```

'-- Initialize the view and let use choose point theme for applying offset
theView = av.GetActiveDoc
theThemes = theView.GetThemes
'ptTheme = MsgBox.Choice(theThemes, "Select Point Theme", "Choose")
for each t in theThemes
  if (t.GetName = "Theme2.shp") then
    ptTheme = t
  end
end
ptTheme.SetActive(True)
ptFTab = ptTheme.GetFTab
ptFTab.GetSelection.SetAll
'-- Create a new shape file to accept offset point data
class = Point
shpFileName = "Offset_UTM.shp"
def = FileDialog.Put(shpFileName.asFileName, "*.shp",

```

```

"Creating offset point shapefile " + shpFileName.AsString)
if (def <> nil) then
tbl = FTab.MakeNew(def, class)
if (tbl.HasError) then
if (tbl.HasLockError) then
MsgBox.Error("Unable to acquire Write Lock for file "
+ def.GetBaseName, "")
else
MsgBox.Error("Unable to create " + def.GetBaseName, "")
end
return nil
end
end
end
'-- Create attribute fields to accept transferred data once point is offset
idField = Field.Make("ID", #FIELD_DECIMAL, 8, 0)
idField.SetVisible( TRUE )
newYField = Field.Make("Latitude", #FIELD_DECIMAL, 10, 3)
newXField = Field.Make("Longitude", #FIELD_DECIMAL, 10, 3)
distanceField = Field.Make("Distance", #FIELD_DECIMAL, 10, 3)
bearingField = Field.Make("Bearing", #FIELD_DECIMAL, 10, 3)
flagField = Field.Make("SpFlag", #FIELD_BYTE, 1, 0)
lbsPtField = Field.Make("LbsPerPt", #FIELD_DECIMAL, 10, 3)
acreField = Field.Make("Acres", #FIELD_DECIMAL, 10, 3)
lbsAcreField = Field.Make("LbsAcre", #FIELD_DECIMAL, 10, 0)
tbl.AddFields({idField, newXField, newYField, distanceField, bearingField, flagField, lbsPtField, acreField, lbsAcreField})
tbl.SetEditable(False)
newTheme = FTheme.Make(tbl)
'-- Add new shapefile to view
theView.AddTheme(newTheme)
newTheme.SetVisible(TRUE)
av.GetProject.SetModified(true)
'--Set new shape file symbol set; define the new color
theColor = Color.Make
theColor.SetRGBList({0,90,255})
'-- Assign the new color to the theme
newLegend = Legend.Make( #SYMBOL_MARKER )
newLegend.GetSymbols.Get(0).SetColor(theColor)
newTheme.SetLegend(newLegend)
newTheme.UpdateLegend
'-- Collect all the points into a list and make the line
pointList= {}
ptTheme.EditTable
pTableName = "Attributes of " + ptTheme.GetName
ptTable = av.FindDoc(pTableName)
ptTableWin = ptTable.GetWin
ptTableWin.close
theVTab = ptTable.GetVTab
XField = theVTab.FindField("Longitude")
YField = theVTab.FindField("Latitude")
for each rec in theVTab.GetSelection
aPoint = Point.Make(theVTab.ReturnValue(XField,rec), theVTab.ReturnValue(YField, rec))
pointList.Add(aPoint)
end
thePlyLn = Polyline.Make( {pointList})
'-- Return the total length of the centerline. This equals 100% of line length
totalLength = thePlyLn.ReturnLength
'-- Now back to offset calculations; make the Point theme editable
ptFTab.SetEditable(True)
'-- Retrieve the offset value from global variable
offset = _offsetDist
offsetPercent = offset/totalLength
'-- Make sure all records are selected

```

```

ptFTab.GetSelection.SetAll
'-- Calc offset point locations
for each rec in ptFTab
  ptA = ptFTab.ReturnValue(ptFTab.FindField("Shape"), rec)
  bearingVal = theVTab.ReturnValue(ptFTab.FindField("Bearing"), rec)
  distVal = theVTab.ReturnValue(ptFTab.FindField("Distance"), rec)
  flagVal = theVTab.ReturnValue(ptFTab.FindField("SpFlag"), rec)
  if (_appType = "NC") then
    lbsPerPtVal = theVTab.ReturnValue(ptFTab.FindField("LbsPerPt"), rec)
  end
  acreVal = theVTab.ReturnValue(ptFTab.FindField("Acres"), rec)
  lbsAcreVal = theVTab.ReturnValue(ptFTab.FindField("LbsAcre"), rec)
'-- check for spflag value of 1
if ((flagVal = 1) and (rec > 0)) then
  spflag2 = ptFTab.ReturnValue(ptFTab.FindField("SpFlag"), rec-1)
  if (spflag2 <> 0) then
    '-- Determine new point location from bearing and distance calculation
    X1 = ptA.GetX
    Y1 = ptA.GetY
    int_Bearing = bearingVal - 180
    if (int_Bearing < 0) then
      int_Bearing = 360 + int_Bearing
    end
    if ((int_Bearing >= 0) and (int_Bearing <= 360)) then
      if (int_Bearing = 360) then
        int_Bearing = 0
      end
      tx = _offsetDist * (90 - int_Bearing).AsRadians.Cos
      ty = _offsetDist * (90 - int_Bearing).AsRadians.Sin
      X2 = X1 + tx
      Y2 = Y1 + ty
      newPt = Point.Make(X2,Y2)
      newX = newPt.GetX
      newY = newPt.GetY
    end
  else
    ptPos = thePlyLn.PointPosition(ptA)
    distAlong = (ptPos/100)*totalLength
    newDist = distAlong - offset
    distPerct = (newDist/totalLength)*100

    newPt = thePlyLn.Along(distPerct)
    newX = newPt.GetX
    newY = newPt.GetY
  end
else
  ptPos = thePlyLn.PointPosition(ptA)
  distAlong = (ptPos/100)*totalLength
  newDist = distAlong - offset
  distPerct = (newDist/totalLength)*100
  newPt = thePlyLn.Along(distPerct)
  newX = newPt.GetX
  newY = newPt.GetY
end
'-- Add new point to offset shapefile
pt = Point.Make(newX, newY)
theView.SetEditableTheme(newTheme)
shpField = newTheme.GetFTab.FindField("Shape")
newTheme.GetFTab.BeginTransaction
rec = newTheme.GetFTab.AddRecord
newTheme.GetFTab.SetValue(shpField, rec, pt)
newTheme.GetFTab.EndTransaction

```

```

newTheme.GetFTab.GetSelection.ClearAll
newTheme.GetFTab.GetSelection.Set(rec)
newTheme.GetFTab.UpdateSelection
newTheme = theView.FindTheme(shpFileName)
'-- Add other feature attributes to FTab
newFTab = newTheme.GetFTab
if (newFTab.IsEditable = "FALSE") then
  newFTab.SetEditable(True)
end
for each rec in newFTab.GetSelection
  newFTab.SetValue(idField,rec,rec+1)
  newFTab.SetValue(newXField, rec, newX)
  newFTab.SetValue(newYField, rec, newY)
  newFTab.SetValue(bearingField, rec, bearingVal)
  newFTab.SetValue(distanceField, rec, distVal)
  newFTab.SetValue(flagField, rec, flagVal)
  if (_appType = "NC") then
    newFTab.SetValue(lbsPtField, rec, lbsPerPtVal)
  end
  newFTab.SetValue(acreField, rec, acreVal)
  newFTab.SetValue(lbsAcreField, rec, lbsAcreVal)
end
'-- Toggle editing off
theView.SetEditableTheme(nil)
end
'-- Remove non-offset theme from project view
ptFTab.SetEditable(False)
newTheme.SetActive(False)
ptTheme.SetActive(True)
theView.CutThemes
'-- Activate offset theme
newTheme.SetActive(True)
'-- Clear selection
for each t in theView.GetActiveThemes
  t.ClearSelection
end
'-- Refresh the view
theView.Invalidate

```

### **Add centerline connecting points**

```

'-- Get the view and its projection, if any
theView = av.GetActiveDoc
thePrj = theView.GetProjection
if (thePrj.IsNull) then
  hasPrj = false
else
  hasPrj = true
end
'-- Initialize Offset Table
for each t in theView.GetActiveThemes
  if (t.HasTable) then
    ptTheme = t
    theTable = t.EditTable
  end
end
theTable = av.FindDoc("Attributes of Offset_UTM.shp")
theTableWin = theTable.GetWin
theTableWin.Close
theVTab = theTable.GetVTab
XField = theVTab.FindField("Longitude")
YField = theVTab.FindField("Latitude")

```



```

IDField = theVTab.FindField("LineID")
VertField = theVTab.FindField("ID")
_pCount = 0
for each rec in theVTab.GetSelection
  _pCount = _pCount + 1
end
'-- Create new shape file to receive line segments
shpFileName = "Centerline.shp"
def = FileDialog.Put(shpFileName.asFilename, "*.shp", "Creating temporary shapefile...")
if(def=nil) then exit end
def.SetExtension("shp")
outputFTab = FTab.MakeNew(def, Polyline)
outputFTab.AddFields({Field.Make("ID", #FIELD_LONG, 8, 0)})
outputShapeFld = outputFTab.FindField("Shape")
outputIDFld = outputFTab.FindField("ID")
'-- Select all the points
theBitmap = theVTab.GetSelection
theBitmap.SetAll
theVTab.SetSelection(theBitmap)
'-- Collect all the points into a list and make the line
pointList = {}
for each rec in theVTab.GetSelection
  aPoint = Point.Make(theVTab.ReturnValue(XField, rec), theVTab.ReturnValue(YField, rec))
  pointList.Add(aPoint)
end
newRec = outputFTab.AddRecord
newLine = Polyline.Make({pointList})
outputFTab.SetValue(outputShapeFld, newRec, newLine).AsPolyline
theBitmap.ClearAll
theVTab.UpdateSelection
'-- Add the new theme to the view
newTheme = FTheme.Make(outputFTab)
theView.AddTheme(newTheme)
'-- Add new lines to centerline shapefile
outputFTab.SetValue(outputShapeFld, newRec, newLine).AsPolyline
'-- Calculate the centerline lengths
newFTab = newTheme.GetFTab
'-- Make the FTAB editable
newFTab.SetEditable(TRUE)
theLine = newFTab.ReturnValue(newFTab.FindField("Shape"), 0)
lenField = Field.Make("Length", #FIELD_DOUBLE, 16, 3)
newFTab.AddFields({lenField})
for each rec in newFTab
  theLength = theLine.ReturnLength
  newFTab.SetValue(lenField, rec, theLength)
end
newFTab.SetEditable(FALSE)
theView.Invalidate

```

### **Breaks centerline for turns and when applicator makes large distance moves**

```

'-- Initialize the view and get the point theme
theView = av.GetActiveDoc
ptTheme = theView.FindTheme("Offset_UTM.shp")
ptTheme.SetActive(True)
ptFTab = ptTheme.GetFTab
ptFTab.GetSelection.SetAll
'-- Clear any existing graphics from the view
gLst = theView.GetGraphics
if (gLst.Count > 0) then
  gLst.Empty
end

```

```

'-- Determine the number of records in selection set
numRecs = ptFTab.GetSelection.Count
numRecs = numRecs - 1
'-- Select all records
if (ptFTab.GetSelection.Count = 0) then
    ptFTab.GetSelection.SetAll
end
'-- Get the point information
for each rec in ptFTab.GetSelection
    ptX = ptFTab.ReturnValue(ptFTab.FindField("Longitude"),rec)
    ptY = ptFTab.ReturnValue(ptFTab.FindField("Latitude"), rec)
    ptBearing = ptFTab.ReturnValue(ptFTab.FindField("Bearing"), rec)
    flagCheck = ptFTab.ReturnValue(ptFTab.FindField("SpFlag"), rec)
    if (flagCheck = 1) then
'-- break line
        bearing2 = ((number.GetPi/2) - ptBearing)
        xCoord = (0.5 * bearing2.Cos)
        yCoord = (0.5 * bearing2.Sin)
        nwPt = Point.Make((ptX-xCoord),(ptY+yCoord))
        nwPt2 = Point.Make((ptX+xCoord),(ptY-yCoord))
        theLine = Line.Make(nwPt, nwPt2)
        splitLine = theLine.asPolyline
'-- Make the polyline theme editable
        plnTheme = theView.FindTheme("Centerline.shp")
        plnTheme.SetActive(True)
        ptTheme.SetActive(False)
        theView.SetEditableTheme(plnTheme)
        if (splitLine.IsNotNull) then
            return nil
        else
            if (plnTheme <> nil) then
                plnTheme.GetFtab.BeginTransaction
                theField = plnTheme.GetFtab.FindField("Shape")
                theType = theField.GetType
                if (theType = #FIELD_SHAPELINE) then
                    plnTheme.Split(splitLine)
                end
                plnTheme.GetFtab.EndTransaction
                theView.SetEditableTheme(nil)
                plnTheme.SetActive(False)
                ptTheme.SetActive(True)
            end
            av.GetProject.SetModified(true)
        end
    elseif (flagCheck = 2) then
'-- check that next record is also flagged
        flagCheck2 = ptFTab.ReturnValue(ptFTab.FindField("SpFlag"), rec+1)
        if (flagCheck2 = 1) then
            '-- break line again
                bearing2 = ((number.GetPi/2) - ptBearing)
                xCoord = (0.5 * bearing2.Cos)
                yCoord = (0.5 * bearing2.Sin)
                nwPt = Point.Make((ptX-xCoord),(ptY+yCoord))
                nwPt2 = Point.Make((ptX+xCoord),(ptY-yCoord))
                theLine = Line.Make(nwPt, nwPt2)
                splitLine = theLine.asPolyline
'-- Make the polyline theme editable
                plnTheme = theView.FindTheme("Centerline.shp")
                plnTheme.SetActive(True)
                ptTheme.SetActive(False)
                theView.SetEditableTheme(plnTheme)
                if (splitLine.IsNotNull) then

```

```

        return nil
    else
        if (plnTheme <> nil) then
            plnTheme.GetFtab.BeginTransaction
            theField = plnTheme.GetFtab.FindField("Shape")
            theType = theField.GetType
            if (theType = #FIELD_SHAPELINE) then
                plnTheme.Split(splitLine)
            end
            plnTheme.GetFtab.EndTransaction
            theView.SetEditableTheme(nil)
            plnTheme.SetActive(False)
            ptTheme.SetActive(True)
        end
        av.GetProject.SetModified(true)
    end
end
end
elseif (flagCheck = 3) then
'-- check to see if rec is last rec in set
    if (rec = numRecs) then
'-- don't break line
        else
'-- check that next record is also flagged
            flagCheck2 = ptFTab.ReturnValue(ptFTab.FindField("SpFlag"), rec+1)
            if (flagCheck2 = 1) then
'-- break line again
                bearing2 = ((number.GetPi/2) - ptBearing)
                xCoord = (0.5 * bearing2.Cos)
                yCoord = (0.5 * bearing2.Sin)
                nwPt = Point.Make((ptX-xCoord),(ptY+yCoord))
                nwPt2 = Point.Make((ptX+xCoord),(ptY-yCoord))
                theLine = Line.Make(nwPt, nwPt2)
                splitLine = theLine.asPolyline
'-- Make the polyline theme editable
                plnTheme = theView.FindTheme("Centerline.shp")
                plnTheme.SetActive(True)
                ptTheme.SetActive(False)
                theView.SetEditableTheme(plnTheme)
                if (splitLine.IsNull) then
                    return nil
                else
                    if (plnTheme <> nil) then
                        plnTheme.GetFtab.BeginTransaction
                        theField = plnTheme.GetFtab.FindField("Shape")
                        theType = theField.GetType
                        if (theType = #FIELD_SHAPELINE) then
                            plnTheme.Split(splitLine)
                        end
                        plnTheme.GetFtab.EndTransaction
                        theView.SetEditableTheme(nil)
                        plnTheme.SetActive(False)
                        ptTheme.SetActive(True)
                    end
                    av.GetProject.SetModified(true)
                end
            end
        end
    end
end
end
end
end
'-- Remove the lines from centerline falling between offset points with values of 1-1, 2-1, or 3-1
plnFTab = plnTheme.GetFTab

```

```

theBitmap = plnFTab.GetSelection
theBitmap.ClearAll
theQuery = "[Length] = 0"
plnFTab.Query(theQuery,theBitmap, #VTAB_SELTYPE_NEW)
plnFTab.UpdateSelection
ptTheme.SetActive(False)
plnTheme.SetActive(True)
theView.setEditableTheme(plntheme)
plnFTab.BeginTransaction
plnTheme.ClearSelected
plnFTab.EndTransaction
theView.SetEditableTheme(Nil)
for each rec in plnFTab
  ptVal1 = 0
  ptVal2 = 0
  ptVal3 = 0
'-- Clear any previous selections
  plnFTab.GetSelection.ClearAll
'-- Set the selection to the current record
  plnFTab.GetSelection.Set(rec)
'-- Select all the offset points that intersect the line
  ptFTab.SelectByFTab(plnFTab, #FTAB_RELTYPE_ISWITHINDISTANCEOF, 0.1, #VTAB_SELTYPE_NEW)
  theView.Invalidate
'-- If there are more than 2 points along the line, skip it
  if (ptFTab.GetSelection.Count = 2) then
    for each r in ptFTab.GetSelection
      ptVal1 = ptFTab.ReturnValue(ptFTab.FindField("SpFlag"), r)
      ptVal2 = ptFTab.ReturnValue(ptFTab.FindField("SpFlag"), r-1)
      if (((ptVal1 = 1) and (ptVal2 = 1)) or
          ((ptVal1 = 2) and (ptVal2 = 1)) or
          ((ptVal1 = 1) and (ptVal2 = 2)) or
          ((ptVal1 = 1) and (ptVal2 = 3))) then
        theView.setEditableTheme(plntheme)
        plnFTab.BeginTransaction
        plnTheme.ClearSelected
        plnFTab.EndTransaction
        theView.SetEditableTheme(Nil)
      end
    end
  end
end
end
'-- Number the centerline segments
numRec = 1
idField = plnFTab.FindField("ID")
plnFTab.GetSelection.SetAll
plnFTab.SetEditable(True)
for each rec in plnFTab.GetSelection
  plnFTab.SetValue(idField,rec, numRec)
  numRec = numRec + 1
end
plnFTab.EndTransaction
theView.SetEditableTheme(Nil)
theView.Invalidate

```

**Select applicator width from ADF; for each point draw a transect based on point bearing; subdivide transect into equal segments based on ADF (number of sub-polygons)**

```

'-- Initialize the view and get the point theme for polygon generation
theView = av.GetActiveDoc
ptTheme = theView.FindTheme("Offset_UTM.shp")
ptTheme.SetActive(True)
ptFTab = ptTheme.GetFTab

```

```

clTheme = theView.FindTheme("Centerline.shp")
clFTab = clTheme.GetFTab
'-- Get the transect length from spreader width global variable
csLength = _spreaderWidth
'-- Set the Distance variable from the spreader width global variable
theDist = _spreaderWidth/2
'-- Create a new shapefile to accept new transects
class = Polyline 'create polyline class
shpFileName = "Transects.shp" 'make shapefile definition
def = FileDialog.Put(shpFileName.asFileName, "*.shp", "Creating shapefile " +
shpFileName)
tbl = FTab.MakeNew(def, class)
'-- Create attribute fields to accept transferred data once point is offset
idField = Field.Make("ID", #FIELD_DECIMAL, 8, 0)
idField.SetVisible( TRUE )
clIIDField = Field.Make("CL_ID", #FIELD_DECIMAL,5,0)
lbsPtField = Field.Make("LbsPerPt", #FIELD_DECIMAL, 10, 3)
acreField = Field.Make("Acres", #FIELD_DECIMAL, 10, 3)
lbsAcreField = Field.Make("LbsAcre", #FIELD_DECIMAL, 10, 0)
tbl.AddFields({idField,clIIDField,lbsPtField,acreField,lbsAcreField})
tbl.SetEditable(False)
newTheme = FTheme.Make(tbl)
'-- Add new shape file to view
theView.AddTheme(newTheme)
newTheme.SetVisible(TRUE)
av.GetProject.SetModified(true)
'-- Cycle for each polyline segment to develop transects perpendicular to each line for each rec in clFTab
'-- Clear any previous selections
clFTab.GetSelection.ClearAll
'-- Set the selection to the current record
clFTab.GetSelection.Set(rec)
'-- Clear any existing graphics from the view
gLst = theView.GetGraphics
if (gLst.Count > 0) then
gLst.Empty
end
'-- Create empty list to hold temporary centerline
plyLnList = {}
'-- Get the current selected polyline segment of the centerline
clPLine = clFTab.ReturnValue(clFTab.FindField("Shape"), rec)
clID = clFTab.ReturnValue(clFTab.FindField("ID"), rec)
thePlyLn = Polyline.MakeNull
plyLnList.Add(clPLine.Clone)
thePlyLn = plyLnList.Get(0)
'-- Return the total length of the centerline
totalLength = thePlyLn.ReturnLength
'-- Select the points in the Offset_UTM theme that intersect the segment
ptFTab.SelectByFTab(clFTab, #FTAB_RELTYPE_ISWITHINDISTANCEOF ,0.1, #VTAB_SELTYPE_NEW)
theView.Invalidate
'-- Transect deifnation with the selected centerline as the polyline; Initialize previous bearing variable
prevBearing = 0
'-- For each point, get the point information
for each rec in ptFTab.GetSelection
thePoint = ptFTab.ReturnValue(ptFTab.FindField("Shape"), rec)
lbsPerPt = ptFTab.ReturnValue(ptFTab.FindField("lbsPerPt"), rec)
acre = ptFTab.ReturnValue(PtFTab.FindField("Acres"), rec)
lbsAcre = ptFTab.ReturnValue(ptFTab.FindField("lbsAcre"), rec)
'-- Calculate distance along line
ptPos = thePlyLn.PointPosition(thePoint)
distAlong = totalLength * (ptPos/100)
'-- Calculate distance ahead of point where cross section will be applied
thePnt = thePlyLn.Along(ptPos)

```

```

xPt1 = thePnt.GetX
yPt1 = thePnt.GetY
newPnt = thePlyLn.Along(ptPos + 0.0001)
xPt2 = newPnt.GetX
yPt2 = newPnt.GetY
deltaX = xPt2 - xPt1
deltaY = yPt2 - yPt1
'-- Calc bearing
allowNeg = False
bearing1 = (deltaY / deltaX).ATan
if (deltaX < 0) then
  if (deltaY >= 0) then
    bearing1 = bearing1 + Number.GetPi
  else
    bearing1 = bearing1 - Number.GetPi
  end
end
if ((bearing1 < 0) and (not allowNeg)) then
  bearing1 = (Number.GetPi *2) + bearing1
end
'-- Compare bearing to previous bearing for break; first check if record is first or last
if (rec = 0) then
  prevBearing = bearing1
else
  if (bearing1 - prevBearing > 20) then
    bearing1 = prevBearing
  else
    prevBearing = bearing1
  end
end
'-- Calculate angle from bearing that is 90 degrees from direction of travel
bearing2 = ((number.GetPi/2) - bearing1)
'-- Set point positions for the new endpoints of the transect
xCoord1 = (theDist * bearing2.Cos)
yCoord1 = (theDist * bearing2.Sin)
xCoord2 = (theDist * bearing2.Cos)
yCoord2 = (theDist * bearing2.Sin)
'-- Calc the new endpoints
nwPnt = Point.Make((xPt1-xCoord1),(yPt1+yCoord1))
nwPnt2 = Point.Make((xPt1+xCoord2),(yPt1-yCoord2))
'-- Draw polyline graphic based on the 2 points
lin = Line.Make(nwPnt, nwPnt2)
plin = lin.AsPolyline
'-- Cut line into new temporary line
theView.SetEditableTheme(newTheme)
shpField = newTheme.GetFTab.FindField("Shape")
newTheme.GetFTab.BeginTransaction
rec = newTheme.GetFTab.AddRecord
newTheme.GetFTab.SetValue(shpField, rec, plin)
newTheme.GetFTab.EndTransaction
newTheme.GetFTab.GetSelection.ClearAll
newTheme.GetFTab.GetSelection.Set(rec)
newTheme.GetFTab.UpdateSelection
newTheme = theView.FindTheme(shpFileName)
'-- Add other feature attributes to FTab
newFTab = newTheme.GetFTab
if (newFTab.IsEditable = "FALSE") then
  newFTab.SetEditable(True)
end
for each rec in newFTab.GetSelection
  newFTab.SetValue(idField,rec,rec+1)
  newFTab.SetValue(cIIDField,rec, cIID)

```

```

        newFTab.SetValue(distField,rec, distAlong)
        newFTab.SetValue(lbsPtField, rec, lbsPerPt)
        newFTab.SetValue(acreField, rec, acre)
        newFTab.SetValue(lbsAcreField, rec, lbsAcre)
    end
'-- Toggle editing off
    theView.SetEditableTheme(nil)
end
end
theView.Invalidate

```

### Create sub-polygons

```

'-- Initialize the transects theme and create the FTab
theView = av.GetActiveDoc
theThemes = theView.GetThemes
InTheme = theView.FindTheme("Transects.shp")
InFTab = InTheme.GetFTab
InFTab.SetEditable(True)
'-- Select all records
InFTab.GetSelection.SetAll
'-- Determine the number of records in FTab
numRecs = (InFTab.GetSelection.Count) -1
'-- Determine the step size for increments
stepSize = 100/ numZones
'-- Create the polygon shapefile and set-up for entry of the polygons as drawn below.
newThemeName = av.Run("CreatePolygonOutputFile",nil)
for each t in theView.GetThemes
    if (t.GetName = newThemeName) then
        newTheme = t
    end
end
shpFileName = newTheme.GetName
'-- Select transects that correspond to each centerline segment before processing
'-- Determine the number of centerline segments
clTheme = theView.FindTheme("Centerline.shp")
clFTab = clTheme.GetFTab
clNum = clFTab.GetNumRecords
for each i in 1..clNum
    theBitmap = InFTab.GetSelection
    theBitmap.ClearAll
    theQuery = "[CL_ID] = " + i.AsString
    InFTab.Query(theQuery,theBitmap, #VTAB_SELTYPE_NEW)
    InFTab.UpdateSelection
    recNum = 0
'-- For each line and the next line
    for each rec in InFTab.GetSelection
        recNum = recNum + 1
'-- Set up the graphics list
        gl = theView.GetGraphics
        gl.Empty
'-- Initialize 2 blank point lists
        ptList1 = {}
        ptList2 = {}
        lin1 = InFTab.ReturnValue(InFTab.FindField("Shape"), rec )
        InID = InFTab.ReturnValue(InFTab.FindField("ID"), rec)
        lbsPerPt = InFTab.ReturnValue(InFTab.FindField("lbsPerPt"), rec)
        acre = InFTab.ReturnValue(InFTab.FindField("Acres"), rec)
        lbsAcre = InFTab.ReturnValue(InFTab.FindField("lbsAcre"), rec)
'-- Divide into equal segments based on step size
        linLength = lin1.ReturnLength
        for each j in 0 .. (_numZones)

```

```

    newPt = lin1.Along(stepSize * j)
    ptGraphic = GraphicShape.Make(newPt)
    gl.Add(ptGraphic)
    ptList1.Add(newPt)
end
if (recNum < (numRecs)) then
    lin2 = lnFTab.ReturnValue(lnFTab.FindField("Shape"), rec + 1)
'-- Divide into equal segments
    linLength = lin2.ReturnLength
    for each k in 0 .. (_numZones)
        newPt = lin2.Along(stepSize * k)
        ptGraphic = GraphicShape.Make(newPt)
        gl.Add(ptGraphic)
        ptList2.Add(newPt)
    end
else
    lin2 = lnFTab.returnValue(lnFTab.FindField("Shape"), rec - 1)
'-- Divide into equal segments
    linLength = lin2.ReturnLength
    for each k in 0 .. (_numZones)
        newPt = lin2.Along(stepSize * k)
        ptGraphic = GraphicShape.Make(newPt)
        gl.Add(ptGraphic)
        ptList2.Add(newPt)
    end
end
'-- Initialize polyID number
idNum = 0
'-- Now draw the new polygon from points
for each z in 0 .. (_numZones-1)
    idNum = idNum + 1
    pt1 = ptList1.Get(z)
    pt2 = ptList2.Get(z)
    pt3 = ptList2.Get(z+1)
    pt4 = ptList1.Get(z+1)
    newPlygn = Polygon.Make({ {pt1,pt2,pt3,pt4} })
'-- Put polygon into new shape file
    theView.SetEditableTheme(newTheme)
    shpField = newTheme.GetFTab.FindField("Shape")
    ptIDField = newTheme.GetFTab.FindField("PointID")
    polyIDField = newTheme.GetFTab.FindField("Poly_ID")
    lbsPtField = newTheme.GetFTab.FindField("LbsPerPt")
    acreField = newTheme.GetFTab.FindField("Acres")
    lbsAcreField = newTheme.GetFTab.FindField("lbsAcre")
    newTheme.GetFTab.BeginTransaction
    rec = newTheme.GetFTab.AddRecord
    newTheme.GetFTab.SetValue(shpField, rec, newPlygn)
    newTheme.GetFTab.EndTransaction
    newTheme.GetFTab.GetSelection.ClearAll
    newTheme.GetFTab.GetSelection.Set(rec)
    newTheme.GetFTab.UpdateSelection
    newTheme = theView.FindTheme(shpFileName)
'-- Add other feature attributes to FTab
    newFTab = newTheme.GetFTab
    if (newFTab.IsEditable = "FALSE") then
        newFTab.SetEditable(True)
    end
    for each rec in newFTab.GetSelection
        newFTab.SetValue(ptIDField,rec,lnID)
        newFTab.SetValue(polyIDField,rec, idNum)
        newFTab.SetValue(lbsPtField, rec, lbsPerPt)
        newFTab.SetValue(acreField, rec, acre)

```



```

        newFTab.SetValue(lbsAcreField, rec, lbsAcre)
    end
'-- Toggle editing off
    theView.SetEditableTheme(nil)
end
end
    i = i + 1
end
'-- Stop editing, save edits and clear selections
InFTab.SetEditable(False)
InFTab.GetSelection.ClearAll
InFTab.UpdateSelection
InTheme.SetVisible(True)
'-- Clear the graphics list
gl = theView.GetGraphics
gl.Empty
'-- Refresh the view
theView.Invalidate
'-- Remove temporary transect theme from view
theThemes = theView.GetThemes
for each t in theThemes
    if (t.GetName = "Transects..shp") then
        tempTheme = t
    end
end
theView.DeleteTheme(tempTheme)
av.GetProject.SetModified(true)
av.PurgeObjects

```

**Calculate the area (square meters) acreage (acres) for each sub-polygon and add the fields Area and Acres to the polygon theme.**

```

'-- A View with at least one active polygon theme is required.
'-- Get the view and its projection if any.
theView = av.GetActiveDoc
thePrj = theView.GetProjection
if (thePrj.IsNull) then
    hasPrj = false
else
    hasPrj = true
end
'-- Activate the sub-polygon theme and deactivate all others
theThemes = theView.GetThemes
for each t in theThemes
    theFTab = t.GetFTab
'-- Make the FTAB editable, and find out which type of feature it is.
    theType = theFTab.FindField("Shape").GetType
    if (theType = #FIELD_SHAPEPOLY) then
        t.SetActive(True)
        theFTab.SetEditable(True)
'-- Create the fields "Area" & "Acre"
        theAreaField = Field.Make("Area",#FIELD_DOUBLE,16,4)
        theFTab.AddFields({theAreaField})
'-- Loop through the FTAB and find the projected area and perimeter of each shape and set the field values appropriately.
        theShape = theFTab.ReturnValue(theFTab.FindField("shape"),0)
        for each rec in theFTab
            theFTab.QueryShape(rec,thePrj,theShape)
            theArea = theShape.ReturnArea
            theAcres = theArea*0.0002471044
            theFTab.SetValue(theAreaField,rec,theArea)
            theFTab.SetValue(theFTab.FindField("Acres"),rec,theAcres)
        end
    end
end

```

```

'-- Select all records
    theFTab.GetSelection.SetAll
'-- Calculate lbs per acre if appType is NC
    if (_appType = "NC") then
'-- Get the high and low number for point values in the dataset
        loPtVal = 0
        hiPtVal = 0
        for each rec in theFTab.GetSelection
            ptVal = theFTab.ReturnValue(theFTab.FindField("PointID"), rec)
            if (rec = 0) then
                loPtVal = ptVal
                hiPtVal = ptVal
            else
                if (ptVal < loPtVal) then
                    loPtVal = ptVal
                end
                if (ptVal > hiPtVal) then
                    hiPtVal = ptVal
                end
            end
        end
'-- make selection based on ptID's and assign lbs/acre
        for each i in loPtVal..hiPtVal
            acreVal = 0
            totAcre = 0
            theBitmap = theFTab.GetSelection
            theBitmap.ClearAll
            theQuery = "[PointID] = " + i.AsString
            theFTab.Query(theQuery,theBitmap,#VTAB_SELTYPE_NEW)
            theFTab.UpdateSelection
            for each rec in theFTab.GetSelection
                acreVal = theFTab.ReturnValue(theFTab.FindField("Acres"), rec)
                totAcre = totAcre + acreVal
            end
            for each rec in theFTab.GetSelection
                lbsPerPt = theFTab.ReturnValue(theFTab.FindField("LbsPerPt"), rec)
                lbsAcre = lbsPerPt/totAcre
                theFTab.SetValue(theFTab.FindField("LbsAcre"), rec, lbsAcre)
            end
        end
        theFTab.GetSelection.ClearAll
        theFTab.SetEditable(False)
    else
        t.GetFTab.GetSelection.ClearAll
        t.SetActive(False)
    end
end
end

```

### Calculate the pounds per acre for each sub-polygon

```

'-- Initialize the View
theView = av.GetActiveDoc
theThemes = theView.GetThemes
for each t in theThemes
    if (t.Is(FTheme)) then
        theFTab = t.GetFTab
        theClass=theFTab.GetShapeClass
        if (theClass.IsSubclassOf(Polygon)) then
            polyTheme = t
            end 'end if...
        end 'end if...
    end 'end if...
end 'end if...

```

```

end
plyFTab = polyTheme.GetFTab
'-- Get the global variable for the range file to be used and import the range from the ADF
  fName = (_appType + ".dbf").AsFileName
  if (File.Exists(fname) = False) then
'-- need to locate the file
    files = FileDialog.ReturnFiles({"*.dbf"}, {"dBASE"}, "Locate Spread Pattern Data Table", 0)
    for each f in files
      newVTab = vTab.Make(f, FALSE, FALSE)
    end
  else
    newVTab = vTab.Make(fName, FALSE, FALSE)
  end
  gui = av.GetProject.GetSelectedGUI
  if (gui.GetType <> "Table") then
    GUIName = "Table"
  else
    GUIName = gui.GetName
  end
  apTable = Table.MakeWithGUI(newVTab, GUIName)
  apTable.SetName(newVTab.GetName)
  apVTab = apTable.GetVTab
  apVTab.GetSelection.SetAll
  if (_appType = "NC") then
    for each rec in apVTab
      if (rec=0) then
        loVal1 = apVTab.ReturnValue(apVTab.FindField("Low"), rec)
        hiVal1 = apVTab.ReturnValue(apVTab.FindField("High"), rec)
      elseif (rec=1) then
        loVal2 = apVTab.ReturnValue(apVTab.FindField("Low"), rec)
        hiVal2 = apVTab.ReturnValue(apVTab.FindField("High"), rec)
      elseif (rec=2) then
        loVal3 = apVTab.ReturnValue(apVTab.FindField("Low"), rec)
        hiVal3 = apVTab.ReturnValue(apVTab.FindField("High"), rec)
      end
    end
  elseif (_appType = "AC") then
    for each rec in apVTab
      if (rec=0) then
        loVal1 = apVTab.ReturnValue(apVTab.FindField("Low"), rec)
        hiVal1 = apVTab.ReturnValue(apVTab.FindField("High"), rec)
      elseif (rec=1) then
        loVal2 = apVTab.ReturnValue(apVTab.FindField("Low"), rec)
        hiVal2 = apVTab.ReturnValue(apVTab.FindField("High"), rec)
      elseif (rec=2) then
        loVal3 = apVTab.ReturnValue(apVTab.FindField("Low"), rec)
        hiVal3 = apVTab.ReturnValue(apVTab.FindField("High"), rec)
      elseif (rec=3) then
        loVal4 = apVTab.ReturnValue(apVTab.FindField("Low"), rec)
        hiVal4 = apVTab.ReturnValue(apVTab.FindField("High"), rec)
      end
    end
  else
    for each rec in apVTab
      if (rec=0) then
        loVal1 = apVTab.ReturnValue(apVTab.FindField("Low"), rec)
        hiVal1 = apVTab.ReturnValue(apVTab.FindField("High"), rec)
      elseif (rec=1) then
        loVal2 = apVTab.ReturnValue(apVTab.FindField("Low"), rec)
        hiVal2 = apVTab.ReturnValue(apVTab.FindField("High"), rec)
      elseif (rec=2) then
        loVal3 = apVTab.ReturnValue(apVTab.FindField("Low"), rec)

```

```

        hiVal3 = apVTab.ReturnValue(apVTab.FindField("High"), rec)
    elseif (rec=3) then
        loVal4 = apVTab.ReturnValue(apVTab.FindField("Low"), rec)
        hiVal4 = apVTab.ReturnValue(apVTab.FindField("High"), rec)
    end
end
end
end
'-- Make sure all records are selected
plyFTab.GetSelection.SetAll
'-- Calculate pounds per sub-polygon
for each rec in plyFTab.GetSelection
    lbsVal = plyFTab.ReturnValue(plyFTab.FindField("LbsAcre"),rec)
    polyNum = plyFTab.ReturnValue(plyFTab.FindField("Poly_ID"),rec)
    polyArea = plyFTab.ReturnValue(plyFTab.FindField("Area"), rec)
    polyAcres = plyFTab.ReturnValue(plyFTab.FindField("Acres"), rec)
'-- compare lbsVal to ranges to determine which row to extract the correct multiplier from
theField = _appType + polyNum.AsString
rangeFactor = 0
if (_appType = "NC") then
    if (lbsVal > 0) then
'-- find proper range
        if ((lbsVal < hiVal1) or (lbsVal = hiVal1)) then
'-- subpoly value from table comes from row 1
            rangeFactor = apVTab.ReturnValue(apVTab.FindField(theField),0)
        elseif ((lbsVal > loVal2) or (lbsVal = loVal2)) then
'-- check against hiVal2
            if ((lbsVal < hiVal2) or (lbsVal = hiVal2)) then
'-- subpoly value comes from table row 2
                rangeFactor = apVTab.ReturnValue(apVTab.FindField(theField),1)
            end
            elseif ((lbsVal > loVal3) or (lbsVal = loVal3)) then
'-- check against hiVal3
                if ((lbsVal < hiVal3) or (lbsVal = hiVal3)) then
'-- subpoly value comes from table row3
                    rangeFactor = apVTab.ReturnValue(apVTab.FindField(theField),2)
                end
            end
            end
        else
            if (lbsVal > 0) then
'-- find proper range
                if ((lbsVal < hiVal1) or (lbsVal = hiVal1)) then
'-- subpoly value from table comes from row 1
                    rangeFactor = apVTab.ReturnValue(apVTab.FindField(theField),0)
                elseif ((lbsVal < hiVal2) or (lbsVal = hiVal2)) then
'-- subpoly value comes from table row 2
                    rangeFactor = apVTab.ReturnValue(apVTab.FindField(theField),1)
                end
                elseif ((lbsVal < hiVal3) or (lbsVal = hiVal3)) then
'-- subpoly value comes from table row3
                    rangeFactor = apVTab.ReturnValue(apVTab.FindField(theField),2)
                end
                elseif ((lbsVal < hiVal4) or (lbsVal = hiVal4)) then
'-- subpoly value comes from table row4
                    rangeFactor = apVTab.ReturnValue(apVTab.FindField(theField),3)
                end
            end
        end
        end
    end
    lbsPoly = lbsVal * rangeFactor
'-- Apply that value to the polygon
    plyFTab.SetEditable(True)
    plyFTab.SetValue(plyFTab.FindField("LbsPoly"),rec,lbsPoly)

```

```
plyFTab.SetEditable(True)
end
```

### **Takes a point file and spears through a polygon layer summing intersecting polygons**

```
theView = av.GetActiveDoc
thethemes = theView.GetThemes
polyThm = msgbox.Choice(theThemes, "Select App PolyTheme", "")
polyFTab = polyThm.GetFTab
polyFields = polyFTab.GetFields
PolyAppField = msgbox.Choice(polyFields, "Select the pndsPer Acre field", "")
polyShape = polyFTab.FindField("Shape")
pntTheme = msgbox.Choice(theThemes, "Now Select the Grid Pt Theme", "")
pntFTab = pntTheme.GetFTab
pntFTab.SetEditable(true)
theFields = pntFTab.GetFields
pndsApplied = Field.Make("PndsPerPoint", #FIELD_DECIMAL, 10,3)
pntFTab.ADDFields({pndsApplied})
pointShape = pntFTab.FindField("Shape")
for each rec in pntFTab
  aPoint = pntFTab.ReturnValue(pointShape, rec)
  pointTotal = 0
  for each rek in polyFTab
    aPoly = polyFTab.ReturnValue(polyShape, rek)
    if (aPoly.Intersects(aPoint))
      then
        polypounds = polyFTab.ReturnValue(polyAppField, rek)
        pointTotal = pointTotal + polyPounds
      end
    end
  end
  pntFTab.SetValue(pndsApplied, rec, pointTotal)
end
pntFTab.SetEditable(false)
```

## REFERENCES

- AGR-1. 2002. Lime and fertilizer recommendations. Lexington, Ky.: University of Kentucky.
- AGR-1. 1998. Fertilizer and lime recommendations. Lexington, Ky.: University of Kentucky.
- AgView. 1999. GIS Solutions Inc., Springfield, IL.
- Anglund, E.A. and P.D. Ayers. 2003. Field evaluation of response times for a variable-rate (pressure-based and injection) liquid chemical applicator. *Appl. Eng. in Agri.* 19(3): 273-282.
- Arslan, S. and T.S. Colvin. 1998. Laboratory test stand for combine grain yield monitors. *Appl. Engr. Agr.* 14(4): 369-371.
- ASAE Standards, 47th Ed. 2000. S341.2. Procedure for measuring distribution uniformity and calibrating broadcast spreaders. St. Joseph, Mich: ASAE.
- ASAE Standards, 44th Ed. 1997. S341.2. Procedure for measuring distribution uniformity and calibrating broadcast spreaders. St. Joseph, Mich. ASAE.
- Babcock, B.A. and G.R. Pautsch. 1998. Moving from uniform to variable-rates on Iowa corn: effects on rates and returns. *J. Agr. Res. Econ.* 23(2): 385-400.
- Bashford, L.L., S. Al-Hames, M. Schroeder, and M. Ismail. 1995. Mapping corn and soybean yields using a yield monitor and GPS. In Site-Specific Management for Agricultural Systems, ASA, CSSA, and SSSA, Madison, WI. 691-707.
- Bongiovanni, R. and J. Lowenberg-DeBoer. 2000. Economics of variable-rate lime in Indiana. *Prec. Agr.* 2:55-70.
- Bullock, D.S., J. Lowenberg-DeBoer, S.M. Swinton. 2002. Adding value to spatially managed inputs by understanding site-specific yield response. *Agr. Econ.* 27:23-245.
- Cambouris, A.N., M.C. Nolin, and R.R. Simard. 1999. Precision management of fertilizer phosphorous and potassium for potato in Quebec, Canada. In P.C. Robert et al. (ed.) Proceeding of the 4<sup>th</sup> International Conference on Precision Agriculture, ASA, CSSA, and SSSA, Madison, WI. 847-857.
- Carr, P.M., G.R. Carlson, J.S. Jacobsen, G.A. Nielsen, and E.O. Skogley. 1991. Farming soils, not fields: A strategy for increasing fertilizer profitability. *J. Prod. Agr.* 4: 57-61.
- Chaplin, J., E. Roytburg, and J. Kaplan. 1995. Measuring the spatial performance of chemical applicators. In Site-Specific Management for Agricultural Systems, ASA, CSSA, and SSSA, Madison, WI. 651-669.
- Cointault, F., P. Sarrazin, and M. Paindavoine. 2003. Measurement of the motion of fertilizer particles leaving a centrifugal spreader using a fast imaging system. *Prec. Agr.* 4: 279-295.
- Doerge, T.A. 1999. Yield map interpretation. *J. Prod. Agr.* 12: 54-61.
- Dorr, G. J., and D. J. Pannel. 1992. Economics of improved spatial distribution of herbicide and weed control in crops. *Crop Protection.* 11(4): 385-391.
- English, C.B., S.B. Mahajanashetti, and R.K. Roberts. 1999. Economics and environmental benefits of variable-rate application of nitrogen to corn fields: role of variability and weather. Paper presented at the Am. Agr. Econ. Assoc. Meeting, Nashville, TN. Aug. 8-11.
- ESRI. 2003. ArcPad<sup>®</sup>, version 6.0.2.12. Redlands, Cal.: Environmental Systems Research Institute, Inc.
- ESRI. 2001. ArcView GIS<sup>®</sup>, version 3.3. Redlands, Cal.: Environmental Systems Research Institute, Inc.

- ESRI. 1999. ArcView<sup>®</sup>, version 3.2. Redlands, Cal.: Environmental Systems Research Institute, Inc.
- Fairchild, D., and M. Duffy. 1993. Working group report on profitability. In P.C. Robert et al. (ed.) Soil Specific Crop Management, ASA Misc. Publ, CSSA, and SSSA, Madison, WI. pp 245-253.
- Fulton, J. P., S. A. Shearer, G. Chabra, and S. F. Higgins. 2001. Performance assessment and model development of a variable-rate, spinner fertilizer disc applicator. *Trans. ASAE*. 44(5): 1071-1081.
- Fulton, J.P., S. A. Shearer, T.S. Stombaugh, M.E. Anderson, T.F. Burks and S.F. Higgins. 2003. Simulation of Fixed and Variable-Rate Application of Granular Materials. *Trans. of ASAE*. 46(5): 1311-1321.
- GIS. 1999. AgView, version 1.7.14. Springfield, Ill.: GIS Solutions, Inc.
- Grift, T.E. and J.W. Hofstee, 2002. Testing an online spread pattern determination sensor on a broadcast fertilizer spreader. *Trans. of ASAE*. 45(3):561-567.
- Goense, D. 1997. The accuracy of farm machinery fro precision agriculture: a case study for fertilizer application. *Netherlands J. Agr. Sci.* 45: 201-217.
- Hofstee, J.W. 1995. Handling and spreading of fertilizers: Part 5, the spinning disc type fertilizer spreader. *J. Agr. Engr. Res.* 62: 143-162.
- Jasa, P.J., R.D. Grisso, and J.C. Wilcox. 2000. Yield monitor accuracy at reduced flow rates. ASAE Paper No. 001085. St Joseph, MI: ASAE.
- Kettle, L.Y. and C.L. Peterson. 1998. An evaluation of yield monitors and GPS systems on hillside combines operating on the steep slopes in the Palouse. ASAE Paper No.981046. St Joseph, MI: ASAE.
- Leer, S. 2003. Survey: Information gaps exist in precision agriculture. Purdue Agricultural News. Press release from Purdue Ag. Communications. Feb. 11, 2003.
- Linsley, C. M., and F. C. Bauer. 1929. Test your soil for acidity. Circular 346. Urbana, Ill.: University of Illinois Agricultural Experiment Station.
- Lowenberg-DeBoer, J. and A. Aghib. 1999. Average returns and risk characteristics of site-specific P and K management: Eastern Corn Belt on-farm trial results. *J. Prod. Agr.* 12: 276-282.
- Lowenberg-DeBoer, J. and S.M. Swinton. 1997. Economics of site-specific management in agronomic crops. In Site-Specific Management for Agricultural Systems, ASA, CSSA, and SSSA, Madison, WI. 369-396.
- Mallarino, A.P., D.J. Wittry, D. Dousa, and P.N. Hinz. 1999. Variable-rate phosphorus fertilization: on-farm research mehods and evaluation for corn and soybean. In P.C. Robert et al. (ed.) Proceeding of the 4<sup>th</sup> International Conference on Precision Agriculture, ASA, CSSA, and SSSA, Madison, WI. 687-696.
- Marchenko, N. M., and B. P. Chernikov. 1977. The ways for spreader development. *Mekh. I. Elektriph. S.H.* (7): 3-6.
- Molin, J.P., L.A.A. Menegatti, L.L. Pereira, L.C. Cremonini, and M. Evangelista. 2002. Testing a fertilizer spreader with VRT. In F.S. Zazuets and J. Xin (eds.) Proceedings of the World Congress of Computers in Agriculture and Natural Resources. 13-15, March 2002. ASAE publication No. 701P0301. pp. 232-237.
- Möller, N. and J.E.T. Svensson. 1991. Modern techniques in application of granular fertilisers. Paper read before The Fertiliser Society in London. December 19, 1991. Proceedings No. 311.

- Mowitz, D. 2003. Precision begins at home: get machinery operating precisely before turning to precision agriculture (Business Perspective). *Successive Farming*. Feb. 2003. 101(2):13.
- Mueller, T.G., F.J. Pierce, O. Schabenberger, and D.D. Warncke. 2001. Map quality for site-specific management. *Soil Sci. Soc. Am. J.* 65: 1547-1558.
- Olieslagers, R., H. Ramon, and J. De Baerdemaeker. 1996. Calculation of fertilizer distribution patterns from a spinning disc spreader by means of a simulation model. *J. Agr. Eng. Res.* 63(2): 137-152.
- Olieslagers, R., H. Ramon, and J. De Baerdemaeker. 1997. Performance of a continuously controlled spinning disc spreader for precision application of fertilizer. In *Precision Agriculture 1997*, papers presented at the first European Conference on Precision Agriculture, Warwick University Conference Centre, UK, 7-10 September 1997 / European Conference on Precision Agriculture. Oxford ; Herndon, VA : BIOS Scientific Pub., c1997. 661-668.
- Parish, R. L. 1991. Effect of rough operating surface on rotary spreader distribution pattern. *Appl. Eng. in Agric.* 7(1): 61-63.
- Parish, R. L. 1987. The effect of speed on performance of a rotary spreader for turf. *Appl. Eng. in Agric.* 3(1): 17-19.
- Parish, R. L., and P. P. Chaney. 1986. Speed effect on drop-type spreader application rate. *Appl. Eng. in Agric.* 2(2): 94-96.
- Pettersen, J. M., J. A. Svendsen, and S. Ovland. 1991. A method of studying the influence of fertilizer particle size on the distribution from a twin-disc spreader. *J. Agric. Eng. Res.* 50(4): 291-303.
- Pierce, F.J. and D.D. Warncke. 2000. Soil and crop response to variable-rate liming for two Michigan fields. *Soil Sci. Soc. Am. J.* 64: 774-780.
- Qui, Z. and T. Prato. 1999. Integrated economic and environmental assessment of variable-rate technology for nitrogen application in corn production. Paper presented at the Am. Agr. Econ. Assoc. Meeting, Nashville, TN. Aug. 8-11.
- Reichenberger, L., and J. Russnogle. 1989. Farm by the foot. *Farm J.* 113(6): 11-15.
- Roth, L.O., R.W. Whitney, and D.K. Kuhlman. 1985. Application uniformity and some non-symmetrical distribution patterns of agricultural chemicals. *Trans. ASAE.* 28(1): 47-50.
- Searcy, S. W. 1995. Engineering system for site-specific management: Opportunities and limitations. In *Site-Specific Management for Agricultural Systems*, ASA, CSSA, and SSSA, Madison, WI. 603-612.
- SAS. 2001. The SAS System for Windows, release 8.02. SAS Institute Inc., Cary, NC.
- Schnitkey, G.D., J.W. Hopkins, and L.G. Tweenten. 1996. An economic evaluation and precision fertilizer application on corn-soybeans fields. In P.C. Robert et al. (ed.) *Proceeding of the 3<sup>rd</sup> International Conference on Precision Agriculture*, ASA, CSSA, and SSSA, Madison, WI. 977-987.
- Schueller, J. K. 1989. Spatially variable fluid fertilizer applicator design concepts. *J. Fert. Issues* 6(4): 100-102.
- Schueller, J.K. and M.W. Wang. 1994. Spatially-variable fertilizer and pesticide application with GPS and DGPS. *Comp. Elec. Agr.* 11:69-83.
- Sigma Plot 2002. 2001. Scientific Graphing Software, version 8.0. Chicago, Ill.: SPSS, Inc.
- Sigma Plot. 1997. Scientific Graphing Software, version 4.00. Chicago, Ill.: SPSS, Inc.
- Sogaard, H. T., and P. Kierkegaard. 1994. Yield reduction resulting from uneven fertilizer distribution. *Trans. ASAE* 37(6): 1749-1752.



- Strubbe, G., B. Missotten, and J. DeBaerdemaeker. 1996. Mass flow measurement with a curved plate at the exit of an elevator. *Prec. Agr.* 703-712.
- Swinton, S.M. and J. Lowenberg-Deboer. 1998. Evaluating the profitability of site-specific farming. *J. Prod. Agr.* 11: 439-446.
- SST. 1999. SSToolbox, version 3.1.1. Stillwater, Okla.: Site-Specific Technologies Development Group.
- Surfer. 1996. Surface Mapping System, version 6.04. Golden Colo.: Golden Software, Inc.
- Thrikawala, S., A. Weersink, G. Kachanoski, and G. Fox. 1999. Economic feasibility of variable-rate technology for nitrogen on corn. *Am. J. Agr. Econ.* 81: 914-927.
- Tri-State. 2000. Tri-state fertilizer recommendations for corn, soybeans, wheat, and alfalfa. Extension Bulletin E-2567 published by Purdue University, Michigan State University, and The Ohio State University.
- USDA. 2003. Agriculture Fact Book, 2001-2002. United States Department of Agriculture. Office of Communications, United States Government Printing Office, Washington, DC. <http://www.usda.gov>.
- U.S. Census Bureau, 2002. United States Census 2000, Issued July 2002. United States Department of Commerce, Washington, DC. <http://www.census.gov>.
- Van Bergeijk, J., D. Goense, L.G. van Wlligenberg, and L. Speelman. 2001. Dynamic weighing for accurate fertilizer application and monitoring. *J. Agr. Engr. Res.* 80(1): 25-35.
- Watkins, K.B., Y. Lu, and W. Huang. 1998. Economic and environmental feasibility of variable-rate nitrogen fertilizer application with carry-over effects. *J. Agr. Res. Econ.* 23(2): 401-426.
- Wang, D., T. Prato, Z. Qui, N.R. Kithchen, and K.A. Sudduth. 2003. Economic and environmental evaluation of variable-rate nitrogen and lime application for claypan soil fields. *Prec. Agr.* 4: 35-52.
- Weisz, R., R. Heiniger, J.G. White, B. Knox., and L. Reed. 2003. Long-term variable-rate lime and phosphorous application for piedmont no-till field crops. *Prec. Agr.* 4: 311-330.
- Wibawa, W.D., D.L. Dlundlu, L.J. Swenson, D.G. Hopkins, and W.C. Dahnke. 1993. Variable fertilizer application based on yield goal, soil fertility, and soil map unit. *J. Prod. Agr.* 6: 255-261.
- Yang, C., G.L. Anderson, J.H. King, Jr., and E.K. Chandler. 1999. Comparison of uniform and variable-rate fertilization strategies using grid soil sampling, variable-rate technology, and yield monitoring. In P.C. Robert et al. (ed.) *Proceeding of the 4<sup>th</sup> International Conference on Precision Agriculture*, ASA, CSSA, and SSSA, Madison, WI. 675-686.
- Yule, I.J., P.J. Cain, E.J. Evans, and C. Venus. 1996. A spatial inventory approach to farm planning. *Comp. Elec. Agr.* 14:151-161.

# VITA

## JOHN PATRICK FULTON

### PERSONAL INFORMATION

---

**Birth:** Born September 26, 1971 to Thomas Morrow and Barbara Ann Fulton in Troy, Ohio.

### EDUCATION

---

- May 1999**                      **Masters of Science in Agricultural Engineering,**  
University of Kentucky, Lexington, Kentucky.  
**Emphasis:** Power and Machinery  
**Thesis:** Evaluation of a mechanical system for reconstructing soil on surface  
mined land.
- June 1994**                      **Bachelor of Arts in Physics with a minor in Math**  
Wittenberg University, Springfield, Ohio.

### EMPLOYMENT EXPERIENCE

---

- 1999 to Present**              **Engineer Associate,** Biosystems and Agricultural  
Engineering Department, University of Kentucky.
- 1996 – 1999**                      **Agricultural Engineer,** Biosystems and Agricultural  
Engineering Department, University of Kentucky.
- 1993 - 1994**  
(Summers Only)              **Assistant Test Engineer,** Hartzell Fan, Inc., Piqua, Ohio.  
Industrial Ventilation Company.
- 1990 – 1994**  
(Summers excluded)        **Student Assistant,** Wittenberg University, Springfield, Ohio.  
Assistant Manager for the athletic center.
- 1978 – Present**                **Assistant Manager,** Fulton Farms, Troy, Ohio.  
2000 acre irrigated fruit, vegetable, and grain crop farm.

### PATENT

---

- Wells L.G. and J.P. Fulton. 2000. Soil Regeneration Apparatus and Method. United States Patent and Trademark Office. Patent Number 6,056,066.

## **PUBLICATIONS**

---

### **Refereed**

- Fulton, J.P., S.A. Shearer, T.S. Stombaugh, M.E. Anderson, T.F. Burks and S.F. Higgins. 2003. Simulation of Fixed and Variable-Rate Application of Granular Materials. *Trans. of ASAE*. Vol. 46(5): 1311–1321.
- Dillon, C.R., S.A. Shearer, J.P. Fulton, and M. Kanakasabai. 2003. Optimal Path Nutrient Application Using Variable Rate Technology. In S. Blackmore and G. Grenier (ed.) Proc. of the Fourth European Conference on Precision Agriculture, pp. 171-176. Berlin, Germany, 16-19 June.
- Burks, T.F., S.A. Shearer, J.P. Fulton, and C.J. Sobolik. 2004. Influence of dynamically varying inflow rates on clean grain elevator yield monitor accuracy. Accepted for publication in *Applied Engineering in Agriculture*.
- Burks, T.F., S.A. Shearer, J.P. Fulton, and C.J. Sobolik. 2003. Combine Yield Monitor Tests Facility Development. *Applied Engineering in Agriculture*. Vol. 19(1): 5-12.
- Fulton, J.P., L.G. Wells and T.D. Smith. 2002. A Mechanical System for Soil Reconstruction. *Applied Engineering in Agriculture*. Vol. 18(5): 517-524.
- Fulton, J.P., S.A. Shearer, G. Chabra and S.F. Higgins. 2001. Performance Assessment and Model Development of a Variable-Rate, Spinner-Disc Fertilizer Applicator. *Trans. of ASAE*. Vol. 44(5): 1071-1081.
- Fulton, J.P. and L.G. Wells. Evaluation of a Mechanical System for Reconstructing Soil on Surface Mined Land. Submitted to *Applied Engineering in Agriculture*.

### **Extension**

- T.S. Stombaugh, S.A. Shearer, and J.P. Fulton. 2002. PA-5: Elements of Precision Agriculture: GPS Simplified. Cooperative Extension Service, University of Kentucky.
- S.A. Shearer, J.P. Fulton, S.G. McNeill, S.F. Higgins, and T.G. Mueller. 1999. PA-1: Elements of Precision Agriculture: Basics of Yield Monitor Installation and Operation. Cooperative Extension Service, University of Kentucky.

### **Meeting Papers**

- Fulton, J.P., S.A. Shearer, T.S. Stombaugh, and S.F. Higgins. 2003. Comparison of Variable-Rate Granular Application Equipment. ASAE Paper No. 031125. Annual International Meeting, Riviera Hotel and Convention Center, Las Vegas, Nevada, July 27-30.
- Shearer, S.A., J.P. Fulton, T.S. Stombaugh, and D.W. Hancock. 2003. Extraction of Machine Performance Data from GPS and Yield Monitor Data. ASAE Paper No. 031085. Annual International Meeting, Riviera Hotel and Convention Center, Las Vegas, Nevada, July 27-30.
- Shearer, S.A., M.D. Montross, T.S. Stombaugh, R. Prewitt, J.P. Fulton, and S. Sokhansanj. 2003. Use of Spatial Technologies for Tracking the Efficiency of Biomass Harvesting. ASAE Paper No. 036087. Annual International Meeting, Riviera Hotel and Convention Center, Las Vegas, Nevada, July 27-30.
- Fulton, J.P., S.A. Shearer, T.S. Stombaugh, S.F. Higgins and C.R. Dillon. 2002. 'As-Applied' Model Validations for Variable-Rate Application of Granular Materials. In P.C. Robert et al. (ed.) Proc. 6th International Conference on Precision Agriculture. ASA Misc. Publ., ASA, CSSA, and SSSA, Madison, WI.

- Fulton, J.P., S.A. Shearer, T.S. Stombaugh, and S.F. Higgins. 2002. Simulation of Variable-Rate Application of Granular Materials. ASAE Paper No. 021168. Annual International Meeting, Hyatt Regency Chicago, Chicago, Illinois, July 28-31.
- Burks, T.F., S.A. Shearer, J.P. Fulton, and T.S. Stombaugh. 2002. Assessment of yield monitor accuracy using the ASAE X-587 Draft Test. In. P.C. Robert et al. (ed.) Proc. 6th International Conference on Precision Agriculture. ASA Misc. Publ., ASA, CSSA, and SSSA, Madison, WI.
- Shearer, S.A., T.S. Stombaugh, J.P. Fulton, and T.G. Mueller. 2002. Considerations for development of a variable-rate controller test standard. ASAE Paper No. 021191. Annual International Meeting, Hyatt Regency Chicago, Chicago, Illinois, July 28-31.
- T.S. Stombaugh, S.A. Shearer, and J.P. Fulton. 2002. Elements of a Dynamic GPS Test Standard. ASAE Paper No. 021150. Annual International Meeting, Hyatt Regency Chicago, Chicago, Illinois, July 28-31.
- T.S. Stombaugh, S.A. Shearer, and J.P. Fulton. 2002. Standards for Comparison of GPS Receiver Performance. In. P.C. Robert et al. (ed.) Proc. 6th International Conference on Precision Agriculture. ASA Misc. Publ., ASA, CSSA, and SSSA, Madison, WI.
- Fulton, J.P., S.A. Shearer, T.S. Stombaugh, and S.F. Higgins. 2001. Pattern Assessment of a Spinner Disc Variable-Rate Fertilizer Applicator. ASAE Paper No. 011116. Annual International Meeting, Sacramento Convention Center, Sacramento, California, July 29 through August 1.
- Burks, T.F., S.A. Shearer, J.P. Fulton and C. J. Sobolik. 2001. Influence of Dynamically Varying Inflow Rates on Clean Grain Elevator Yield Monitor Accuracy. ASAE Paper No. 011182. Annual International Meeting, Sacramento Convention Center, Sacramento, California, July 29 through August 1.
- Thomasson, J.A., S.A. Shearer, S.A., R.L. Hoskinson, R.K. Fink, J.R. Wooten, T.G. Mueller, J.P. Fulton, and S.F. Higgins. 2001. Decision support system for agriculture (DSS4Ag) applied to fertilization of corn and cotton. ASAE Paper No. 011018. Annual International Meeting, Sacramento Convention Center, Sacramento, California, July 29 through August 1.
- Fulton, J.P., S.A. Shearer, M.E. Anderson, T.F. Burks and S.F. Higgins. 2000. Simulated Application Errors for Granular Materials for Fixed and Variable-Rate Application. ASAE Paper No. 001153. Annual International Meeting, Midwest Express Center, Milwaukee, Wisconsin, July 9-12.
- Burks, T.F., S.A. Shearer, and J.P. Fulton. 2000. Assessment of Fertilizer Application Accuracy with the Use of Navigational Aids. ASAE Paper No. 001154. Annual International Meeting, Midwest Express Center, Milwaukee, Wisconsin, July 9-12.
- Burks, T.F., S.A. Shearer, C. J. Sobolik, and J.P. Fulton. 2000. Combine Yield Monitor Test Facility Development. ASAE Paper No. 001084. Annual International Meeting, Midwest Express Center, Milwaukee, Wisconsin, July 9-12.
- L.G. Wells, S.A. Shearer, J.P. Fulton and L.W. Murdock. 2000. Assessment of Remote Sensing for Implementation of Precision Tillage. ASAE Paper No. 001097. Annual International Meeting, Midwest Express Center, Milwaukee, Wisconsin, July 9-12.
- Shearer, S.A., T.G. Mueller, C.R. Dillon, J.P. Fulton, N.J. Hartsock, and J. Stull. 2000. A GIS-based simulation model for estimating the potential benefits of variable-rate fertilizer application. ASAE Paper No. 001105. Annual International Meeting, Midwest Express Center, Milwaukee, Wisconsin, July 9-12.
- Shearer, S.A., R.L. Hoskinson, R.K. Fink, T.G. Mueller, J.A. Thomasson, J.P. Fulton, and M. Ellis. 2000. Use of the decision support system for agriculture (DSS4Ag) for corn fertilization in

Kentucky. In. P.C. Robert et al. (ed.) Proc. 5th International Conference on Precision Agriculture. ASA Misc. Publ., ASA, CSSA, and SSSA, Madison, WI.

- Fulton, J.P., S.A. Shearer, G. Chabra and S.F. Higgins. 1999. Field Evaluation of a Spinner Disc Variable-Rate Fertilizer Applicator. ASAE Paper No. 991101. Annual International Meeting, Sheraton Centre, Toronto, Canada, July 18-21.
- Shearer, S.A., T.F. Burks, J.A. Thomasson, T.G. Mueller, J.P. Fulton, S.F. Higgins, and S.Samson. 1999. Yield prediction using a neural network classifier trained using soil landscape features and soil fertility data. ASAE Paper No. 993041. Annual International Meeting, Sheraton Centre, Toronto, Canada, July 18-21.
- Fulton, J.P. and L.G. Wells. 1998. Evaluation of a Prototype Mechanism for Soil Reconstruction. ASAE Paper No. 981033. International Meeting, Orlando, Florida, July 12-16.
- Fulton, J.P. and L.G. Wells. 1997. A Mechanical System for Soil Reconstruction. ASAE Paper No. 971095. International Meeting, Minneapolis, Minnesota. August 10-14.
- Shearer, S.A., S.F. Higgins, S.G. McNeill, G.A. Watkins, R.I. Barnhisel, J.C. Doyle, J.H. Leach, and J.P. Fulton. 1997. Data Filtering and Correction Techniques for Generating Yield Maps from Multiple Combine Systems. ASAE Paper No. 971034. Annual International Meeting, Minneapolis Minnesota, August 10-14.
- Fulton, J.P., L.G. Wells, S.A. Shearer and R.I. Barnhisel. 1996. Spatial Variation of Soil Physical Properties: A Precursor to Precision Tillage. ASAE Paper No. 961002. International Meeting, Phoenix, Arizona. July 14-18.

## **GRANTS**

---

### **Principle Investigator**

- Voice Recognition for Concurrent Field Scouting and Machine Operation. J.P. Fulton, S.A. Shearer, T.G. Mueller, S.G. McNeil, Precision Agriculture Special Grant from USDA/CSREES - Phase III Funding. \$63,820 (Funded).

### **Co-Principal Investigator**

- Equipment Enhancement to Support Variable-Rate Response Surface Development. S.A. Shearer, S.F. Higgins, T.G. Mueller, T.S. Stombaugh, C.R. Dillon, J.P. Fulton. Precision Agriculture Special Grant from USDA/CSREES - Phase III Funding. \$63,662 (Funded).
- Outreach Education for Precision Agriculture. T. S. Stombaugh, S.A. Shearer, J.P. Fulton, T.G. Mueller and C.R. Dillon. Precision Agriculture Special Grant from USDA/CSREES – Phase III Funding. \$63,447 (Funded).
- Dynamic Testing of Force-Impetus Yield Monitors Under Rough Terrain Conditions. T.F. Burks, S.A. Shearer, L. G. Wells, S.G. McNeill, J.P. Fulton and S.F. Higgins. Precision Agriculture Special Grant from USDA/CSREES – Phase II Funding. \$35,349 (Funded).

## RESEARCH EXPERIENCE

---

- University of Kentucky's Precision Agriculture Research Team (<http://www.bae.uky.edu/precag/>)
- Indoor Yield Monitor Test Facility
- Application Assessment of Granular Application for Spinner Spreaders
- Biomass Collection and Transportation Research
- Variable-Rate Input Studies
- GIS Analysis
- GPS Testing Facility
- Soil Regenerator
- **Other Research Activities**
  - Generate DEMs utilizing survey grade GPS.
  - Soil compaction research on reclaimed mining sites.
  - Hartzell Fan Inc. – Performance testing of industrial fans.

## EXTENSION EXPERIENCE

---

- Perform on-farm visits to help farmers install yield monitors and GPS receivers.
- Assist farmers in transferring yield data from the yield monitor to their home computer.
- Guest speaker at various conference/extension meetings and at University of Kentucky field days.
- **Precision Agriculture In-Service Training**, October, 2000, Princeton, KY

## OTHER EXPERIENCES

---

- Fulton Farms - family operated 2000 acre irrigated fruit, vegetable, and grain farm.
- ValleyHill Farms ([www.valleyhillfarms.com](http://www.valleyhillfarms.com))

## HONORS AND ACTIVITIES

---

- **Society of Physic Students (SPS)**, Wittenberg University  
Vice-President between May 1993 - May 1994
- **The Society for Engineering in Agricultural, Food, and Biological Systems (ASAE)** – member since 1995
- Member of ASAE committee PM-54 Precision Agriculture
- **Alpha Epsilon** – Agricultural Engineering Honorary
- **Gamma Sigma Delta** - Agricultural Honorary
- Wittenberg Dean's List (Fall 1991, Spring 1992, Fall 1993, Winter 1994)
- Graduated with honors from Wittenberg - *cum laude*
- Community Service: Masonic Home for the Elderly, Springfield, Ohio
- Varsity Men's Basketball (3 years)
- FFA and 4-H member
- Intramural Basketball, Softball and Volleyball